



Analysis of Fire Effects  
on Tank Cars

# **Users Manual**

**For AFTAC 4.00**

**Beta 06**

Prepared by: Dr. Scott R. Runnels  
*Scott Runnels Consulting*

For: The RSI-AAR Railroad Tank Car Safety Research & Test Project

January 24, 2013

**Beta Draft**



Copyright 2001-2013 The RSI-AAR Tank Car Safety Research & Test Project



## **LICENSE AGREEMENT FOR USE OF AFFTAC FOR WINDOWS SOFTWARE**

### LICENSE AGREEMENT FOR USE OF AFFTAC FOR WINDOWS SOFTWARE

The purpose of this License Agreement ('Agreement') is to set forth the terms and conditions that shall govern the use of the 'AFFTAC 4.00' software ('AFFTAC') by the licensee (the 'Licensee') to whom AFFTAC has been distributed without charge through The RPI/AAR Tank Car Safety and Research Project (comprised of The Railway Progress Institute and the Association of American Railroads, collectively 'Licensor'). The parties agree as follows:

#### TERMS

1. **LIMITED LICENSE.** Licensor hereby grants to the Licensee and the Licensee hereby accepts a non-transferable, non-exclusive limited license to use AFFTAC and any licensed supporting materials ('Licensed Materials'). Notwithstanding the foregoing, the Licensee's right to use AFFTAC is subject to the restrictions set forth in Sections 1(a)-1(e), below.

- a. The Licensee may not disassemble, decompile or otherwise reverse-engineer AFFTAC.
- b. The Licensee shall not remove or alter any copyright notices and other proprietary rights legends of Licensor or of any other entity contained in, or on, AFFTAC.
- c. The Licensee shall not misrepresent to a third party that the Licensee or any party other than Licensor:
  - (i) has title to AFFTAC; or (ii) is in any way responsible for the creation of the content of AFFTAC.
- d. Licensor shall have the right, at its sole discretion and without incurring any liability to the Licensee, to modify AFFTAC or discontinue its development, sale, or support.
- e. The Licensee shall not modify AFFTAC or combine AFFTAC with any other software.

2. **OWNERSHIP OF INTELLECTUAL PROPERTY.** Licensors own all intellectual property rights (including but not limited to all patents, trademarks, copyrights, trade secrets, and data rights) pertaining to AFFTAC, including translations, compilations, partial copies and derivative works thereof, and such rights shall remain in Licensor or its licensors. The Licensee agrees that, except for the limited license granted herein, this Agreement does not grant the Licensee any rights to patents, copyrights, trade secrets, trademarks (whether registered or unregistered), data rights or any other rights or licenses with respect to AFFTAC. AFFTAC may not be sold, leased, or sublicensed, in whole or in part, by the Licensee except with Licensor's prior written consent. The Licensee acknowledges Licensor's intellectual property rights in AFFTAC, and agrees that it will not challenge such rights in any way.

- a. **Derivative Works.** The Licensee may not create any derivative works of AFFTAC. In the event that the Licensee creates any derivative works of AFFTAC, the Licensee hereby agrees that such property shall be the sole property of Licensor. The Licensee hereby waives all 'moral rights' and any other ownership rights therein.
- b. **All Rights Reserved.** Licensor reserves all rights not expressly granted to the Licensee. AFFTAC is protected by copyright laws and international copyright treaties, as well as other intellectual property laws and treaties.

3. **NO WARRANTIES.** LICENSOR AND ITS LICENSORS HEREBY DISCLAIM ALL EXPRESS OR IMPLIED CONDITIONS, REPRESENTATIONS AND WARRANTIES, INCLUDING ANY IMPLIED

WARRANTY OF MERCHANTABILITY, FITNESS FOR A PARTICULAR PURPOSE, DATA ACCURACY, QUIET ENJOYMENT OR NON-INFRINGEMENT, EXCEPT TO THE EXTENT THAT SUCH DISCLAIMERS ARE HELD TO BE LEGALLY INVALID. THE LICENSEE AGREES TO HOLD LICENSOR AND ITS LICENSORS HARMLESS FOR ANY CLAIMS OR LIABILITY ARISING FROM THE LICENSEE'S USE OF OR RELIANCE UPON AFFTAC FOR ANY PURPOSE.

4. TERM AND TERMINATION. This Agreement shall commence on execution of the installation software.

5. ASSIGNMENT AND SUBLICENSE. The Licensee may not assign, sublicense or transfer any of its rights or obligations under this Agreement.

6. GOVERNING LAW. Disputes which cannot be settled amicably will be governed by the laws of the District of Columbia, USA. Choice of law rules of any jurisdiction and the United Nations Convention on Contracts for the International Sale of Goods will not apply. The venue for litigation will be the appropriate courts located in the District of Columbia.

7. IMPORT AND EXPORT LAWS. AFFTAC may be subject to U.S. and local export laws and may be subject to export or import regulations of other countries. The Licensee agrees to comply strictly with all such laws and regulations and acknowledges that it has the responsibility to obtain such licenses to export, re-export or import as may be required after delivery to the Licensee.

8. ENTIRE AGREEMENT; SEVERABILITY; WAIVER.

This Agreement constitutes the entire agreement between the parties with regard to the subject matter of this Agreement and supersedes all previous communications, whether oral or written, between the parties with respect to such subject matter. No waiver or modification of any of the provisions hereof shall be binding unless in writing and signed by duly authorized representatives of Licensee and Licensor. Any provision of this Agreement that is held to be invalid by a court of competent jurisdiction shall be severed from this Agreement, and the remaining provisions shall remain in full force and effect. Neither the course of conduct between the parties nor trade usage shall modify or alter this Agreement. Failure or delay by either party to enforce compliance with any term or conditions of this Agreement shall not constitute a waiver of such term or condition.

## Contents

<b>INTRODUCTION.....</b>	<b>11</b>
HISTORY .....	11
SOFTWARE COMPONENTS: GUI, COMPUTATIONAL MODULE, AND DATABASES.....	12
INSTALLATION, SYSTEM REQUIREMENTS, AND TECHNICAL ASSISTANCE .....	14
ACKNOWLEDGEMENTS.....	15
<b>THE SCOPE AND INTERACTION OF AFFTAC’S MODELS.....</b>	<b>17</b>
PHYSICS ASPECTS OF A TYPICAL SIMULATION.....	17
HEAT TRANSFER ASSUMPTIONS.....	19
PRESSURE RELIEF DEVICE MODELING.....	20
TANK FAILURE MODELING .....	22
MATERIAL EXPANSION MODELING.....	23
<b>CREATING AND RUNNING AFFTAC SIMULATIONS.....</b>	<b>25</b>
SETTING UP AN ANALYSIS.....	25
RUNNING AN ANALYSIS .....	28
VIEWING AND USING RESULTS .....	28
ADMINISTRATIVE INFORMATION.....	30
TABLE OF CAPABILITY SETUP OPTIONS .....	30
<b>THE LADINGS DATABASE .....</b>	<b>33</b>
<i>Using Default Ladings .....</i>	<i>33</i>
<i>Editing Ladings.....</i>	<i>36</i>
<b>DETAILS OF THE OVERALL THERMAL MODEL .....</b>	<b>39</b>
ESSENTIAL CONSTRUCTS .....	39
CONSTRUCTS OF RADIATIVE HEAT EXCHANGE .....	41
TEMPERATURES OF THE LADING AND THE TANK WALL.....	44
<i>Radiative Heat Exchange with the Tank Wall .....</i>	<i>44</i>
<i>Convective Heat Exchange with Tank Wall.....</i>	<i>44</i>
<i>Temperature Change in the Tank Wall Adjacent to the Vapor.....</i>	<i>45</i>
<i>Temperature Change of the Lading and Tank Wall Adjacent to the Liquid.....</i>	<i>45</i>
<b>THE LEGACY TPS MODEL AND DATABASE .....</b>	<b>47</b>
MANAGING THE LEGACY TPS MODEL DATABASE .....	47
SETTING UP A TPS IN THE LEGACY MODEL .....	48
<i>Bare.....</i>	<i>48</i>
<i>FRA Standard.....</i>	<i>50</i>
<i>Temperature-Independent Insulation.....</i>	<i>50</i>
<i>Temperature-Dependent Insulation .....</i>	<i>50</i>
<i>Steel Jacketed (2 component) Insulation .....</i>	<i>50</i>
LEGACY TPS MODEL THEORY.....	51

<i>Bare Tank or Non-Jacketed Tank with Partial Insulation Coverage</i> .....	52
<i>Partial Insulation Coverage Inside Jacket</i> .....	54
HEAT FLUX INTO LADING AND THE TANK WALL OVER VAPOR SPACE.....	57
CONDUCTANCES FOR MULTI-LAYER TPSS .....	57
<b>THE GENERALIZED TPS MODEL AND DATABASE.....</b>	<b>61</b>
USING THE GENERALIZED TPS MODEL .....	63
GENERAL TPS MODEL THEORY.....	64
<i>Area in Contact</i> .....	66
<i>Right Side's Exposed Area</i> .....	66
<i>Left Side's Exposed Area</i> .....	67
<i>Flux Computation</i> .....	67
<b>STRENGTH MODELS .....</b>	<b>69</b>
LEGACY STRENGTH MODEL.....	69
THE STRENGTH MODEL DATABASE .....	70
<i>Validated Entries in the Failure Model Database</i> .....	75
LARSON-MILLER MODEL THEORY.....	75
<i>Burst Pressure for the Larson-Miller Failure Model</i> .....	80
<i>Interactions with Other Models</i> .....	81
ULTIMATE TENSILE STRENGTH DATA.....	82
<b>PRESSURE RELIEF DEVICES AND THE PRD DATABASE.....</b>	<b>83</b>
SPECIFYING A PRD DIRECTLY DURING THE EDITING SEQUENCE .....	85
SPECIFYING A PRD USING THE PRD DATABASE.....	85
<i>Specifics for a PRV</i> .....	88
<i>Specifics for a Vent with Rupture Disk</i> .....	88
THEORY FOR MODELING FLOW THROUGH A PRD .....	88
<i>Choked Flow Model</i> .....	89
<i>Estimation of the PRD's Area using the Choked Flow Model</i> .....	90
<i>Low Speed Vapor Flow</i> .....	91
<i>Two-Phase Flow</i> .....	91
<i>Liquid Ejection in the Shell Full Condition</i> .....	93
MODELING THE OPENING AND CLOSING OF PRDS.....	95
<i>Spring-Loaded Pressure Relief Valve (PRV)</i> .....	95
<i>Frangible Disk</i> .....	97
<b>MODELS FOR INTERNAL PRESSURE, STRESS, AND STRAIN .....</b>	<b>99</b>
MODELING PRESSURE INSIDE THE TANK .....	99
MODELING TANK DEFORMATION .....	101
<i>Thermal Expansion</i> .....	101
<i>Elastic Strain</i> .....	103
<i>Plastic Strain</i> .....	103
<i>Combined Strain</i> .....	103
<b>NUMERICS.....</b>	<b>105</b>
<i>Dampening</i> .....	105



<i>Overshoot</i> .....	106
<b>TUTORIAL 1: A SIMPLE ANALYSIS</b> .....	<b>107</b>
<b>TUTORIAL 2: ADDING A LADING</b> .....	<b>113</b>
<b>BIBLIOGRAPHY</b> .....	<b>117</b>
<b>APPENDIX A: DEFAULT LADINGS</b> .....	<b>119</b>
VAPOR PRESSURE .....	119
SPECIFIC HEAT.....	120
SPECIFIC VOLUME.....	120
HEAT OF VAPORIZATION.....	121
COMPRESSIBILITY FACTOR .....	122
RATIO OF SPECIFIC HEATS .....	122
<b>APPENDIX B: CHOKED VAPOR FLOW DERIVATION AND AREA ESTIMATION METHOD</b> .....	<b>123</b>
APPLICATIONS OF THE FIRST LAW OF THERMODYNAMICS.....	123
<i>Application to Quasi-Static Process</i> .....	<i>123</i>
<i>Application to a Control Volume</i> .....	<i>126</i>
MASS FLOW FOR AN IDEAL GAS .....	131
AFFTAC'S SUB-SONIC VAPOR FLOW MODEL .....	133
<b>APPENDIX C: THERMODYNAMIC IDENTITIES FOR AN IDEAL GAS</b> .....	<b>135</b>
<b>APPENDIX D: DERIVATION OF PRD AREA ESTIMATION FORMULA</b> .....	<b>137</b>
<b>APPENDIX E: DERIVATION OF SHELL-FULL LIQUID EXPULSION PRESSURE</b> .....	<b>141</b>
<b>APPENDIX F: GOVERNING EQUATIONS FOR THE GENERALIZED TPS MODEL</b> .....	<b>145</b>
CONVECTION AND RADIATION COMMUNICATION AREAS .....	145
CONDUCTION COMMUNICATION AREAS .....	146
HEAT BALANCE EQUATIONS.....	148
<i>Area in Contact</i> .....	<i>148</i>
<i>Right Side's Exposed Area</i> .....	<i>149</i>
<i>Left Side's Exposed Area</i> .....	<i>149</i>
<i>Boundary Conditions</i> .....	<i>149</i>
ANGULAR DEPENDENCE .....	150
NONLINEAR SOLVER .....	152



# Introduction

## History

The AFFTAC computer program was originally developed by Dr. Milton Johnson at IITRI circa 1984 under funding from the United States Federal Railroad Administration to predict the effects of fire on railroad tank cars. It makes predictions of key state variables such as the lading temperature, temperature of the tank wall, pressure inside the tank, flow through the pressure relief device, and failure (if relevant) of the tank wall. In the years following its initial development, AFFTAC was expanded to provide more information and handle more types of vents, as well as be more accessible to users. Eventually in 1992, it was ported to the PC.

Beginning in 2000, AFFTAC entered a new phase of development with Dr. Scott Runnels as its custodian. The first task undertaken in this new phase was the development of a graphical user interface (GUI) to assist the user in managing data and analysis.

A third phase of development began circa 2008 with three new efforts. The first was a new, more general thermal protection system model. After that, an effort was undertaken to use AFFTAC to validate model parameters for liquid/two-phase flow through pressure relief devices. More recently, a new creep and failure model was added. Significant advances in testing and software quality assurance have been made in this third phase as well. A regression test system and database of over 50 regression tests have been established; many of those tests are carefully designed verification tests. All of the regression tests and the recent validation work are described in a separate companion document entitled *AFFTAC Verification and Validation Testing*. As of this release, that document, along with this manual, are updated and released as part of each AFFTAC formal release.

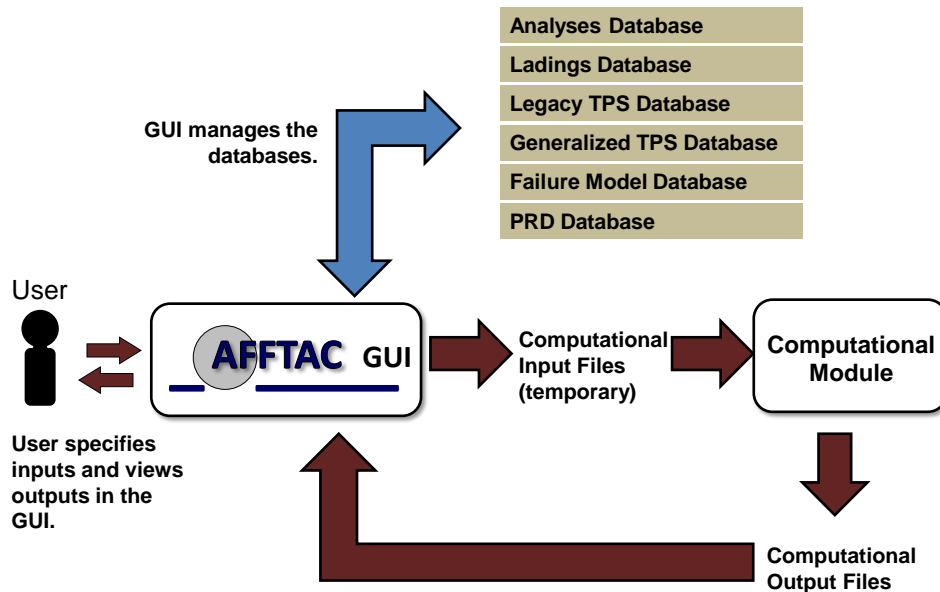


Figure 1.1: Overview of AFFTAC operations and components

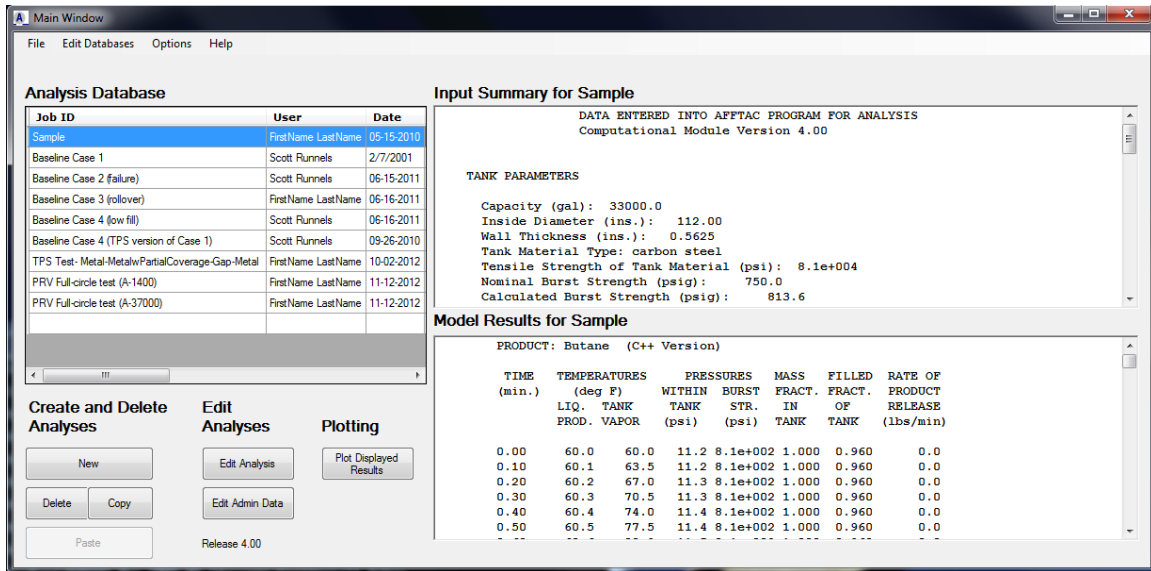
## Software Components: GUI, Computational Module, and Databases

An overview of how the AFFTAC software package components interact is shown in Figure 1.1. The user interacts with the GUI, which writes an ASCII file that the Computational Module reads. The GUI manages the execution of the Computational Module and the displaying of the results from its computations. User interaction is eased through the use of databases that store different aspects of the analysis in convenient ways.

In the GUI, you set up analyses which are grouped together and displayed in the Main Window as shown in Figure 1.2. Analyses have several inputs, some of which are straightforward numerical inputs and choices. Others, however, make reference to one of the databases that contain detailed information about specific aspects of an AFFTAC simulation. For example, in your analysis you must choose a lading by name. That lading is specified in detail in the Ladings Database, which is the database containing its thermodynamic properties.

Likewise, you may choose a thermal protection system (TPS) model by name, where that system is described in detail in one of the two TPS databases.

When you run AFFTAC, it automatically reads its database files. You do not have a choice regarding which files it reads; it reads the ones in the installation directory.



**Figure 1.2: Example of AFFTAC's Main Window where, in the left-most pane, the Analysis Database is displayed**

Although they are read automatically, they are not saved automatically. You should use caution to ensure changes you make to the database files are saved when you want to keep them.

In general, the management of the various databases is a well integrated and natural part of using AFFTAC. However, it is still helpful to know what the databases are and what they contain. The details of the various models supported by these databases are described later. For now, a brief summary is provided below.

- (1) **Analysis.db**: This file contains the inputs for the analyses you have performed and saved.
- (2) **Ladings.db**: This file contains the thermodynamic properties of several ladings, which are referred to by name in your analyses. These ladings may be edited and also new ones may be added.
- (3) **Insulations.db** and **TPS.db**: These two files contain descriptions of various thermal protection system configurations; one of these descriptions must be referred to by name in your analysis. The Insulations.db file contains the descriptions for the legacy TPS models that were implemented by Dr. Milt Johnson decades ago. These models have undergone some revision since 2000, but remain largely unchanged. They are simpler than the new general TPS model, the inputs for which are contained in TPS.db. Because it is simpler and so well tested, the legacy TPS model provides an important resource for comparison. Also it contains some capabilities not yet in the generalized TPS model, for example time-dependent behavior of insulations.
- (4) **PRV.db**: Although named as an acronym for pressure relief valve, this database contains specifications for two kinds of pressure relief devices (PRDs), those being valves and vents with frangible disks. Use of this database gives you access

- to pre-established PRV setups calibrated in an extensive validation exercise, which is discussed in the *AFFTAC Verification and Validation Testing* document. It also gives you more freedom in how you specify PRD performance. However, in setting up an analysis, you do not have to use this database; the GUI also still allows you to input values directly into the analysis to describe the pressure relief device. That method is more restrictive, but is in some ways faster, especially if you want to vary a PRD parameter in a study.
- (5) **Strength.db:** This database contains specifications for tank material failure models, particularly the Larson-Miller creep and failure model as well as ultimate tensile strength data expressed in tabular and formulaic form as a function of temperature. You may reference these inputs by name when choosing to use the Strength Database. However, you do not have to use this database. The GUI also still allows you to specify tank material names directly as part of the analysis. Doing so calls upon legacy failure models that are hard-coded inside the Computational Module. All of this will be explained in greater detail in later chapters.
- (6) **Regression.db:** This database contains the specifications for the regression tests, which are used to help maintain AFFTAC's quality. You need not worry about the regression tests. However, some of the regression tests may prove interesting and are therefore shipped with the release.

## **Installation, System Requirements, and Technical Assistance**

AFFTAC 4.00 is designed for systems running MS-Windows XP, Vista, and 7 operating systems. It should be compatible with Windows 8 but it has not yet been tested on that operating system.

The AFFTAC 4.00 graphical user interface was developed in Microsoft Visual Studio 2008, version 9.0.30729.1 SP, Microsoft .NET Framework Version 3.5 SP1. Assistance can be obtained from:

Dr. Scott R. Runnels  
Scott Runnels Consulting  
630 Camino Encantado  
Los Alamos, NM 87544  
505-695-9241  
SRunnels@srconsult.com  
www.srconsult.com

## **Acknowledgements**

Special thanks go to John Sbragia whose careful testing of AFFTAC has revealed multiple deficiencies that, once fixed, improved the reliability and robustness of the code. Also, thanks go to Todd Treichel for his skillful management of the AFFTAC project.

The original development of AFFTAC for Windows and the initial three databases were funded by the RPI-AAR Railroad Tank Car Safety Research & Test Project and was performed under Southwest Research Institute project number 18-6965. Development past 2000 was continued by Scott Runnels Consulting under the same funding source.

Thanks go to Tom Dalrymple for his advice during the designing of the graphical user interface and suggesting the use of databases in the original AFFTAC for Windows, as well as the overall project management during 2000-2002. Thanks also to those who tested the earlier versions, including Bill Bitting, Al Henzi, Thomas Petrunich, and Andy Rohrich.

The late Dr. Milton Johnson's contributions to the earlier versions of this manual are gratefully acknowledged. Much of his contributions remain in this revision, in particular the "Aside" comments and Appendix A. Likewise, Mr. Joe Cardinal at Southwest Research Institute also provided helpful input on earlier versions of this manual.





# **The Scope and Interaction of AFFTAC's Models**

AFFTAC is a simulator combining the effects of several physical phenomena that, together, comprise a complex nonlinear system. In this chapter, the scope and interaction of those multiple physics models are described.

AFFTAC is best thought of as a transient, quasi-two-dimensional model. The heat transfer through the tank wall is one-dimensional. However, some models in AFFTAC support variation in the insulation properties as a function of angle around the tank. Conversely, the liquid and vapor are at a uniform temperature at any point in time and in that sense AFFTAC is a zero-dimensional model. Yet, the tank may be modeled as rolled over, meaning the location of the liquid surface and its interaction with the location of the pressure relief device is accommodated. In short, separate assumptions regarding dimensionality are made. The individual models are then combined in a consistent way.

## **Physics Aspects of a Typical Simulation**

Heat is added to the system on the outside of the tank car through heat exchange with the fire. This heat is transported to the inside of the tank through the tank wall and thermal protection system, eventually reaching the lading. The heat is transported to the lading by contact with the wall and by radiation to and from its interior surfaces. The lading responds by heating up; the liquid thermally expands and evaporates causing the vapor pressure to increase. If the tank is in a shell full condition, i.e., when it is completely full of liquid, the liquid's thermal expansion results in an increase in pressure inside the tank. When vapor is present, the pressure also increases but is due instead to the vapor

pressure. Either way, when the pressure inside the tank reaches a sufficient level, the tank's pressure relief device opens and allows lading to be released. A supporting model for the pressure relief device is provided as part of the AFFTAC simulator. Flow of vapor, liquid, or a mixture, depending on the rollover condition and the amount of liquid present, is accommodated by these models.

The simulation is carried out starting at time = 0 and, under normal circumstances, ending at a user-specified time. However, as the simulation proceeds, the lading could eventually be completely expelled, causing the simulation to end earlier. Another possibility for early termination occurs when the pressure relief device is not able to accommodate the expulsion of lading quickly enough. In that case, the pressure inside the tank car builds up to be high enough to rupture the tank.

In addition to the models for the pressure relief device and the flow through it, AFFTAC has other supporting models that play key roles in the simulation. There are models for how the insulating layers of the tank wall change with time and temperature. There are also auxiliary models, including a stress model that computes the strain in the tank wall and subsequent change in the tank volume. Finally, there is a temperature-dependent and temperature- and pressure- dependent failure model for the tank wall's structural layer.

An overview of the AFFTAC simulation is shown in Figure 2.1 and a summary of the models is shown in Figure 2.2. As shown in Figure 2.1, each of the models are linked and executed in a time-marching loop that proceeds through the simulation in small time increments. The equations describing these models are all linked and, in principle, must be solved simultaneously at each point in time. In practice, however, they are separated and solved in an alternating fashion where some values from the previous time step are used to update other values. Then, those newly updated values are used to update the first set of values. In reality, there are more than just two groups like this. At multiple steps in the calculations, a mixture of old values and newly updated values are used to propagate the calculation forward. At the end of each time step, all variables will have been updated. This method is often referred to as "nonlinear lagging" or "operator splitting". **This aspect of the calculations is very important to understand** when delving into the theoretical descriptions in the chapters that follow. In all of the chapters, you will notice that some values, which you know to be transient and part of the overall solution, will be assumed known for that part of the theory. By considering all parts of the theory in the same context, you will see how all values are eventually updated.

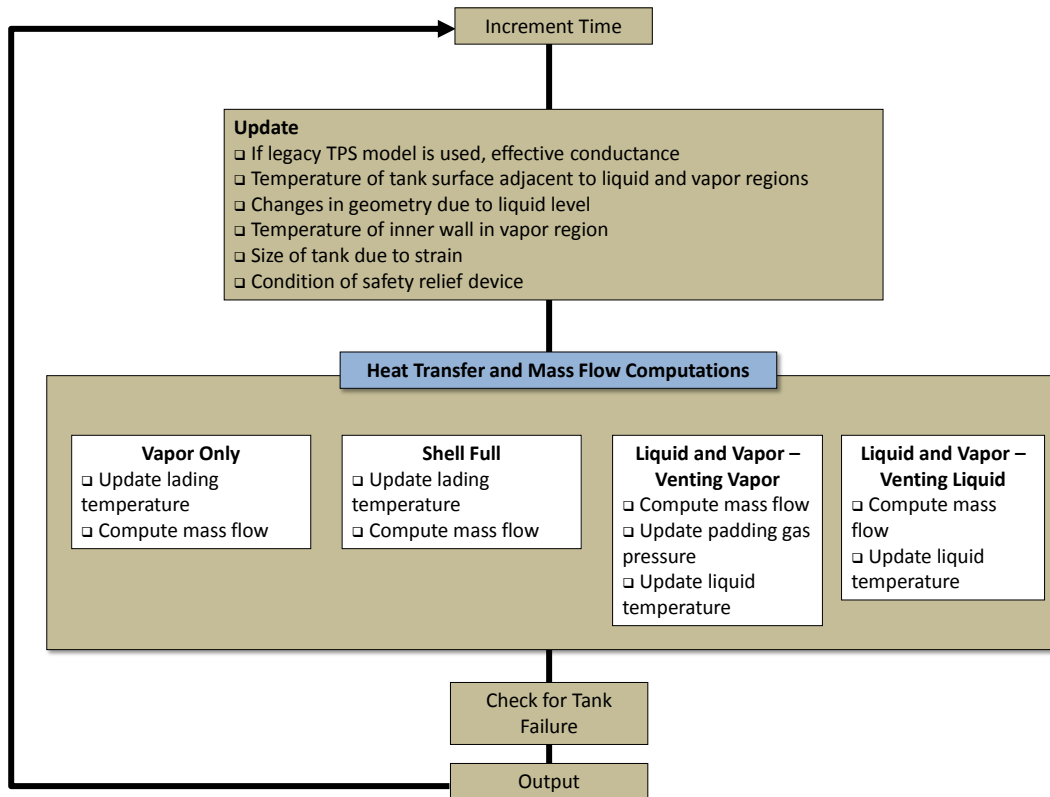


Figure 2.1: Conceptual flow chart of the AFFTAC model computations

## Heat Transfer Assumptions

Heat transfer is a primary driver in AFFTAC and so, in a sense, the heat transfer model is the core, driving model. It has multiple aspects that are addressed in multiple places in this manual. Here, some of the key overarching assumptions and approaches are described.

First, the fire is modeled as a fixed temperature surface, some arbitrary distance from the tank, held at a fixed temperature during the simulation, e.g., 1,500 deg-F. In a “pool fire” simulation, this surface surrounds the tank entirely. The lading inside the tank is assumed to be well mixed and at a uniform temperature. The liquid and vapor phases are assumed to be in thermodynamic equilibrium with each other and thus are at the same temperature.

Second, the tank car’s innermost surface is considered to have two different temperature regions, one for the segment of the tank adjacent to the liquid lading and one for the segment adjacent to the vapor. This division is established because it is assumed the liquid has such a great thermal mass and is in intimate contact with the tank wall’s innermost surface. Thus the tank wall in contact with the liquid is assumed to be at the same temperature as the lading. In contrast, the tank wall adjacent to the vapor does not have intimate contact, nor does the vapor have any appreciable thermal mass. Therefore,

the tank wall's innermost surface temperature can be very different from the vapor temperature. In fact, the temperature of the tank wall adjacent to the vapor is among the most important state variables, for it is that temperature that will impact the strength and ultimate life of the tank wall.

Third, a variety of models can be chosen for computing the heat transfer between the tank's innermost surface, outermost surface, and the fire. These are the thermal protection system or "TPS" models. When the TPS model is invoked at any time during the simulation, it is given the current temperature of the interior surface of the tank wall and the temperature of the flame. Using those two boundary conditions, it computes the temperature of the tank's outermost surface and the heat flux through the TPS. The TPS model is invoked at least twice, once for the segment of the tank wall adjacent to the liquid, and again for that adjacent to the vapor. In simulations where the TPS is specified to have angular dependence, it is invoked multiple times, one for each angular segment you specify.

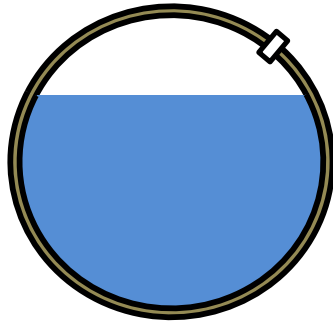
Fourth, the heat transferred into the lading is computed in two ways. One way is the heat conducted through the tank wall adjacent to the liquid. That heat flux is provided by the TPS model, as mentioned above. Another aspect is the heat radiated and convected from the inner surface of the tank wall into the lading. The radiation occurs between the tank's innermost surface adjacent to the vapor and the top surface of the liquid while the convection is between the tank's innermost surface and the vapor. Either way, whether exchanged with the vapor or liquid phase, the heat is considered to be exchanged with the lading as a whole, which again is at one uniform temperature at each point in time. Other heat-related mechanisms include thermodynamic work associated with discharging lading through the pressure relief device and the associated heat of vaporization.


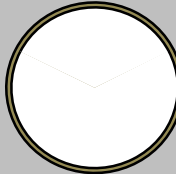
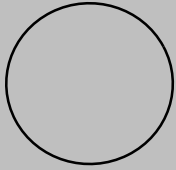

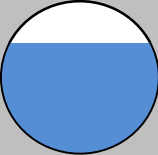
Fifth, a heat balance on the innermost tank wall is used to determine the temperature of the tank wall for the portion of the tank over the vapor region.

## **Pressure Relief Device Modeling**

AFFTAC accommodates pressure relief devices (PRDs) that, under appropriate conditions, allow lading to be discharged. Depending on the amount of liquid lading present and the angle of tank rollover, the discharge may be purely liquid, purely vapor, or a mix. The details of how the pressure relief device's opening and closing action are modeled as well as the fluid flow through it are described in a separate chapter.

One important note to make here, however, is that you have two ways of entering specifications for the PRD. One is to specify them directly as numerical entries as part of an analysis. Another way is to choose from a list of PRDs that are contained in a separate database, which you can also edit.



	<p><b>Lading</b></p> <p>The vapor and liquid are at the same uniform temperature. Properties are taken from the Ladings Database.</p>
	<p><b>Thermal Protection System</b></p> <p>Models the conduction, radiation, convection inside the wall, insulation, jacket. Multiple temperatures for different parts of the wall are computed. There is a legacy and a new general TPS model.</p>
	<p><b>Tank Wall</b></p> <p>While also modeled in the TPS, separate strength models determine how much it expands due to pressure and heating. There are also multiple models that can be used to determine strength and failure.</p>
	<p><b>Relief Device</b></p> <p>Lading in various states may be discharged through the relief device. Multiple flow models are used for different discharge scenarios.</p>
	<p><b>Interior Heat Transfer</b></p> <p>Heat is exchanged between the lading surface and the interior tank wall over the vapor space. It is also conducted through the tank wall to the liquid.</p>

**Figure 2.2: Overview of AFFTAC’s primary models**

## **Tank Failure Modeling**

The strength of the tank is a very important model in AFFTAC. It provides a determination regarding whether the tank will burst during the simulation.

There is more than one strength model from which to choose in AFFTAC. The legacy model only requires the current, highest temperature of the tank wall. From that temperature and knowledge of the material from which the tank wall is constructed, the legacy model computes a current value for the tank's ultimate tensile strength. That value is compared to the stress required to contain the pressure inside the tank. If it is insufficient, the tank bursts.

In addition to the legacy model, AFFTAC now also offers a Larson-Miller creep and failure model that has been validated very successfully against recently acquired data. Instead of only using the current temperature to determine the tank material's strength, the Larson-Miller model computes the damage accumulated at the microscopic level as the tank material is heated and stretched. As this accumulated damage is computed, it is used to compute the amount of "life", so to speak, of the tank wall that has been depleted. Once all of the life has been depleted, the tank is said to have burst.

The tank strength model interacts with AFFTAC's thermal model in fairly intricate ways. If the legacy TPS model is used, then the highest temperature experienced by the tank wall is that adjacent to the vapor and that temperature is used as input into relatively straightforward algebraic equations to compute an ultimate tensile strength. In contrast to this, AFFTAC's new Larson-Miller model operates differently because it depends on the history of each point around the tank. In the Larson-Miller model, 180 points are established around the tank, at one degree intervals, and those "tracking points" are used to track the temperature-pressure-life-remaining metrics at their respective locations. Thus, when the legacy TPS model is used, the Larson-Miller tracking points are fed either the tank wall temperature adjacent to the liquid or the vapor, depending on their location. As the liquid level rises or falls, the temperature fed into each Larson-Miller tracking point may change.

If the general TPS model is invoked with significant angular dependence to the insulation, the interactions are different still. For the legacy strength model, a search must be made through the TPS segments for the highest temperature, and that temperature is fed to the algebraic equations mentioned above. But for the Larson-Miller model, each of its 180 tracking points uses the temperatures in their respective TPS segments.

Thus, one can imagine a variety of complex scenarios arising depending on the type of simulation carried out. For example, consider a setup using the general TPS model with angular dependence such that significant defects in the insulation exist around the liquid level. As the liquid expands or lading is discharged, there may be significant changes into the input of the strength model for those points. This type of complexity testifies to

the need for a computer model to understand it and also to the need for careful use and understanding of the model.

## **Material Expansion Modeling**

Both the liquid lading and the tank itself can expand during a simulation. The liquid lading may expand due to heating. The tank may expand due to heating and also due to stress. The interaction of these expansions is very important when the tank is completely full of liquid, i.e., the “shell full” condition. In that case, further expansion of the liquid can lead to tremendous stresses in the tank wall that can result in failure. Thus there is an important interaction between the models computing the expansion of the liquid, its possible release through the PRD, the expansion of the tank wall due to heat and stress, and the tank failure model.





# Creating and Running AFFTAC Simulations

## Setting up an Analysis

Each analysis in AFFTAC is stored in AFFTAC's Analysis Database. The Analysis Database is central to AFFTAC and is displayed in AFFTAC's Main Window, as in Figure 3.1. To create a new analysis from scratch using default values, click on the **New** button in the Main Window. To create a new analysis that is based on an existing one, highlight the existing one, click **Copy** and then click **Paste**. When you do, a new analysis will be created that is identical to the one you copied except for its title and its administration information, which you will eventually specify. You may edit that analysis by highlighting it and clicking **Edit Analysis**.

It is valuable to understand that each analysis you create in the Analysis Database will contain two kinds of entries:

1. **Numerical and Logical Data** – These are straightforward entries having to do with direct data about the simulation. For example, the length of the simulation is a numerical entry that is part of an analysis.
2. **References to the Other Database Entries** – These are names of components, such as ladings, thermal protection systems, and pressure relief devices (PRDs), that contribute to the simulation setup. An example is the lading name. If you select “Butane” for the lading, that name is used to pull thermodynamic properties from the Ladings Database under the name “Butane” and provide them to the Computational Module for the simulation. Thus the single entry “Butane” in the analysis specification contains a great deal of information, including multiple

tables of data. Other examples include the TPS setup, the tank material, and can also include the pressure relief device.

The process of setting up a simulation is divided into four steps which are conducted using four sequential windows: **Edit Analysis Conditions**, **Edit Tank Car Properties**, **Select TPS Model**, and **Setup Lading**. These four windows are shown in Figure 3.2.

### **Edit Analysis Conditions Window**

In this window, you may set basic analysis conditions, including the flame type and the length of the simulation. From this window you can launch a sub-window that allows you to set the time step and the frequency of printouts.

### **Edit Tank Car Properties Window**

In this window, you set up the properties of the tank car, including the material from which the tank is made and the safety relief device properties. Both the material setup and the PRD setup may be handled in two ways. You may choose to use the legacy models and setup methods by making choices directly in this window. Or you may choose to use the PRD Database with the click of the appropriate button. These new databases will be discussed at length in subsequent chapters.

### **Select TPS Window**

In this window, you choose the type of thermal protection system on the tank car by selecting one of the systems that is displayed. AFFTAC has two completely separate TPS models, the legacy model and a new, more general model. The specification for these two models are in separate databases, each of which may be managed using windows launched from this window.

### **Setup Lading Window**

In this window, you select the lading from a list of ladings stored in the Ladings Database. You may edit this database to create new ladings by clicking the **Manage Ladings Database** button. Also in this window, you specify the fraction of tank filled by the lading, its initial temperature, and the padding gas, if present.

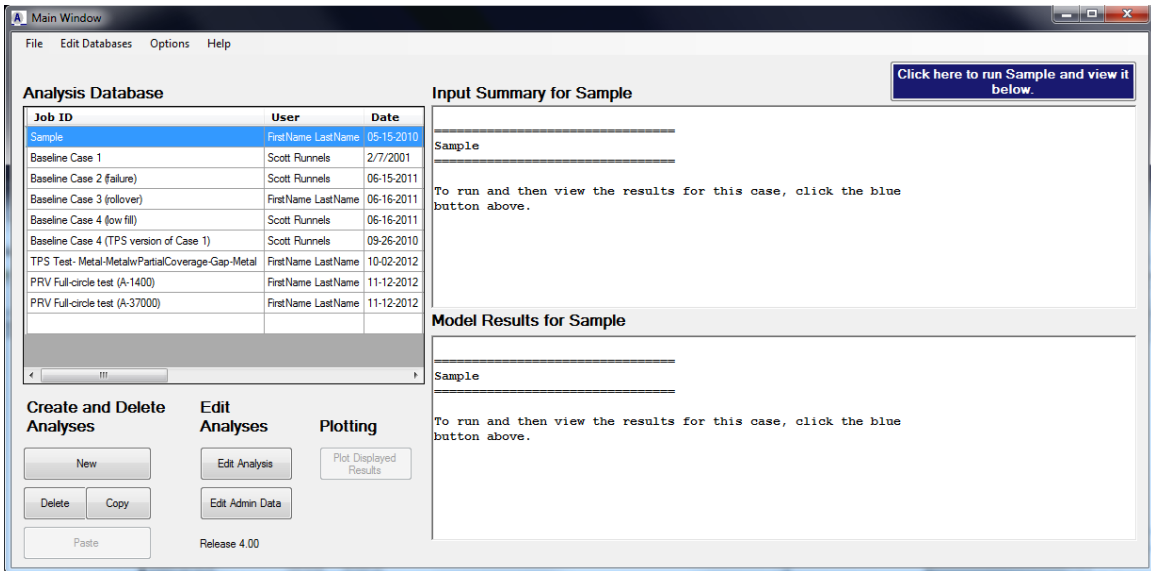


Figure 3.1: AFFTAC's Main Window in which the Analysis Database is displayed in the left-most pane

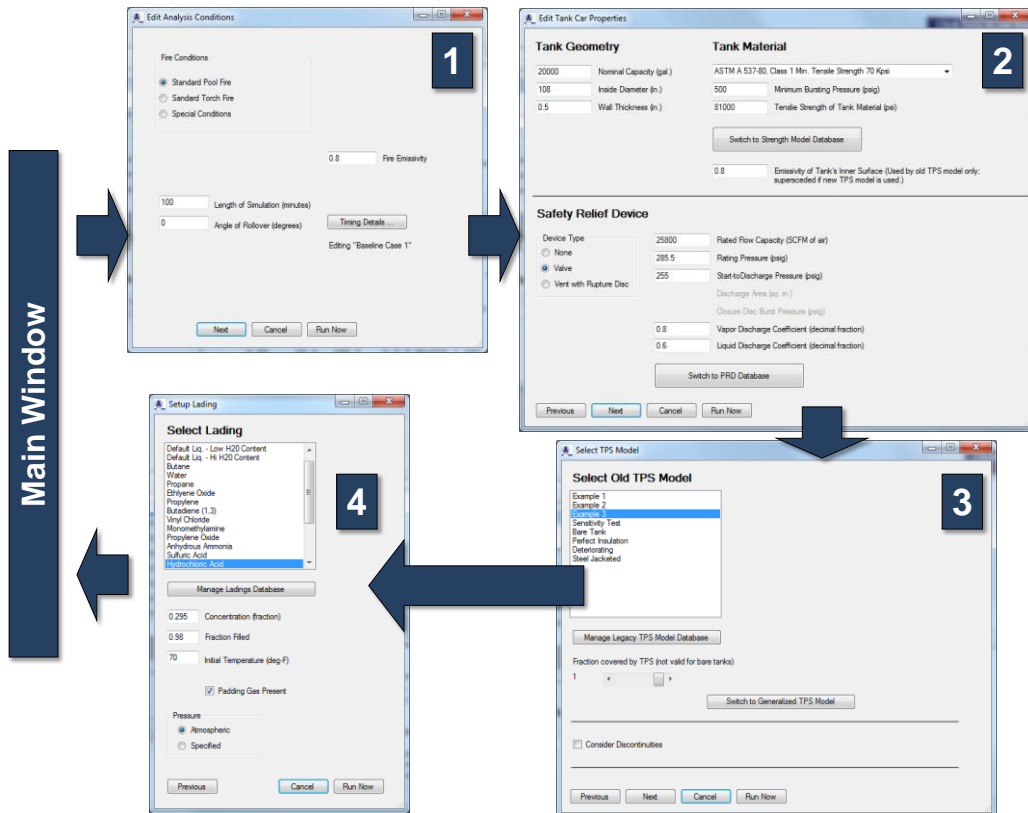


Figure 3.2: Illustration of the four-step editing process for setting up AFFTAC simulations

## Running an Analysis

There are two ways to initiate the execution of an analysis. One is to highlight the analysis in the Analysis Database of the Main Window and then click the dark blue panel in the upper right portion of the Main Window. The other is to click the **Run Now** button in any of the four editing windows. In this latter option, the changes you have made during the editing sequence are automatically made part of the current highlighted analysis. However, those changes are not saved permanently to the Analysis Database until you choose the menu option **File-Save Analyses Database**.

The analysis is carried out by AFFTAC's Computational Module, which is a stand-alone executable invoked by the GUI. When you request the simulation to be run, the GUI writes the necessary input files for the Computational Module. It then runs the Computational Module, which executes in an DOS window that opens to display the simulation's progress. Once the simulation is completed, the GUI reads the Computational Module's output files and displays them in the two panels on the right-hand-side of the Main Window.

## Viewing and Using Results

After a simulation is completed, the results are displayed on the right-hand-side of the Main Window. The top right panel of the Main Window displays a partial summary of your inputs for the problem. The panel below it is some of the key numerical output values. Typical results are shown in Figure 3.3. These results may be visualized by clicking the **Plot Displayed Results** button in the Main Window which displays a window like that shown in Figure 3.4. The plot window has several controls that allow some modification to the displayed plots. Clicking on a plot copies it to the Microsoft clipboard from which it can be pasted into a number of other applications.

To print the results and input summary, in the Main Window, select the menu option **File-Print Currently Shown Results**. Also, you may copy the contents of the displayed textual output to the Microsoft clipboard by painting the text displayed in the Main Window and typing Ctrl-C. These contents may then be pasted into a variety of Microsoft Windows applications such as Word or PowerPoint.

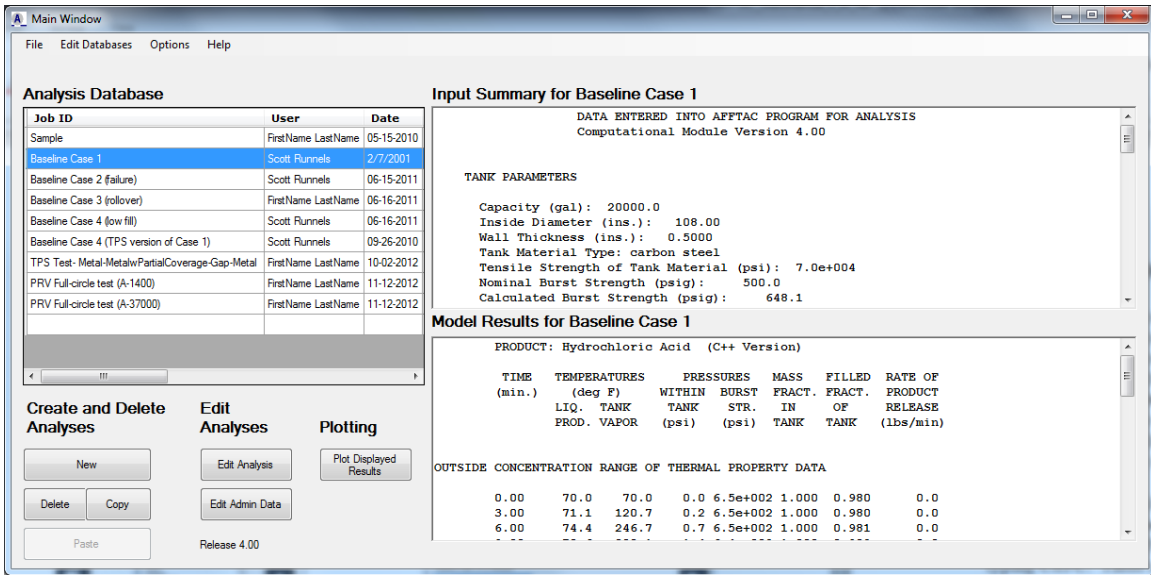


Figure 3.3: AFFTAC's Main Window, displaying the results of an analysis on the right

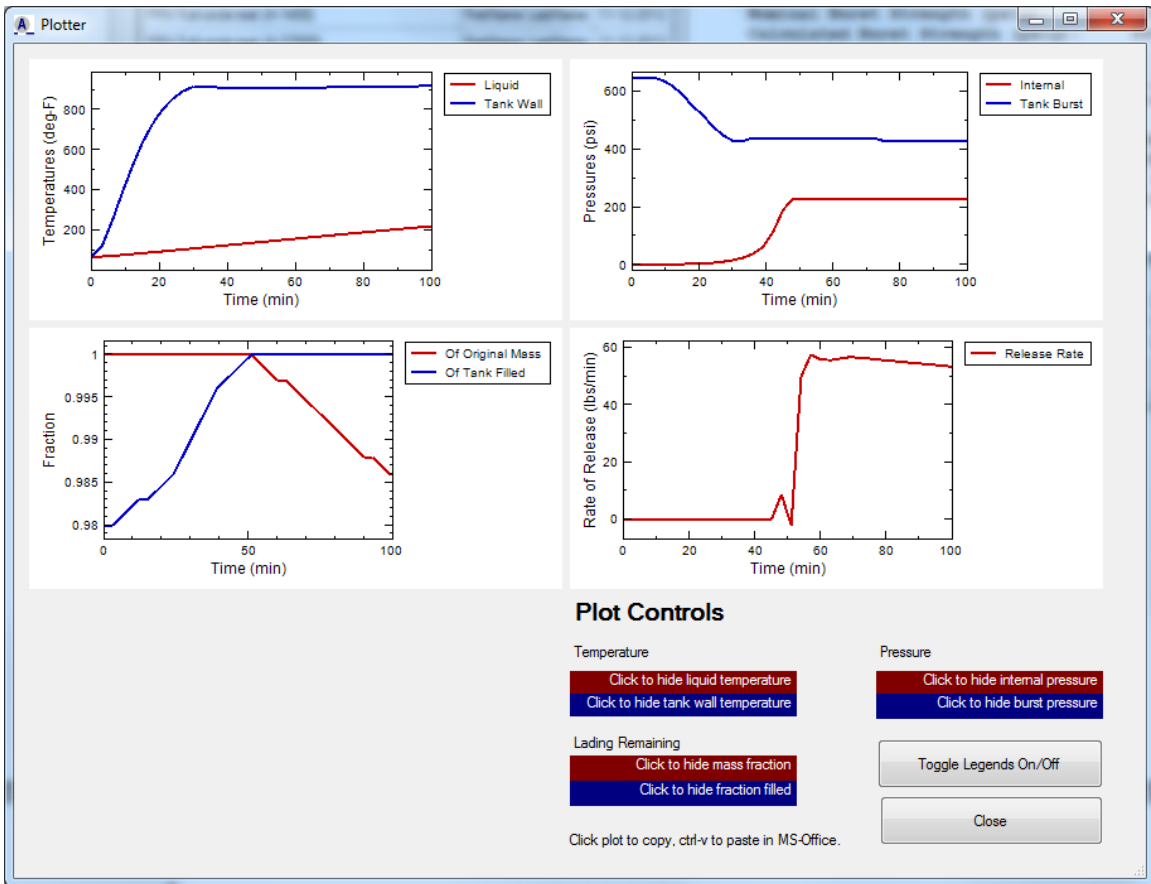
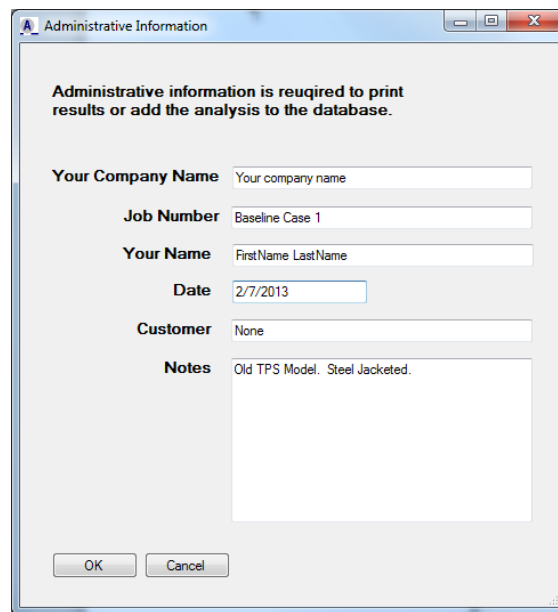


Figure 3.4: AFFTAC's plotting window, graphically displaying the results of an analysis

## Administrative Information

Administrative information is required in order to print the results of an analysis or to save it in the database. To add the administrative information, highlight the analysis and click the **Edit Admin Data** button in the Main Window. The window used for entering that administrative information is shown in Figure 3.5. Your name and company may be more permanently set by selecting the menu option **Options-User Information** in the Main Window. The rest of the user-specific information you add in the window is shown in Figure 3.5.



Administrative Information

Administrative information is required to print results or add the analysis to the database.

Your Company Name: Your company name

Job Number: Baseline Case 1

Your Name: FirstName LastName

Date: 2/7/2013

Customer: None

Notes: Old TPS Model. Steel Jacketed.

OK Cancel

**Figure 3.5: Administrative information window that must be completed for a simulation to be printed or added to the Analysis Database**

## Table of Capability Setup Options

AFFTAC is approximately forty years old and has been enhanced many times during its history. As with any code of that age and type, efforts are made to maintain legacy capabilities while adding enhancements. As a result of that, AFFTAC has a variety of input options and style of input methods. In many places in this manual, you will find that you have the option of using a legacy model or a new model. And you will find that you have the option of inputting values in different ways. To help avoid confusion, the table on the next page is provided to clarify these aspects.

As the table indicates, some aspects of the simulation may only be entered directly into the analysis by specifying values. Others have multiple options. For example, if the legacy PRD setup method is used, the values are entered directly in the analysis. If you choose to use the new PRD setup method, you will instead access the PRD Database and enter the values there.

<b>Table of Capability Setup Options</b>		
	Specified directly by inputting values in the analysis	Specified by naming an entry in one of the databases (not the Analysis Database, to which everything is connected) and then inputting the values in that database
<b>Length of Simulation</b>	Yes	No
<b>Tank Geometry</b>	Yes	No
<b>Tank Failure</b>	Yes for legacy	Yes for Larson-Miller
<b>Tank Wall Emissivity</b>	Yes for legacy	Yes for general TPS
<b>Pressure Relief Device</b>	Yes for legacy	Yes for PRD database
<b>Thermal Protection System</b>	No	Yes, two different databases, one for legacy one for general model
<b>Other Heat Transfer Mechanisms</b>	Yes	No
<b>Lading Properties</b>	No	Yes
<b>Lading Initial Conditions</b>	Yes	No
<b>Padding Gas</b>	Yes	No

**Table 3.1:** This table provides an overview of what methods may be used for inputting values for different models in AFFTAC. Because there is a mix of legacy and new modeling capability, input options vary.





# The Ladings Database

As shown in the previous chapter's Table 3.1, lading properties are described by entering values into the Ladings Database. Then, when setting up an analysis, the lading is referred to by its name. When the simulation is run, AFFTAC extracts the appropriate thermodynamic data from the database and writes it to a file for the Computational Module to read. The Ladings Database may be edited by choosing the **Edit Databases-Ladings** menu option in the Main Window, or by clicking the **Manage Ladings Database** button in the Setup Lading window, which is displayed during the editing of an analysis.

When you choose to manage the Ladings Database, a window like that shown in Figure 4.1 is displayed. In this window, ladings can be edited by highlighting them and clicking the **Edit** button. New ladings can be created by either highlighting an existing one and clicking **Copy** then **Paste**, which creates a copy of the highlighted lading, or by clicking **New**, which creates a new lading from scratch. You can exit the window with or without saving your changes to the database file. If you choose not to save them to the file, they will still be available for the current AFFTAC session and AFFTAC will ask you if you want to save them when you try to exit the session.

## Using Default Ladings

The first three entries in the database are default ladings. These cannot be used for an analysis but instead serve as a template from which new ladings can be created when not all of the thermodynamic properties are known. The process for creating a new lading from a default lading is similar to creating one from any other existing lading. Simply highlight the default lading of interest, click **Copy** and then click **Paste**. However, when pasting from a default lading, the dialog box shown in Figure 4.2 appears. This window asks for the name of the new lading, the molecular weight, and the density at ambient.

The creation of the new lading cannot proceed without these values. The use of default ladings is not recommended. If they are used, you should understand how their thermodynamic properties were chosen, as described in Appendix A.

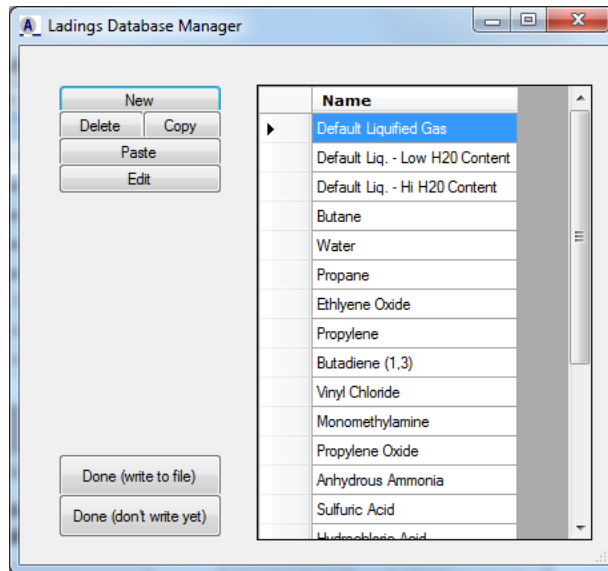


Figure 4.1: The window used for managing the Ladings Database

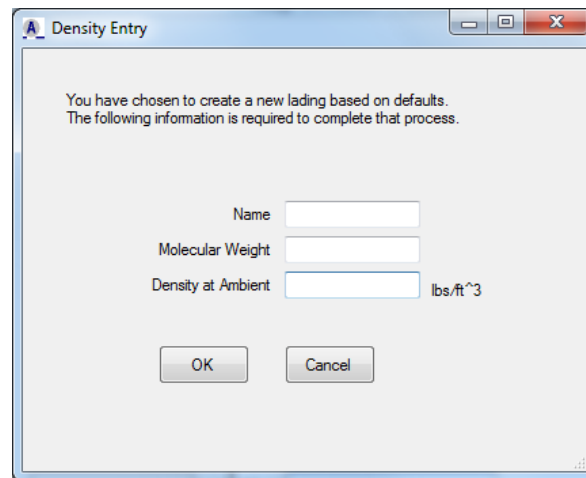


Figure 4.2: Dialogue box asking for additional information when creating a new lading from a default lading

**Edit Lading Properties**

Name:

Type of Lading:  Solution  Substance

Molecular Weight:

Lading has a critical temperature

Emissivity:

Depends on Temp:

- Specific Heat (BTU/lb F)
- Specific Volume (ft<sup>3</sup>/lb)
- Heat of Vaporization (BTU/lb)
- Vapor Pressure (psia)
- Compressibility Factor
- Cp/Cv

**Edit Lading Properties**

Name:

Type of Lading:  Solution  Substance

Molecular Weight:  Solute  Solvent

Lading has a critical temperature

Emissivity:

Depends on Temp	Value at Low Concentration	Low Concentration	Value at High Concentration	High Concentration	
<input checked="" type="checkbox"/>	<input type="button" value="Edit Table"/>	<input type="text" value="5"/>	<input type="button" value="Edit Table"/>	<input type="text" value="0.32"/>	Specific Heat (BTU/lb F)
<input checked="" type="checkbox"/>	<input type="button" value="Edit Table"/>	<input type="text" value="5"/>	<input type="button" value="Edit Table"/>	<input type="text" value="0.32"/>	Specific Volume (ft <sup>3</sup> /lb)
<input checked="" type="checkbox"/>	<input type="button" value="Edit Table"/>	<input type="text" value="5"/>	<input type="button" value="Edit Table"/>	<input type="text" value="0.32"/>	Heat of Vaporization (BTU/lb)
<input checked="" type="checkbox"/>	<input type="button" value="Edit Table"/>	<input type="text" value="0.32"/>	<input type="button" value="Edit Table"/>	<input type="text" value="0.38"/>	Vapor Pressure – Solute (psia)
<input checked="" type="checkbox"/>	<input type="button" value="Edit Table"/>	<input type="text" value="0.32"/>	<input type="button" value="Edit Table"/>	<input type="text" value="0.38"/>	Vapor Pressure – Solvent (psia)
<input checked="" type="checkbox"/>	<input type="button" value="Edit Table"/>				Compressibility Factor – Solute
<input checked="" type="checkbox"/>	<input type="button" value="Edit Table"/>				Compressibility Factor – Solvent
<input checked="" type="checkbox"/>	<input type="button" value="Edit Table"/>				Cp/Cv – Solute
<input checked="" type="checkbox"/>	<input type="button" value="Edit Table"/>				Cp/Cv – Solvent

**Figure 4.3: Example Edit Lading Properties window where the thermodynamics properties of the lading are entered for a substance (top) or solution (bottom)**

## Editing Ladings

When you double-click a lading or highlight it and then click the **Edit** button, the Edit Lading window like those shown in Figure 4.3 appears. This multi-faceted window allows for the input of the thermodynamic properties of the lading.

The Edit Lading Properties window changes its appearance depending upon the options chosen. The most significant change is when you select the substance or solution option<sup>1</sup>. In the upper window of Figure 4.3, the **Substance** option is chosen. In this mode, you need only enter thermodynamic properties for the substance. In the lower part of Figure 4.3, is the same window with the **Solution** option chosen, where you are required to enter some of the thermodynamic properties for the solvent and solute at high and low concentrations. To the extent possible, those concentrations should bracket the solution concentration used in the analysis. Inaccuracies can result from the bracketing being too wide.

You may enter any of the lading's thermodynamic properties as a constant or as a function of temperature. If they are a constant, the values are simply typed into the associated entry box. AFFTAC converts that constant value into a table of two rows, each with the same value you entered. To enter properties that vary as a function of temperature, you must enter the data by first clicking the appropriate **Edit Table** button that appears next to the property name.

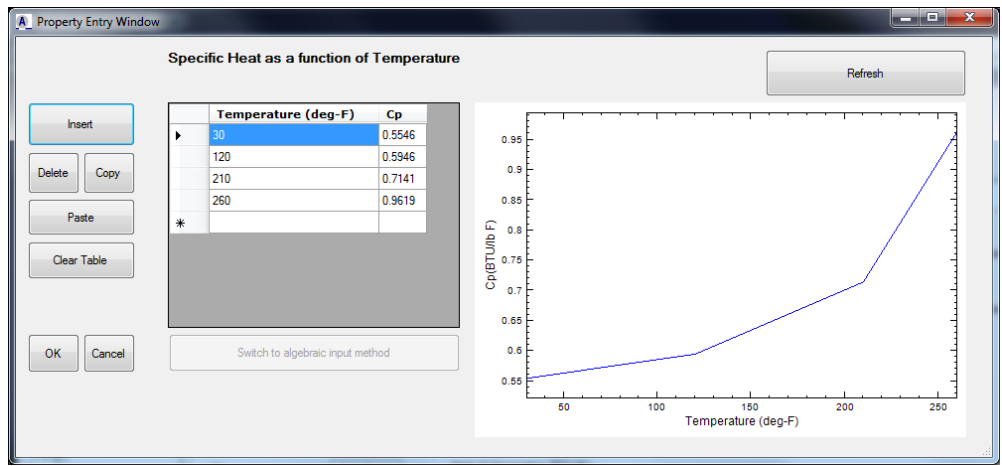
Shown in Figure 4.4 is the **Property Entry** window for one of the lading's specific heat. The table may be edited by entering the values as a function of temperature. The recommended method is to clear the table first using the **Clear Table** button, enter the temperature values, using the **ENTER** key to create new rows as you go, and then to enter the property values, using the **ENTER** key to move down the rows.

Clicking **Refresh** will update the plot using the values you enter into the table. By clicking on the plot itself, the plot is copied to the Microsoft clipboard and can then be pasted into a variety of Microsoft Windows applications such as PowerPoint and Word.

It is important to remember that the AFFTAC Computational Module allows only 8 data points for each property except for vapor pressure, which may have between 3 and 15 data points. Also, there must be an odd number of data points entered for vapor pressure.

---

<sup>1</sup> A *substance* is matter that is comprised of only one type of molecule. A *solution* is a mixture of two or more substances that is homogenous at the molecular level. AFFTAC allows two-component solutions.



**Figure 4.4: Window for editing tabular input of thermodynamic properties**



# Details of the Overall Thermal Model

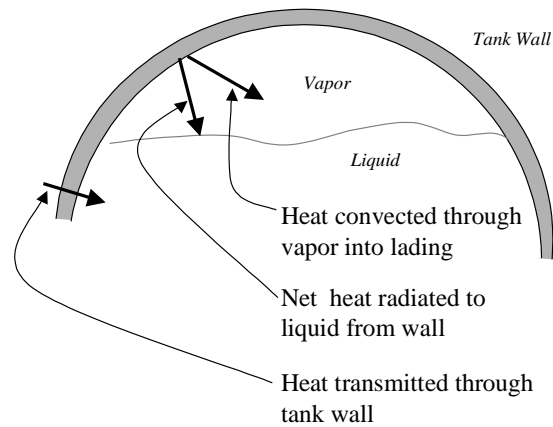
## Essential Constructs

Below are the essential constructs of AFFTAC's thermal transport model. You should be cognizant of these when seeking to understand the theory behind the Computational Module:

1. The liquid and vapor phases of the lading are assumed to be at the same temperature,  $T_{lading}$ , which changes with time but is constant in space. The part of the tank wall adjacent to the liquid phase is also assumed to be at that same temperature.
2. The innermost surface of the tank wall adjacent to the vapor is at a temperature that may be different from the lading temperature. Its temperature is denoted as  $T_{wall-vapor}$ .
3. As shown in Figure 5.1, heat is transferred to the lading by three mechanisms:
  - (i) Conduction to the liquid through the TPS and tank wall,
  - (ii) Convection to the vapor by contact with the inner tank wall, and
  - (iii) Radiation to the liquid surface from the inner tank wall that is adjacent to the vapor.
4. The tank is heated through radiative exchange with the flame, only. Convection with the surrounding air is not included in the model.

Computing 4 and 3 (i) is the responsibility of the TPS model, of which there are two kinds in AFFTAC. They are each discussed in their own, subsequent, chapters. Those models take as a given the innermost surface temperature and the flame temperature. Using those two boundary conditions, they compute the heat flux conducted through the innermost surface. The process of taking the interior temperature as a known value in the TPS computations is a technique known as “nonlinear lagging” or sometimes “operator splitting” and is discussed in the chapter entitled “The Scope and Interaction of AFFTAC’s Models.” The details of the computations in 3 (i) are discussed in the separate chapters on the TPS models.

The details of computing the fluxes in 3 (ii) and 3(iii) are discussed in this chapter. Computing these fluxes also requires knowledge of the temperature of the innermost surface of the tank wall adjacent to the vapor. That key variable,  $T_{wall-vapor}$ , is determined using an equation that balances the net flux into the wall from the outside with the net flux leaving the wall on the inside through convection and radiation to the lading. That heat balance is shown graphically in Figure 5.2. As with 3 (i), this method of computation, which splits governing equations into parts and solves them piecewise, is known as “nonlinear lagging” or “operator splitting” and is discussed in the chapter entitled, “The Scope and Interaction of AFFTAC’s Models.”



**Figure 5.1: Heat flowing into the vapor and liquid phases of the lading**



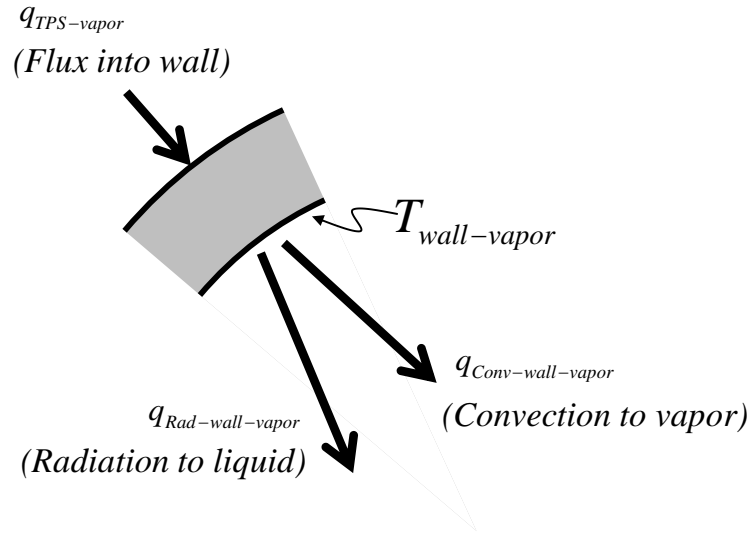


Figure 5.2: Heat balance on the tank wall adjacent to the vapor

## Constructs of Radiative Heat Exchange

As discussed in the previous section, radiative heat exchange occurs between the tank car's outermost surface and the flame as well as the tank's innermost surface and the lading's liquid surface. AFFTAC models all radiative exchange using a classical law [18], and represents every surface as being gray with a constant value of emissivity.

For radiative exchange between two surfaces, the emissive powers of the two surfaces are

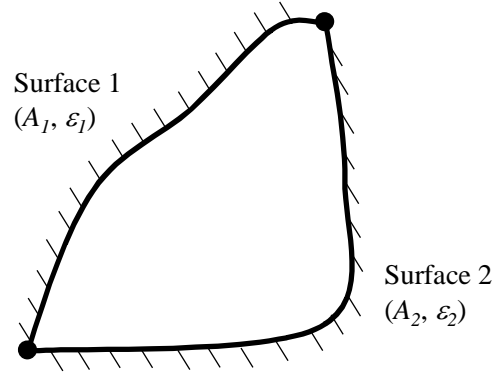
$$\begin{aligned} E_1 &= \varepsilon_1 \sigma T_1^4 \\ E_2 &= \varepsilon_2 \sigma T_2^4 \end{aligned} \quad 5.1$$

where  $\sigma$  is the Stefan-Boltzmann constant. As shown in [18] a heat flux balance between two gray surfaces connected in the logical configuration indicated in Figure 5.3 results in the following relationship:

$$Q_{1-2} = \frac{\sigma(T_1^4 - T_2^4)}{\frac{1 - \varepsilon_1}{A_1 \varepsilon_1} + \frac{1}{A_1 F_{1-2}} + \frac{1 - \varepsilon_2}{A_2 \varepsilon_2}} \quad 5.2$$

where

- $Q_{1-2}$  is the net heat flux from surface 1 to surface 2
- $F_{1-2}$  is the geometric view factor, which represents the line-of-sight exposure between surfaces 1 and 2 as defined in [18], and
- $A_i$  is the area of the surfaces  $i$  ( $i = 1, 2$ ).



**Figure 5.3: Gray body configuration used in AFFTAC**

Rearranging, the above equation becomes

$$\frac{Q_{1-2}}{A_1} \equiv q_{1-2} = \frac{\sigma(T_1^4 - T_2^4)}{\frac{1}{F_{1-2}} + \left(\frac{1}{\varepsilon_1} - 1\right) + \frac{A_1}{A_2} \left(\frac{1}{\varepsilon_2} - 1\right)} \quad 5.3$$

Through this equation the “surface configuration factor,”  $f_{1-2}$ , is defined and used in AFFTAC to scale the radiative flux exchange. That factor,

$$f_{1-2} \equiv \frac{1}{\frac{1}{F_{1-2}} + \left(\frac{1}{\varepsilon_1} - 1\right) + \frac{A_1}{A_2} \left(\frac{1}{\varepsilon_2} - 1\right)} \quad 5.4$$

is used in combination with the surface areas, Stefan-Boltzmann constant, and temperatures of the exchanging surfaces to predict the radiant heat flux on a per-area basis, i.e.,

$$q_{1-2} = f_{1-2} \sigma(T_1^4 - T_2^4) \quad 5.5$$

In computing the radiative exchange between the inside tank wall and the liquid surface, 1 becomes “*liquid*” and 2 becomes “*wall*” to represent the tank wall. The emissivity of the inside tank wall is assumed to be 0.8 when using the legacy TPS model but you may

change that in the Edit Tank Car Properties window. When using the new generalized TPS model, you are allowed to specify that value when editing the TPS setup. The emissivity of the liquid surface is set in the Edit Lading Properties window, accessible through the Ladings Database. A reciprocal relationship is used to compute  $f_{wall-liquid}$ .

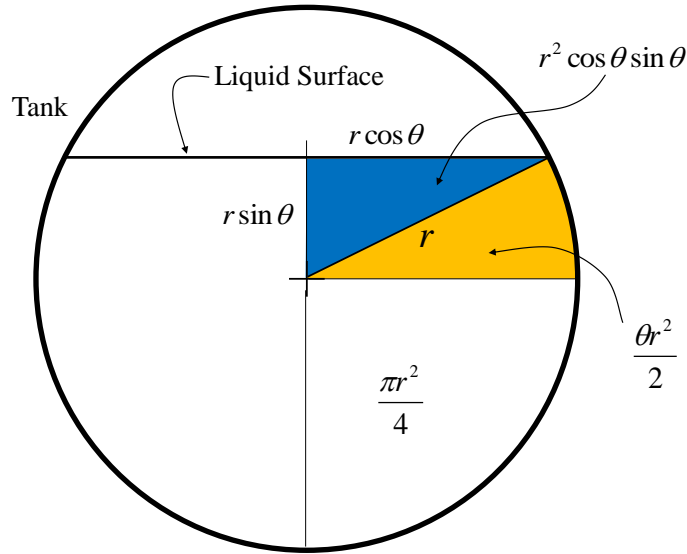
To compute the view factor,  $F_{liquid-wall}$  used in the above equation, the geometry of the liquid surface relative to the tank wall must be computed. Figure 5.4 shows a cross-section of the tank. The area of the bottom quadrant is  $\pi r^2/4$ . The area of the gold region above that is  $\theta r^2/2$ . The area of the blue area is  $r^2 \sin \theta \cos \theta/2$ . Twice the sum of these three areas represents the entire area under the liquid surface. Therefore,

$$A_{liquid} = 2 \times \left[ \frac{1}{4} \pi r^2 + \frac{1}{2} \pi \theta r^2 + \frac{1}{2} r^2 \sin \theta \cos \theta \right] = \frac{1}{2} \pi r^2 + \pi \theta r^2 + r^2 \sin \theta \cos \theta \quad 5.6$$

The ratio of this quantity to the total cross-sectional area ( $\pi r^2$ ) is the same as the fraction of the tank volume occupied by the liquid, i.e.,

$$\frac{V_{liquid}}{V_{total}} = \frac{1}{\pi} \left[ \frac{\pi}{2} + \theta + \sin \theta \cos \theta \right] \quad 5.7$$

This equation is solved through trial and error during the simulation to determine  $\theta$  at each point in time. From this value, the surface area of the liquid and the tank wall over it is computed. In addition, this value is used to determine whether or not liquid or vapor is adjacent to the pressure relief device.



**Figure 5.4: Geometry used to derive the equation relating the angle to the liquid surface endpoint to the fraction of tank filled with liquid**

## Temperatures of the Lading and the Tank Wall

### Radiative Heat Exchange with the Tank Wall

As discussed above, a classical gray-body radiative exchange model is used between the innermost tank wall surface adjacent to the vapor and the surface of the liquid. That net flux, on a per-area basis, is

$$q_{Rad-wall-liquid} = f_{wall-liquid} \sigma (T_{wall-vapor}^4 - T_{lading}^4) \quad 5.8$$

The value of  $f_{wall-liquid}$  is the surface configuration factor for the liquid lading surface and the tank wall above it as captured in Equation 5.4.

### Convective Heat Exchange with Tank Wall

A standard engineering model is used for the convective heat exchange between the vapor and the innermost tank wall surface adjacent to it. For heat flux on a per-area basis, that model is

$$q_{Conv-wall-vapor} = h(T_{wall-vapor} - T_{lading}) \quad 5.9$$

where  $h$  is the film coefficient.

#### Aside

The  $h$  film coefficient is difficult to estimate since it represents fluid flow that can take on a variety of forms. Film coefficients spanning an order of magnitude are reported in the literature depending on the properties of the liquid, whether or not boiling is present at the interface, and the geometry of the interface (e.g., see [5]). An indication of a representative value to use for this parameter can be inferred from the results of the full-scale fire test on a tank car filled with propane [6]. The results of this test indicated that the average conductance over the surface of the car was 300 BTU/hr-ft<sup>2</sup>-deg-F. The conductance of the 5/8 in. thick steel wall can be estimated at approximately 500 BTU/hr-ft<sup>2</sup>-deg-F, which implies that the conductance for the film would be about 750 BTU/hr-ft<sup>2</sup>-deg-F. A value of 1000 BTU/hr-ft<sup>2</sup>-deg-F is recommended as a conservative representative value. When only vapor is present, the convection coefficient is set to 1.0 BTU/hr-ft<sup>2</sup>-deg-F.

In both the legacy and new, generalized TPS model, the convective heat transfer is modeled as an additional “virtual layer” of resistance, because it has exactly the same mathematical form as a heat conductance model (linear in the temperature difference).

### Temperature Change in the Tank Wall Adjacent to the Vapor

In both of the heat flux terms in the preceding two sub-sections, the value for  $T_{wall-vapor}$  is considered known. But, as discussed at the beginning of this chapter and shown in Figure 5.2, it is determined by considering the heat balance on that part of the tank wall. The net heat flux is the heat entering the wall from the outside minus the heat leaving the wall and going into the lading. The difference in those fluxes is used to evolve  $T_{wall-vapor}$  over time as follows:

$$m_{wall-vapor} \frac{dT_{wall-vapor}}{dt} = q_{TPS-vapor} - q_{Rad-wall-liquid} - q_{Conv-wall-vapor} \quad 5.10$$

where each term is on a per-area basis, including  $m_{wall-vapor}$ , which is the mass of the tank wall over the vapor space, on a per-area basis. It is the product of its density and specific heat.

Clearly, the last two heat flux terms are the very ones in the preceding sub-sections that depend on  $T_{wall-vapor}$ . This is not surprising because all of these variables are, in fact, linked simultaneously in time. But as has been mentioned multiple times at this point in the manual, these linked governing equations are split and solved in pieces. Thus, using  $T_{wall-vapor}$  and other values from the previous time step,  $q_{Rad-wall-liquid}$  and  $q_{Conv-wall-vapor}$  are computed. Those values are then used to update  $T_{wall-vapor}$  and other variables as well, such as  $T_{lading}$ .

In Figure 5.2 and the above equation,  $q_{TPS-vapor}$  is the heat conducted from the outer part of the TPS into the tank wall. Along with its counterpart in the liquid region,  $q_{TPS-liquid}$ , it is a principle output of the TPS models and its computation is described in detail in those chapters.

### Temperature Change of the Lading and Tank Wall Adjacent to the Liquid

As already mentioned, AFFTAC assumes the vapor and liquid temperatures are equal and the tank wall adjacent to the liquid is at the same temperature as the liquid. The liquid phase of the lading and the part of the tank wall adjacent to it are lumped into one thermal mass denoted here as  $M_{liquid+Adjacent\_wall}$ . The mass of the vapor is negligible by comparison and although it could be included in principle, it is neglected here. The net flux into the lading is

$$Q_{net} = A_{wall-liquid}q_{TPS-liquid} \times (\text{Fraction Engulfed}) + A_{wall-vapor}q_{Rad-wall-liquid} + A_{wall-vapor}q_{Conv-wall-vapor} \quad 5.11$$

The first term on the right-hand side is the conductive exchange between the tank wall and the liquid, which is scaled by the area of contact between the liquid and tank wall,  $A_{wall-liquid}$ . It is one of the primary outputs of the TPS model. If you refer to the theory sections for both the legacy and new, generalized TPS models, you will see sections where the computation of that quantity is described. Keeping in mind that the thermal model is one-dimensional, the “Fraction Engulfed” term is used to represent the fact that some of the tank may not be engulfed in the flame. It changes depending upon whether a pool fire or a torch fire is being considered.

During times when the pressure relief device is open and lading is being expelled, the amount of work,  $W_{flow}$ , performed by pushing part of itself through the device is subtracted from  $Q_{net}$ . Also, the latent heat of vaporization for the expelled lading is subtracted. Thus the temperature change is given by

$$M_{liquid+adjacentwall} \frac{dT_{lading}}{dt} = Q_{net} + W_{flow} - \dot{m}H_f \quad 5.12$$

Here,  $H_f$  is the latent heat of vaporization.

### Aside

Modeling the tank wall over the vapor space and liquid each as having a uniform temperature is based on the assumption that the conditions are uniform on the respective inside surfaces of the tank. This assumption is not strictly without consequence because the temperature of the inner wall surface could be colder for regions close to the liquid’s surface. The temperature would depend on the length of time the wall has been exposed to the vapor and also the amount of radiant energy that has been received from the hotter part of the wall. Uniform conditions will be closely approached when the liquid level is near the top of the tank, because a slight drop in the liquid level will expose a large area of the inner surface of the tank. Uniform conditions will also be approached when the level of the liquid is low. Although the transient difference in temperature may be larger when the liquid level is near the center of the tank, calculations show that the difference would only have a small effect on the total heat transfer.

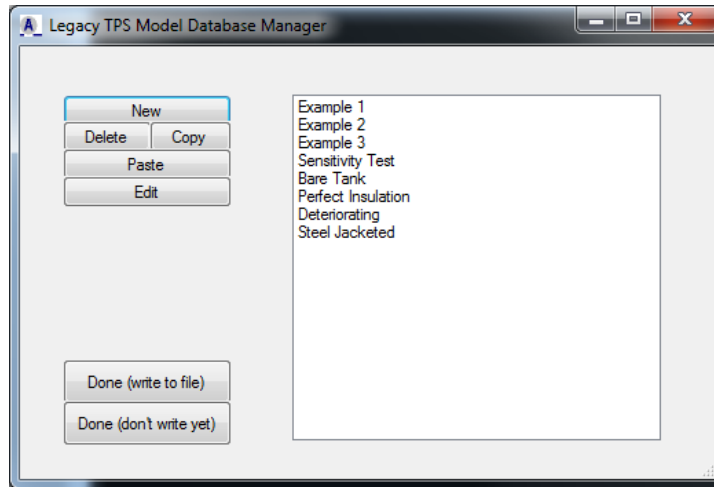
# The Legacy TPS Model and Database

There are two separate models for thermal protection systems (TPSs) in AFFTAC. You are required to choose one of them when setting up an analysis even if the tank is bare; that part is still accommodated as part of the TPS model. The TPS model described in this chapter is the legacy model, which has been in AFFTAC for decades. It provides important capabilities and also provides an important reference point for calculations that use the generalized TPS model, discussed in the next chapter.

The inputs that specify the legacy TPS model are grouped together and stored by name in the Legacy TPS Database, filename Insulations.db. Thus, each named entry in the Legacy TPS Database represents multiple pieces of data. When setting up an analysis, the third editing window requires you to select which TPS model you want to use, the legacy model or the new general TPS model. If you select the legacy TPS model, you will see the list of named entries in the Legacy TPS Model Database. In that same window, you may launch a window from which you may edit the Legacy TPS Model Database. You may also edit the Legacy TPS Model Database from the Main Window by choosing the option **Edit Databases-Legacy TPS Model**.

## Managing the Legacy TPS Model Database

When you choose to manage the Legacy TPS database, the window shown in Figure 6.1 is displayed. In this window, TPS setups can be edited by double clicking them or by highlighting them and clicking the **Edit** button. New TPSs can be created by either highlighting an existing one and clicking **Copy** then **Paste**, which creates a copy of the highlighted TPS, or by clicking **New**, which creates a new insulation using default values.



**Figure 6.1: The Legacy TPS Model Database manager**

When you double-click a TPS or highlight it and then click the **Edit** button, the Legacy TPS Model Setup window appears, like one of those shown in Figure 6.2. This multi-faceted window provides opportunities to create and customize six different TPS types. Its appearance changes depending upon which type of TPS types is chosen.

When you are finished editing a particular TPS setup, you will be returned to the Legacy TPS Model Database Manager window. There are two ways to exit it. One way saves the changes made to the database file. The other way keeps the changes for use in the current AFFTAC session but does not yet save the changes to the database file. This option is important because sometimes it is helpful to try a modification to an existing TPS without committing to it. Be sure to save the file before exiting if you, indeed, want to keep those changes. You may do so by clicking the Main Window menu option **File-Save Legacy TPS Model Database**.

## **Setting up a TPS in the Legacy Model**

Described below are the various types of setups available in the legacy TPS model. Refer again also to Figure 6.2.

### **Bare**

The “Bare” option simply means that there is no thermal protection system. No further input is required of you for this option.



### Steel Jacketed

Default Insulation 9

Type of Insulation

- Bare
- FRA Standard
- Steel Jacketed
- Temperature-independent
- Temperature-Dependent
- Steel Jacketed (2 component)

0.43 Initial conductance (BTU/hr-ft<sup>2</sup> deg-F)

1 Time interval for change (min)

None  
Six (6) mil organic liner  
3/16 inch thick rubber liner

Deteriorates over time

1 Time interval (min)

OK Cancel

### Temperature-Independent

Default Insulation 9

Type of Insulation

- Bare
- FRA Standard
- Steel Jacketed
- Temperature-independent
- Temperature-Dependent
- Steel Jacketed (2 component)

Conductivity's change with time

- Linear Decay
- Constant

0.43 Final conductance (BTU/hr-ft<sup>2</sup> deg-F)

None  
Six (6) mil organic liner  
3/16 inch thick rubber liner

Deteriorates over time

1 Time interval (min)

OK Cancel

### Temperature-Dependent

Default Insulation 9

Type of Insulation

- Bare
- FRA Standard
- Steel Jacketed
- Temperature-independent
- Temperature-Dependent
- Steel Jacketed (2 component)

0.5 Insulation thickness (inches)

K1	K2	K3
0.017	0.019	0.042

None  
Six (6) mil organic liner  
3/16 inch thick rubber liner

Deteriorates over time

1 Time interval (min)

OK Cancel

### Steel Jacketed (2 component)

Default Insulation 9

Type of Insulation

- Bare
- FRA Standard
- Steel Jacketed
- Temperature-independent
- Temperature-Dependent
- Steel Jacketed (2 component)

**Outer Layer**

Conductivity's change with time

- Linear Decay
- Constant

0.5 Insulation thickness (inches)

K1	K2	K3
0.017	0.019	0.042

0.43 Initial conductance (BTU/hr-ft<sup>2</sup> deg-F)

0.43 Final conductance (BTU/hr-ft<sup>2</sup> deg-F)

1 Time interval for change (min)

GroupBox3

- Yes
- No (Use default of 40 BTU/hr-ft<sup>2</sup> deg-F)

**Inner Layer**

None  
Six (6) mil organic liner  
3/16 inch thick rubber liner

Deteriorates over time

1 Time interval (min)

OK Cancel

Figure 6.2 The four types of legacy TPS types that require user input

**FRA Standard**

This TPS sets an overall thermal conductance of 4.0 BTU/hr-ft<sup>2</sup>-deg-F for the TPS, which is the maximum conductance that will pass the FRA performance test specified in Appendix B to CFR 179. Insulation systems that pass the test would likely have conductances that are less than this value.

**Temperature-Independent Insulation**

This type of TPS uses an insulation that is constant with temperature but is allowed to change with time. Two alternatives are offered, one where the conductance of the system is constant and the other where the conductance changes linearly over a given time period from an initial value to a steady-state value.

**Temperature-Dependent Insulation**

If this option is chosen, you may enter three coefficients that are used in the following equation to describe how the thermal conductivity of the tank wall varies as a function of temperature:

$$k = k_1 + k_2T + k_3T^2 \tag{6.1}$$

Note that conductivity typically has units of  $\frac{BTU}{hr - ft^2 - deg F / ft}$ . When conductivity is

computed using the temperature-dependent form, temperature is in thousands of deg F and length is in feet. So the units of conductivity are, in the Computational Module,

$\frac{BTU}{hr - ft^2 - thousands\ of\ deg\ F / ft}$ . The  $k_1$  parameter has those units while the other two

parameters have units that accommodate the temperature function that multiplies them. In summary:

Parameter	Units
$k_1$	$\frac{BTU}{hr - ft^2 - thousands\ of\ deg\ F / ft}$
$k_2$	$\frac{BTU}{hr - ft^2 - (thousands\ of\ deg\ F)^2 / ft}$
$k_3$	$\frac{BTU}{hr - ft^2 - (thousands\ of\ deg\ F)^3 / ft}$

**Steel Jacketed (2 component) Insulation**

As the name implies, this TPS option has two layers. For the inner layer, you may enter an initial and final thermal conductivity value and a time interval over which AFFTAC

will interpolate between those values (just as in the temperature-independent option described above). For the outer layer, you may specify its thickness and also make its conductivity a function of temperature.

## Legacy TPS Model Theory

Before attempting to understand the theory for the legacy TPS model, it is highly recommended that you read the chapter entitled, “Details of the Overall Thermal Model.” The material there will help you understand how the calculations of the TPS model fit in to the overall solution process and also some of the parameters used in the model description.

As discussed in that chapter, the primary role of the TPS model is to compute the heat flux through the TPS. The legacy TPS model operates in two modes, one in which the tank is bare or perhaps partially covered by an insulating layer and another mode in which an air gap exists between the insulated tank and a steel jacket. Although all of the underlying assumptions and approaches are the same for the two modes, it is convenient to describe them separately.

The overall thermal model discussed in the chapter entitled “Details of the Overall Thermal Model” has certain constructs, such as the fact that the lading is a uniform temperature and that same temperature is shared by the part of the tank wall adjacent to the liquid. Likewise, the legacy TPS model has certain constructs. The most important one is that the legacy TPS model assumes the tank’s outermost surface can have up to four distinct temperatures. Since partial insulation coverage is modeled, different outermost temperatures exist for the regions with insulation compared to those regions without insulation. Also, both of those regions may exist in the part of the tank adjacent to the vapor or the liquid. Thus four combinations result as listed in the table below. And to solidify these definitions, the temperatures are shown in Figure 6.3 for the two different cases (jacketed and non-jacketed). Notice in both cases that there is one temperature for the lading, both vapor and liquid, and that same temperature is the temperature of the interior tank wall adjacent to the liquid.

Adjacent to	Insulation Present?	Outermost Temperature in that Region
Liquid	Yes	$T_{outer-Ins-liquid}$
	No	$T_{outer-noIns-liquid}$
Vapor	Yes	$T_{outer-Ins-vapor}$
	No	$T_{outer-noIns-vapor}$

**Table 6.1: The four outermost temperatures in the legacy TPS model when a steel jacket is not present**

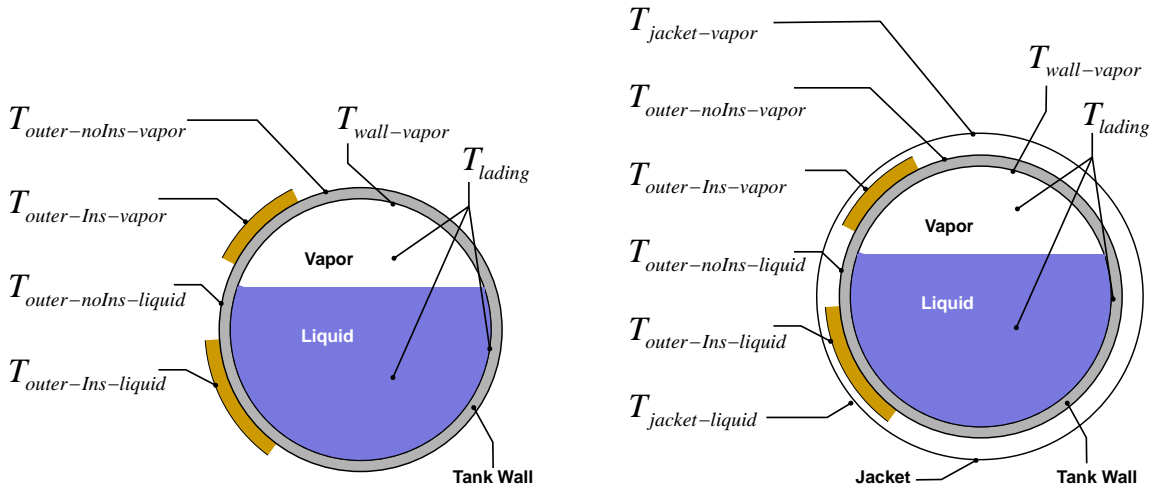


Figure 6.3: Temperature definitions for the case of an unjacketed (Left) and jacketed (Right) TPS

### Bare Tank or Non-Jacketed Tank with Partial Insulation Coverage

Although a bare tank may perform and appear very different than a tank with insulation, from the legacy TPS model's standpoint, the two cases are identical in structure. Specifically, the heat transfer from the inside of the tank wall to the outermost surface is equal to the temperature difference on those two surfaces times a thermal conductivity, divided by a thickness. Granted, the conductivity in the bare tank case will be much higher than in the insulated case, but that does not change the fact that the equations are the same form.

And so, in AFFTAC, the bare tank and insulated tank are treated exactly the same way, with different values for conductivity. The treatment is a heat balance on the outermost surface that accommodates areas with and without insulation. The equations are of the same form for all the regions:

$$\epsilon_f f T_f^4 - \epsilon T_{outer}^4 + c(T_{outer} - T_{inner}) = 0 \quad 6.2$$

where  $T_f$  is the flame temperature,  $c$  is thermal conductance, and  $\epsilon_f$  is the emissivity of the fire. The value for  $c$  and the other variables take on the following meanings in the different regions to which the equation is applied:

Adjacent to	Insulation Present?	$T_{outer}$	$T_{inner}$	$c$
Liquid	Yes	$T_{outer-ins-liquid}$	$T_{lading}$	$c_{Tank+Ins}$
	No	$T_{outer-noIns-liquid}$	$T_{lading}$	$c_{Tank}$
Vapor	Yes	$T_{outer-ins-vapor}$	$T_{wall-vapor}$	$c_{Tank+Ins}$
	No	$T_{outer-noIns-vapor}$	$T_{wall-vapor}$	$c_{Tank}$

**Table 6.2: The values that the variables in Equation 6.2 take on for the four regions of the tank wall present in the legacy TPS model when a steel jacket is not present**

As implied in the definitions above, these nonlinear equations are solved four times, twice for the tank wall adjacent to the liquid and twice for the tank wall adjacent to the vapor. The reason AFFTAC makes the distinction between the liquid and vapor regions was explained in “The Scope and Interaction of AFFTAC’s Models” chapter, but is worth reviewing here. When the liquid lading is touching the tank wall, it provides a great deal of thermal mass in intimate contact with the tank wall. Therefore, the tank wall touching the liquid is assumed to be at the same temperature as the liquid. However, the tank wall adjacent to the vapor has no intimate contact with a large thermal mass. Thus it can be at a different temperature from the lading.

Once the outermost surface temperature is determined for the four regions in Table 6.2 above, it is used in combination with the appropriate innermost surface temperature to compute the heat flux into the innermost layer via conduction

$$q_{region} = c(T_{outer} - T_{inner}) \quad 6.3$$

which is simply the second term in Equation 6.2.

Thus, for the four combinations considered, heat fluxes computed are as shown in the table below.

Adjacent to	Insulation Present?	$q_{region}$
Liquid	Yes	$q_{Ins-liquid}$
	No	$q_{noIns-liquid}$
Vapor	Yes	$q_{Ins-vapor}$
	No	$q_{noIns-vapor}$

**Table 6.3: The heat fluxes computed by Equation 6.3 for the four regions in the legacy TPS model when a jacket is not present.**

To compute the total average flux through the tank wall for the liquid and vapor regions, the fluxes for those regions in the parts that do and do not have insulation are combined using a weighted average:

$$\begin{aligned} q_{TPS-liquid} &= q_{Ins-liquid}F_{Ins} + q_{noIns-liquid}(1 - F_{Ins}) \\ q_{TPS-vapor} &= q_{Ins-vapor}F_{Ins} + q_{noIns-vapor}(1 - F_{Ins}) \end{aligned} \quad 6.4$$

where  $F_{Ins}$  is the fraction of insulation coverage.

### Partial Insulation Coverage Inside Jacket

In this case, the model accommodates a variable amount of coverage from the insulation that is between the steel jacket and the tank wall.

The model assumes that the steel jacket is so thin that it does not support a temperature gradient, i.e., it is a uniform temperature  $T_j$ . The heat transfer equation is solved twice, once for the part of the tank wall touching the liquid, and once for where it is touching the vapor.

Analogous to the previous sub-section, the governing equation can be written once and applied to multiple regions by appropriately defining the variables. When solving for the part of the tank wall adjacent to the liquid, the inner temperature of the tank wall  $T_i$  is set to  $T_{loading}$ . When solving for the part of the tank wall adjacent to the vapor, the inner temperature of the tank wall is set to  $T_{wall-vapor}$ . When solving for the liquid region, the solution obtained for  $T_{outer-Ins}$  is used for  $T_{outer-Ins-liquid}$  and the solution obtained for  $T_{outer-noIns}$  is used for  $T_{outer-noIns-liquid}$ . The exact analogy is used for the vapor region.

The following equation represents the heat balance on the jacket:

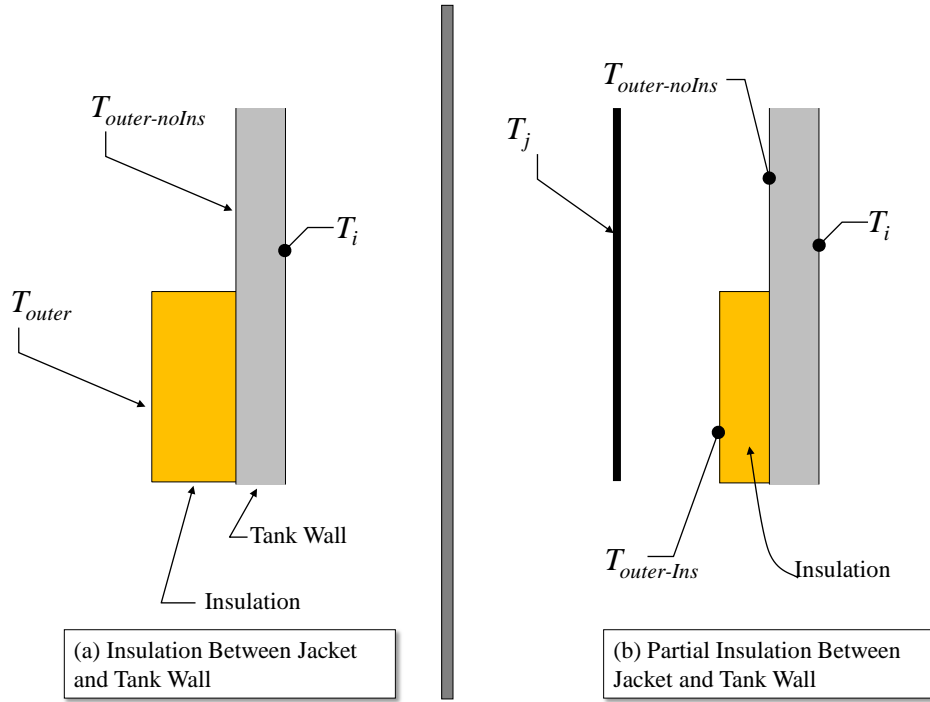
$$\sigma\varepsilon_f T_f^4 - \sigma\varepsilon T_j^4 - \sigma\left(\frac{\varepsilon}{2-\varepsilon}\right)T_j^4 + \sigma\left(\frac{\varepsilon}{2-\varepsilon}\right)T_{outer-noIns}^4(1 - F_{SP}) + \sigma\left(\frac{\varepsilon}{2-\varepsilon}\right)T_{outer-Ins}^4 F_{SP} = 0 \quad 6.5$$

This is the heat balance on the bare tank surface:

$$\sigma\left(\frac{\varepsilon}{2-\varepsilon}\right)T_j^4 - \sigma\left(\frac{\varepsilon}{2-\varepsilon}\right)T_{outer-noIns}^4 - C_w(T_{outer-noIns} - T_i) = 0 \quad 6.6$$

And this is the heat balance on the insulation surface:

$$\sigma\left(\frac{\varepsilon}{2-\varepsilon}\right)T_j^4 - \sigma\left(\frac{\varepsilon}{2-\varepsilon}\right)T_{outer-Ins}^4 - \bar{C}(T_{outer-Ins} - T_i) = 0 \quad 6.7$$



**Figure 6.4: Heat exchange diagram for jacketed systems showing relevant nomenclature**

In the above equations,  $\sigma$  is the Stefan-Boltzmann constant, and the  $f$  parameters are the surface configuration factors. The surface configuration factors rely upon the emissivities, geometric view factors, and areas of the surfaces involved (see Equations 5.2-5.5). The  $C_w$  and  $\bar{C}$  are thermal conductances of the wall and wall+insulation, respectively.

The unknowns in the above equations are  $T_j$ ,  $T_{outer-Ins}$ , and  $T_{outer-noIns}$ . To solve the equations using the Newton-Raphson method, first the left-hand-side of the equations are given names,  $f_1$ ,  $f_2$ , and  $f_3$ :

$$f_1 \equiv \alpha \varepsilon f T_f^4 - \alpha \varepsilon T_j^4 - \sigma \left( \frac{\varepsilon}{2 - \varepsilon} \right) T_j^4 + \sigma \left( \frac{\varepsilon}{2 - \varepsilon} \right) T_{outer-noIns}^4 (1 - F_{SP}) + \sigma \left( \frac{\varepsilon}{2 - \varepsilon} \right) T_{outer-Ins}^4 F_{SP} \quad 6.8$$

$$f_2 \equiv \sigma \left( \frac{\varepsilon}{2 - \varepsilon} \right) T_j^4 - \sigma \left( \frac{\varepsilon}{2 - \varepsilon} \right) T_{outer-noIns}^4 - C_w (T_{outer-noIns} - T_i) \quad 6.9$$

$$f_3 \equiv \sigma \left( \frac{\varepsilon}{2 - \varepsilon} \right) T_j^4 - \sigma \left( \frac{\varepsilon}{2 - \varepsilon} \right) T_{outer-Ins}^4 - \bar{C} (T_{outer-Ins} - T_i) \quad 6.10$$

Second, an array containing the three unknown temperatures and an array containing the three functions are defined:

$$\mathbf{T} \equiv \begin{bmatrix} T_j \\ T_{outer-noIns} \\ T_{outer-Ins} \end{bmatrix} \quad \text{and} \quad \mathbf{f}(\mathbf{T}) \equiv \begin{bmatrix} f_1(\mathbf{T}) \\ f_2(\mathbf{T}) \\ f_3(\mathbf{T}) \end{bmatrix} \quad 6.11$$

The nonlinear system of three equations may now be expressed as follows:

$$\mathbf{f}(\mathbf{T}) = \mathbf{0} \quad 6.12$$

The Newton-Raphson method of solving a nonlinear system such as that in Equation (6.11) is to start with an initial guess,  $\mathbf{T}^0$  and then update that guess as follows:

$$\mathbf{T}^{i+1} = \mathbf{T}^i + \boldsymbol{\delta}^i \quad 6.13$$

Where  $\boldsymbol{\delta}^i$  is the solution to the following linear system of equations:

$$\begin{bmatrix} \frac{\partial f_1}{\partial T_j} & \frac{\partial f_1}{\partial T_{outer-noIns}} & \frac{\partial f_1}{\partial T_{outer-Ins}} \\ \frac{\partial f_2}{\partial T_j} & \frac{\partial f_2}{\partial T_{outer-noIns}} & \frac{\partial f_2}{\partial T_{outer-Ins}} \\ \frac{\partial f_3}{\partial T_j} & \frac{\partial f_3}{\partial T_{outer-noIns}} & \frac{\partial f_3}{\partial T_{outer-Ins}} \end{bmatrix}_{\mathbf{T}^i} \boldsymbol{\delta}^i = -\mathbf{f}(\mathbf{T}^i) \quad 6.14$$

The right hand side is an array of three entries, which are the  $\mathbf{f}$  functions evaluated at the previous guess. The matrix is comprised of partial derivatives of the three functions with respect to the different temperatures, also evaluated at the previous guess.

Working from Equations 6.8-6.10, the partial derivatives are as follows:

$$\begin{aligned} \frac{\partial f_1}{\partial T_j} &= -4\sigma\epsilon T_j^3 - 4\sigma \left( \frac{\epsilon}{2-\epsilon} \right) T_j^3 \\ \frac{\partial f_1}{\partial T_{outer-noIns}} &= 4\sigma \left( \frac{\epsilon}{2-\epsilon} \right) T_{outer-noIns}^3 (1 - F_{SP}) \\ \frac{\partial f_1}{\partial T_{outer-Ins}} &= 4\sigma \left( \frac{\epsilon}{2-\epsilon} \right) T_{outer-Ins}^3 F_{SP} \end{aligned} \quad 6.15$$



$$\frac{\partial f_2}{\partial T_j} = 4\sigma \left( \frac{\varepsilon}{2-\varepsilon} \right) T_j^3 \quad 6.16$$

$$\frac{\partial f_2}{\partial T_{outer-noIns}} = -4\sigma \left( \frac{\varepsilon}{2-\varepsilon} \right) T_{outer-noIns}^3 - C_w$$

$$\frac{\partial f_2}{\partial T_{outer-Ins}} = 0$$

$$\frac{\partial f_3}{\partial T_j} = 4\sigma \left( \frac{\varepsilon}{2-\varepsilon} \right) T_j^3 \quad 6.17$$

$$\frac{\partial f_3}{\partial T_{outer-noIns}} = 0$$

$$\frac{\partial f_3}{\partial T_{outer-Ins}} = -4\sigma \left( \frac{\varepsilon}{2-\varepsilon} \right) T_{outer-Ins}^3 - \bar{C}$$

An initial guess is required to start the Newton-Raphson iterations. For all but the first time step, the solution from the previous time step is sufficient. But for the first time step, the initial guess is provided using an approximation.

The geometric view factor for the flame-tank exchange is assumed to be unity except in the case of a torch fire where it is assumed to be 0.536. The geometric view factor for the jacket-wall exchange is unity.

## Heat Flux Into Lading and the Tank Wall over Vapor Space

Once the nonlinear system is solved to determine the temperatures on the outer surfaces, those values can be used to compute the flux as follows:

$$q_{TPS-liquid} = F_{SP}(T_{outer-Ins-liquid} - T_{lading})\bar{C} + (1 - F_{SP})(T_{outer-noIns-liquid} - T_{lading})C_w \quad 6.18$$

$$q_{TPS-vapor} = F_{SP}(T_{outer-Ins-vapor} - T_{wall-vapor})\bar{C} + (1 - F_{SP})(T_{outer-noIns-vapor} - T_{wall-vapor})C_w \quad 6.19$$

Here,  $\bar{C}$  and  $C_w$  represent the conductivities for the regions with and without insulation

## Conductances for Multi-Layer TPSs

The thermal transport models described in the previous section rely heavily on composite conductances. Considering one-dimensional heat conduction through several layers, it is

well known that the effective conductance,  $C$ , of the composite layer is related to the conductance,  $C_i$ , of each layer as follows:

$$\frac{1}{C} = \sum_{i=1}^n \frac{1}{C_i} \quad 6.20$$

where  $n$  is the number of layers. Here, each  $C_i$  represents a layer in a composite system. Those layers include the tank wall itself, but also insulation and tank linings. Although not shown explicitly in Figure 6.4, other layers may exist (such as a lining). Their conductance is used to modify the  $C_w$  using the equation above.

AFFTAC's legacy TPS model accommodates different behaviors for the insulation layers and linings. For example, you can specify an amount of time during which some layers deteriorate. Also, you can specify a temperature-dependent conductivity. In that case, a nonlinear system must be solved to determine the effective conductance of the entire layer. As discussed earlier in this chapter, the conductivity may be expressed by the user as follows:

$$K(T) = K_1 + K_2T + K_3T^2 \quad 6.21$$

To solve the heat conduction equation when the conductance is of this form, the algorithm divides the insulation layer into 50 elements. It then starts at the inside of the layer and, using the previous value for the effective conductance and the heat flux that it allows, marches through the 50 elements computing the temperature distribution as it proceeds. When it arrives at the outside of the insulation, it checks to see if the temperature matches that predicted by using the previous effective conductance. If it does not, the effective conductance is adjusted and the process is repeated until convergence is achieved.

The other insulation behaviors in AFFTAC's legacy TPS model accommodate different insulations used in tank cars. For example, rubber liners are used on some acid cars. They would initially offer a high value of insulation. A typical value for the conductivity of rubber is 0.1 BTU/hr-ft-deg-F. This value would imply a conductance of 6.4 BTU/hr-ft<sup>2</sup>-deg-F for a 3/16 in. thick rubber liner, which would provide a high degree of resistance to heat flow into the tank. It is likely, however, that the effectiveness of the rubber as a thermal insulator would soon be destroyed on cars that do not have any exterior insulation because the adjacent steel tank wall would soon be heated to over 1000 deg-F, which would melt the surface of the rubber in contact with it. Therefore, in an analysis of this condition, it is recommended that the rubber liner be considered to have an initial conductance of 6.4 BTU/hr-ft<sup>2</sup>-deg-F, but that this would be degraded linearly over a 15 minute period. The rubber liner on an insulated car is likely to remain effective for a much longer time because the exterior insulation would keep the tank wall at a moderate temperature.

Some cars have an organic coating on the inside of the tank. It would offer less resistance to heat flow than a rubber liner because of its small thickness. An estimate of its conductivity is 0.25 BTU/hr-ft-deg-F, which implies a thermal conductance of 500 BTU/hr-ft<sup>2</sup>-deg-F for a 6 mil thickness. Its effectiveness would be expected to be retained for a fairly long period of time because its conductance is high, which means the temperature of the inside of the tank wall would be close to the temperature of the product within the tank. Thus, it is less likely to be damaged by high temperature.

Again, for all such liners, the  $C_w$  value is modified according to Equation 6.20.



# The Generalized TPS Model and Database

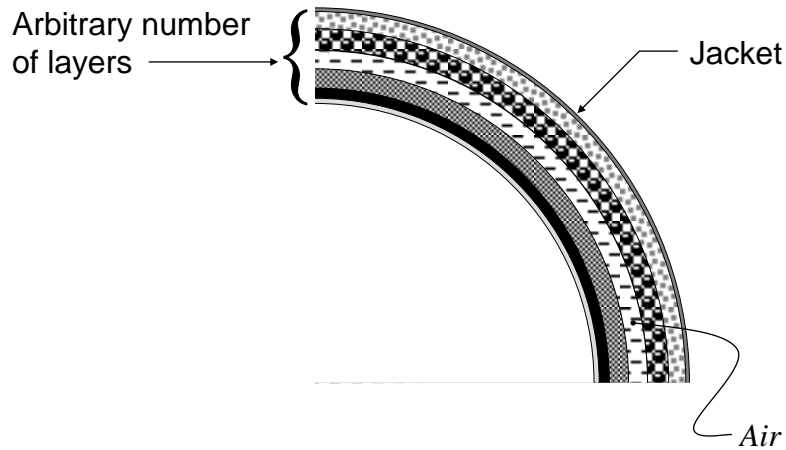
This chapter discusses the scope and use of the generalized TPS model and database, which is a separate modeling option that can be chosen instead of the legacy TPS model described in the previous chapter. The legacy TPS model is very important because it has been part of AFFTAC a long time and, through its many uses, has undergone significant debugging and hardening. Also, it is a relatively simple model and so it inherently has less potential for errors. For those reasons, users are encouraged to always make test runs using the legacy TPS model as a check against runs made using the newer and more complex generalized TPS model described here.

The generalized TPS model offers several sophisticated advances over the legacy model. Because of its complexity, it has also undergone significant testing as described in the accompanying *AFFTAC Verification and Validation Test* document. The capabilities of the generalized TPS model include:

- (1) The ability to accommodate an arbitrary number of material layers in the TPS,
- (2) Each layer of the TPS can have an arbitrary coverage (defects) that varies as a function of position around the tank,
- (3) Each layer of the TPS may have its thermal conductivity specified using tabular data,
- (4) Each layer of the TPS may undergo a change of phase at a certain temperature wherein the thermal conductivity becomes described by a different table.

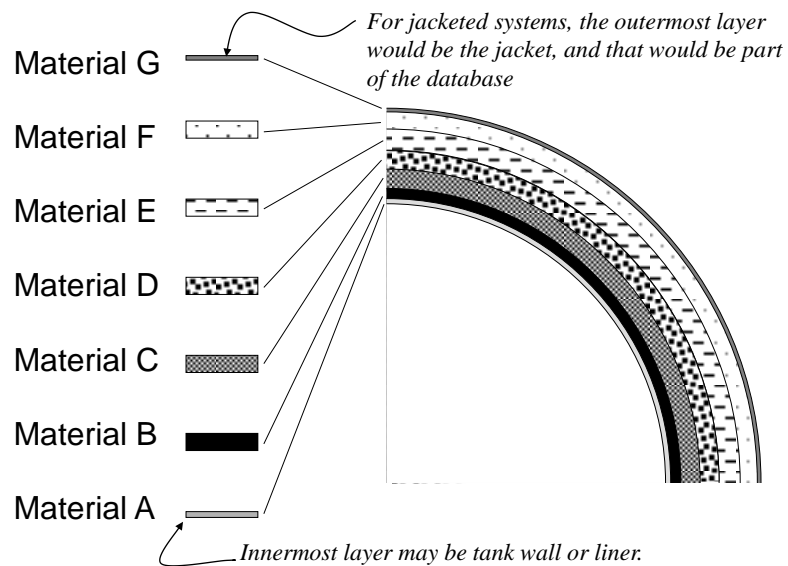
Various aspects of the requirements are represented in Figures 7.1-7.3 on the pages that follow.

- An arbitrary number of layers is accommodated.
- Jacket, tank wall, and liners are also treated as layers.
- Any layer may exhibit partial coverage.



**Figure 7.1: Composite thermal protection system model**

- Layers are named separately and saved in the database.
- Composite systems are assembled from named layers, and also saved in the database.



**Figure 7.2: Summary of how materials can be named and then combined to form a composite thermal protection system**

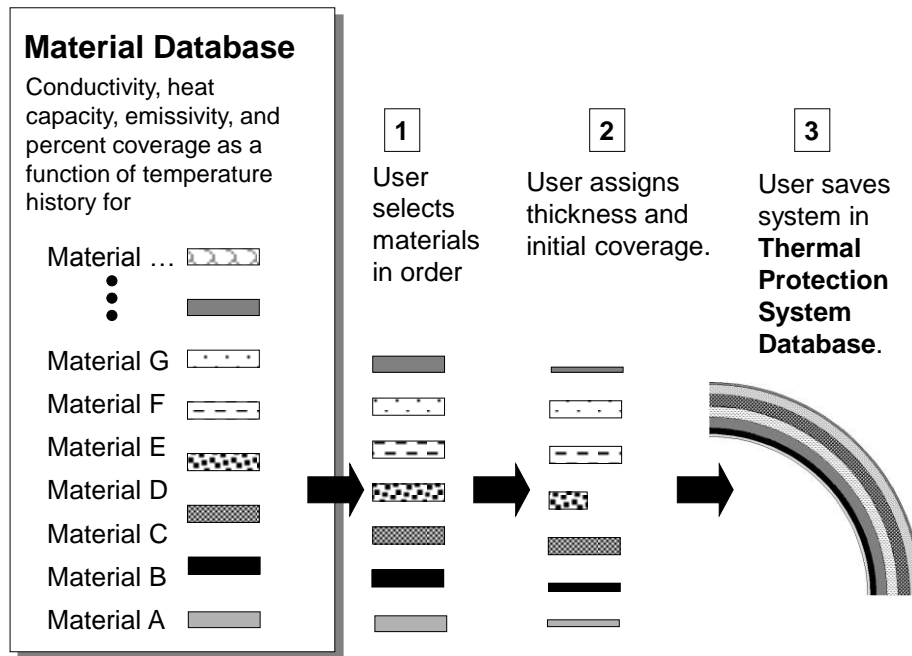


Figure 7.3: Process for specifying a TPS in the generalized TPS model

## Using the Generalized TPS Model

While editing an analysis, the third window of the four-window editing sequence requires you to choose either the legacy TPS model or the generalized TPS model. If you choose the generalized TPS model, you will see the list of previously established TPS setups for that model. You may select one of the setups in the list for your analysis. Also, you may edit that list of setups by clicking the **Manage Generalized TPS Database** button. You may also manage the Generalized TPS Database by choosing the Main Window menu option **Edit Databases- Generalized TPS Model**.

Shown in Figure 7.4 is the window for managing the Generalized TPS Model Database. Toward the far left of the window, bulk materials are defined and, for each one, at least one table describing their thermal conductivity is specified. Multiple thermal conductivity tables can be specified for each material, each table becoming active at a specific temperature. These bulk materials can be used to describe a TPS component (i.e., layer), which are specified in the middle of the window. A component consists of a bulk material, the specification of the layer's thickness, and the emissivity on each surface. Also, the coverage of the component can be specified as a function of angle around the tank in the lower middle portion of the window. Finally, a TPS is constructed on the far right by assembling layers. In Figure 7.4 several TPSs are shown. The layers of the highlighted TPS "SteelJacketedTrend50" are shown in the rightmost list box.

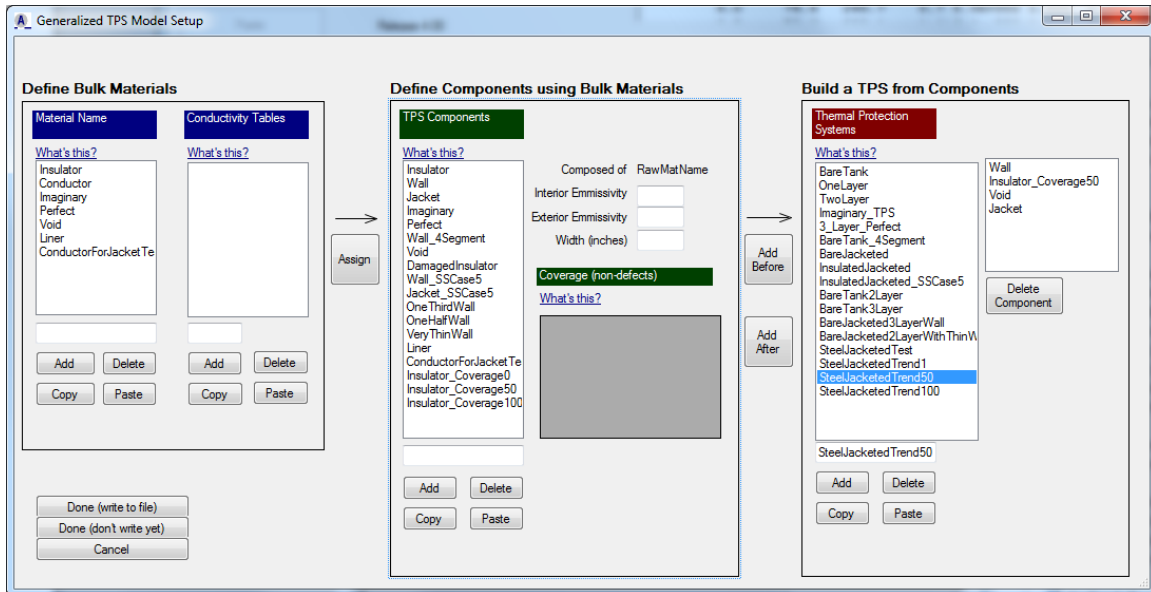


Figure 7.4 Main management and editing window for the Generalized TPS Model Database.

## General TPS Model Theory

Before attempting to understand the theory for the generalized TPS model, it is highly recommended that you read the chapter entitled, “Details of the Overall Thermal Model.” The material there will help you understand how the calculations of the TPS model fit in to the overall solution process and also some of the parameters used in the model development.

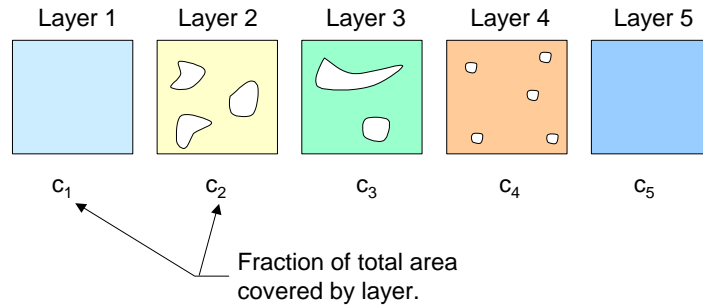
Consider Figure 7.5, which shows each layer of a five-layer system as if the system had been disassembled, and each layer laid out side by side. As the figure shows, each of the inner layers may have a coverage value,  $c_i$ , less than unity. The voids in these layers affect how heat is transferred through the system, as illustrated in Figure 7.6, which shows that there are three temperatures at each material interface. One temperature is that of the area where the two adjacent layers are in contact. Specifically,  $T_2$  is the temperature where Layer 2 and Layer 3 are in contact.  $T_{R2}$  is the temperature of Layer 2’s right side that is exposed to convection and radiation with layers to its right.  $T_{L3}$  is the temperature of Layer 3’s left side that is exposed to convection and radiation with layers to its left. A governing equation is required for each one of these areas.

The new TPS model makes the following assumptions:

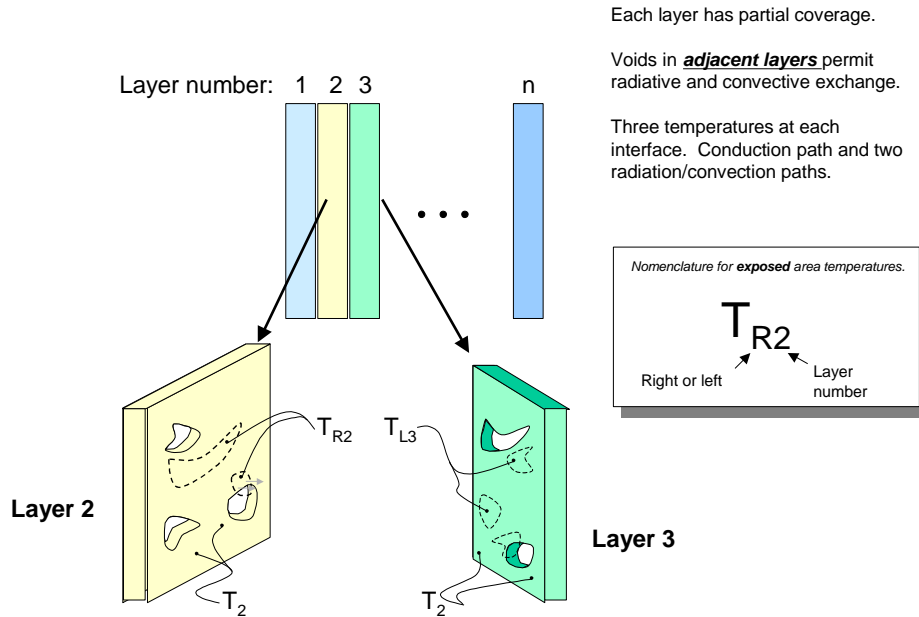
- (1) The voids have a random size distribution, meaning that on average there is no pattern that would cause voids to line up, thereby unduly exposing one layer to another layer several layers away. Instead, the exposure of each layer to other layers is gradually reduced by the coverage of the intermediate layers.
- (2) The voids are large enough such that lateral conduction (i.e., in the plane of Figure 7.5) need not be considered.



Because the generalized TPS model is designed to handle an arbitrary number of layers, each with an arbitrary amount of coverage, there is a non-trivial amount of nomenclature that must be established before the actual governing equations can be written. Appendix F describes that nomenclature and proceeds to give an exhaustive account of the governing equations and solution algorithm. Here, the equations are summarized so you can get a reasonably good understanding of the model's basic theory.



**Figure 7.5: Illustration of a disassembled conceptual TPS, which each layer laid out separately thereby exposing the voids in each layer**



**Figure 7.6: Illustration of conceptual TPS with layer numbers, showing how the voids and non-void areas interact between layers, and establishing temperature nomenclature**

## Area in Contact

Interface  $i$  is the interface between Layer  $i$  and Layer  $i+1$ . Since this area is in contact with two layers, conduction is the only mechanism for heat transfer. A heat balance on the interface states that the heat flowing into it must equal the heat flowing out of it. That requirement is embodied in the following equation:

$$\begin{aligned} \frac{k_i}{w_i} A_i (T_i - T_{i-1}) + \frac{k_i}{w_i} A_{i,L} (T_i - T_{L_i}) + \\ \frac{k_{i+1}}{w_{i+1}} A_{i+1} (T_i - T_{i+1}) + \frac{k_{i+1}}{w_{i+1}} A_{i,R} (T_i - T_{R_{i+1}}) = 0 \end{aligned} \quad 6.1$$

In the above equation, you can see some of the complexities of the nomenclature. In particular, there are area terms, “A” variables, that describe how much area is available for conduction. That value depends on the amount of coverage specified for the layers.

## Right Side’s Exposed Area

Consider again interface  $i$ , but this time, the part of that interface that is exposed due to a lack of coverage in Layer  $i+1$ . Heat conduction still occurs to the left, but radiative and convective heat transfer occurs to the right. Again, a heat balance on the interface states that the heat flowing into it must equal the heat flowing out of it. That requirement is embodied in the following equation, where heat conduction to the left is represented in the first terms and radiative plus convective heat flow is represented in the last terms:

$$\begin{aligned} \frac{k_i}{w_i} A_{i-1,R} (T_{R_i} - T_{i-1}) + \frac{k_i}{w_i} A_{L,R} (T_{R_i} - T_{L_i}) + \\ \sum_{k=i+1}^n A_{R_i L_k} h_{i,k} (T_{R_i} - T_{L_k}) + \sum_{k=i+1}^n A_{R_i L_k} \frac{\sigma (T_{R_i}^4 - T_{L_k}^4)}{1/\varepsilon_{R_i} + 1/\varepsilon_{L_k} + 1} = 0 \end{aligned} \quad 6.2$$

Again, while not all of the nomenclature is defined here (it is in Appendix F), the above equation can still give you a feel for this part of the theory. Part of the heat leaving a surface that is exposed is due to conduction through its own layer; those are the first two terms. The third term represents the convective heat transfer between the exposed area and all of the other exposed areas it sees. Keep in mind that there are an arbitrary number of layers, which explains why the summation sign is needed. The last term is the radiative exchange between the exposed area and all the other exposed areas it sees.

## Left Side's Exposed Area

The equation for the left side's exposed area is exactly analogous to that for the right:

$$\begin{aligned} & \frac{k_i}{w_i} A_{i,L} (T_{L_i} - T_i) + \frac{k_i}{w_i} A_{L,R} (T_{L_i} - T_{R_i}) + \\ & \sum_{k=1}^{i-1} A_{L_i R_k} h_{i,k} (T_{L_i} - T_{R_k}) + \sum_{k=1}^{i-1} A_{L_i R_k} \frac{\sigma (T_{L_i}^4 - T_{R_k}^4)}{1/\varepsilon_{L_i} + 1/\varepsilon_{R_k} + 1} = 0 \end{aligned} \quad 6.3$$

Again, the theory is thoroughly developed in Appendix F, and you are encouraged to explore that material.

## Flux Computation

The key output of the TPS model is the flux into and through the innermost surface of the TPS, which may be a liner or the tank wall itself. Once all of the temperatures in Figure 7.6 and Equations 6.1-6.3 are known, the flux through and into the innermost surface is computed using the conduction term, i.e.,

$$\begin{aligned} q_{TPS-liquid} &= \frac{k_1}{w_1} (T_{L1} - T_{loading}) \\ q_{TPS-vapor} &= \frac{k_1}{w_1} (T_{L1} - T_{wall-vapor}) \end{aligned} \quad 6.5$$



# Strength Models

There are two separate methods for modeling strength in AFFTAC. Both are described in this chapter, starting with the legacy strength model.

## Legacy Strength Model

The legacy strength model is relatively straightforward to explain and use. You make the choice regarding which strength model to use in the Edit Tank Car Properties window, which is the second of the four-window editing sequence for any analysis. The upper right part of that window has two modes, one of which is displayed when using the legacy strength model and the other when using the Strength Model Database. The modes are toggled by clicking the button that says either **Switch to Strength Model Database** or **Switch to Legacy Strength Model**. Figure 8.1 shows the window with the legacy models displayed.

The legacy failure model is based on an estimate of the material's room-temperature ultimate tensile strength, which is a constant, multiplied by a factor that decreases with increasing temperature. More explicitly, in AFFTAC, the tensile strength of the tank wall material is

$$S(T) = S_r f(T) \quad 8.1$$

where  $S_r$  is the hard-coded value of the material's ultimate tensile strength at room temperature and  $f(T)$  is the multiplier that decreases with increasing temperature. Values of  $S_r$  are provided inside AFFTAC for twenty-seven different materials. And for each material, there is a hard-coded model for  $f(T)$ .

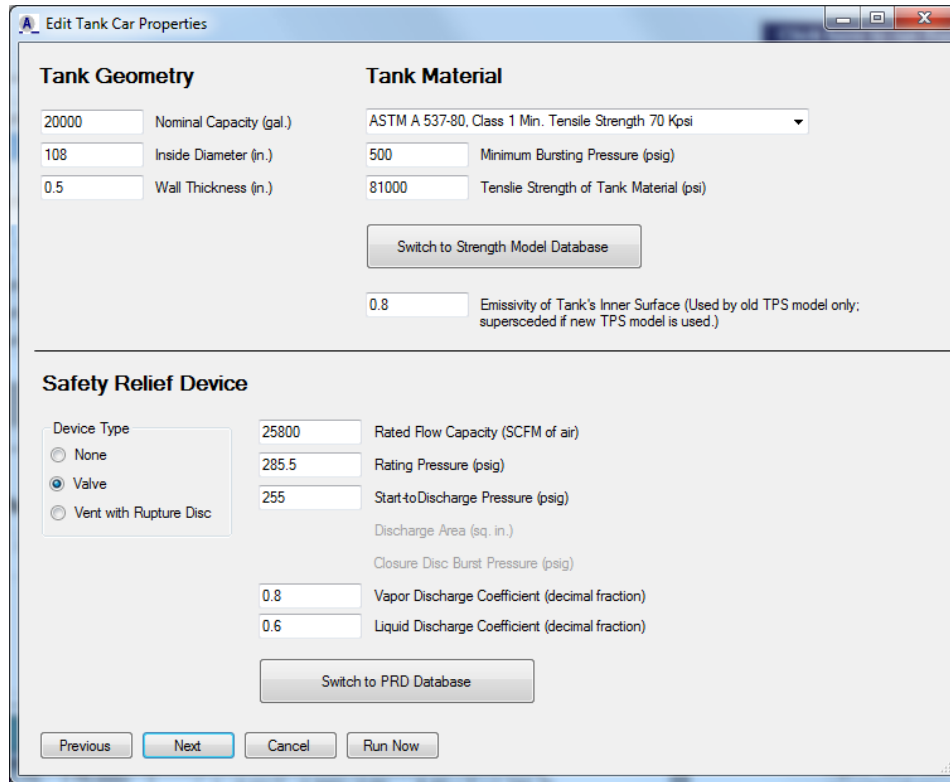


Figure 8.1: Edit Tank Car Properties window in which the legacy model is selected.

Tables 8.1-8.3 on the subsequent pages show these models for each of the materials. The units in the tables are

$$T : R^o / 1000 \quad 8.2$$

$$S_r : \text{Kpsi}$$

Note that the adjustment factor,  $f(T)$ , is not a function of time, meaning that it does not accommodate the widely observed phenomenon of creep.

## The Strength Model Database

The other way to model strength of the tank wall is to use the Strength Model Database by selecting the button **Switch to Strength Model Database** in the same Edit Tank Car Properties Window. The Strength Model Database is like the other databases used in AFFTAC in that by choosing a particular name, you are drawing upon potentially several pieces of data that are transmitted to the Computational Module for a simulation.

The Strength Model Database accommodates two types of strength models which may be used individually or in combination. One is the Larson-Miller creep and failure model; the other is ultimate tensile strength data that you can enter as a function of temperature.

Carbon Steels			
ID	Description	$S_r$	Adjustment Factor
1	ASTM A 515-70, Gr. 55 Min.	55,000	$f = \begin{cases} 1 - 0.54(T - 0.460)^4 & T < 1.260 \\ 1.74 - 1.17(T - 0.460) & T > 1.260 \\ 0. & T > 1.947 \end{cases}$
2	ASTM A 515-70, Gr. 60 Min.	60,000	
3	ASTM A 515-70, Gr. 65 Min.	65,000	
4	ASTM A 515-70, Gr. 70 Min.	70,000	
5	ASTM A 285-70a, Gr. A Min.	45,000	
6	ASTM A 285-70a, Gr. B Min.	50,000	
7	ASTM A 286-70a, Gr. C Min.	55,000	
8	ASTM A 516-70a, Gr. 55 Min.	55,000	
9	ASTM A 516-70a, Gr. 60 Min.	60,000	
10	ASTM A 516-70a, Gr. 65 Min.	65,000	
11	ASTM A 516-70a, Gr. 70 Min.	70,000	
12	AAR TC128-70, Grs. A & B Min.	81,000	
13	ASTM A 537-80, Class 1 Min.	70,000	
14	ASTM A 302-69a, Gr. B Min.	60,000	
15	ASTM A 302-70a, Gr. B Min.	60,000	

**Table 8.1: For carbon steels, hard-coded room temperature tensile strength (column 3) and multiplicative adjustment factor that reduces that strength due to higher temperatures (column 4). Here, temperature, T, is in thousandths of Rankines. See [15].**

Stainless Steels			
ID	Description	$S_r$	Adjustment Factor
16	ASTM A 240-70, Type 304 Min.	75,000	$f = \begin{cases} 1 - 0.45(T - 0.860)/0.90 & 8.60 < T < 1.760 \\ 0.55 - 0.55(T - 1.760)/0.40 & 1.76 < T < 2.16 \\ 0. & T > 2.160 \end{cases}$
17	ASTM A 240-70, Type 304L Min.	70,000	
18	ASTM A 240-70, Type 316 Min.	75,000	$f = \begin{cases} 1 - 0.55(T - 0.860)/0.90 & 8.60 < T < 1.760 \\ 0.45 - 0.45(T - 1.760)/0.40 & 1.76 < T < 2.16 \\ 0. & T > 2.160 \end{cases}$
19	ASTM A 240-70, Type 316L Min.	70,000	

**Table 8.2: For stainless steels, hard-coded room temperature tensile strength (column 3) and multiplicative adjustment factor that reduces that strength due to higher temperatures (column 4). Here, temperature, T, is in thousandths of Rankines. See [16] and [17].**

Aluminum			
ID	Description	$S_r$	Adjustment Factor
20	ASTM B 209-70, Alloy 5052 Min.	75,000	$f = \begin{cases} 1 - 0.55(T - 0.860)/0.90 & 0.610 < T < 1.260 \\ 0. & T > 2.6 \end{cases}$
21	ASTM B 209-70, Alloy 5083 Min.	38,000	
22	ASTM B 209-70, Alloy 5086 Min.	35,000	<p>Here it is noted that the condition in AFFTAC's Computational Module that says TankMatID == 25 should say TankMatID &lt;= 25.</p>
23	ASTM B 209-70, Alloy 5154 Min.	30,000	
24	ASTM B 209-70, Alloy 5254 Min.	30,000	
25	ASTM B 209-70, Alloy 5454 Min.	31,000	
26	ASTM B 209-70, Alloy 5652 Min.	Possible AFFTAC Bug – No value provided	$f = \begin{cases} 1 - 0.48(T - 0.610)/0.25 & 6.1 < T < 8.6 \\ 0.52 - 0.52(T - 0.86)/0.40 & 8.6 < T < 1.26 \\ 0. & T > 1.26 \end{cases}$ <p>Here it is noted that T&gt;.86 might should be T &gt; 1.260 in the Computational Module.</p>
27	ASTM B 209-70, Alloy 6061 Min.	34,000	$f = \begin{cases} 1 - 0.83(T - 0.610)/0.35 & 6.1 < T < 9.6 \\ 0.17 - 0.17(T - 0.96)/0.30 & 9.6 < T < 1.26 \\ 0. & T > 1.26 \end{cases}$ <p>Here it is noted that T&gt;.86 might should be T &gt; 1.260 in the Computational Module.</p>

**Table 8.3: For different types of aluminum, hard-coded room temperature tensile strength (column 3) and multiplicative adjustment factor that reduces that strength due to higher temperatures (column 4). Here, temperature, T, is in thousandths of Rankines. There were possible corrections needed to the legacy strength model found as part of this background research. See [12].**



Before moving into a discussion of these models, it is worth noting that although the legacy hard-coded algebraic models mentioned at the beginning of this chapter are less general and are not available for editing by the user, they have been part of AFFTAC for decades. Therefore, they have been used more and have been part of more tests. Most importantly, however, they are simpler. Therefore, it is recommended that you also use these legacy strength models to provide results that you check against the results produced when using the Strength Model Database. Mistakes in units or errors in the code can be much more easily detected that way.

To use an entry in the Strength Model Database, when editing an analysis, click the **Switch to the Strength Model Database** button in the Edit Tank Car Properties window, which is the second in the four-window editing sequence. When you do that, the list of current entries in the Strength Model Database appears, and you may select one for the current analysis. That editing window, displaying the Strength Model Database, is shown in Figure 8.2

To edit or expand the entries in the database, click the **Edit Database** button, which appears when you click the **Switch to Strength Model Database**. When you click the **Edit Database** button, the Strength Model Database manager window appears, like that shown in Figure 8.3. From that window you may create new or delete existing database entries. If you choose to edit an entry, the window in Figure 8.4 appears, which shows that each strength model can implement either the Larson-Miller strength model, the ultimate tensile strength data, or both. The ultimate tensile strength model is described by the ultimate tensile strength entered as a function of temperature. The Larson-Miller model is described by the “Larson-Miller parameter” entered as a function of stress; the Larson-Miller model will be described in more detail in a later section.

Data is entered for these two models by clicking the appropriate buttons in Figure 8.4, which opens a property data entry window. An example of that window is shown in Figure 8.5 and allows for tabular entry of data (top of Figure 8.5) or, conversely, algebraic data entry (bottom of Figure 8.5).

The Larson-Miller strength model output is in two forms, which occupy two columns in the output viewed in the Main Window. The primary output of the Larson-Miller model is a metric referred to here as “Life Depleted.” This value, which starts at zero, represents the amount of accumulated damage in the tank material due to temperature and stress. It is a non-dimensional value; once it reaches the value of one, the life is completely depleted from the tank wall and it fails, thereby ending the simulation. The “Life Depleted” output might change very slowly at first and then grow rapidly as failure is neared. Therefore, the log of its value is displayed.

Another useful metric output by the Larson-Miller model is the internal tank pressure that would cause the tank wall to fail in one minute, given the damage that has accumulated in the tank wall up to that point in time. That internal burst pressure output takes the place

of the “burst pressure” column of data, which is displayed using the legacy strength model.

Shown in Figure 8.6 is a set of plots from a simulation that uses the Larson-Miller strength model. In the bottom left plot, the life depleted is shown. In the upper right plot, the “burst pressure” is plotted; again, this is the pressure at which the tank would fail in one minute given its accumulated damage.

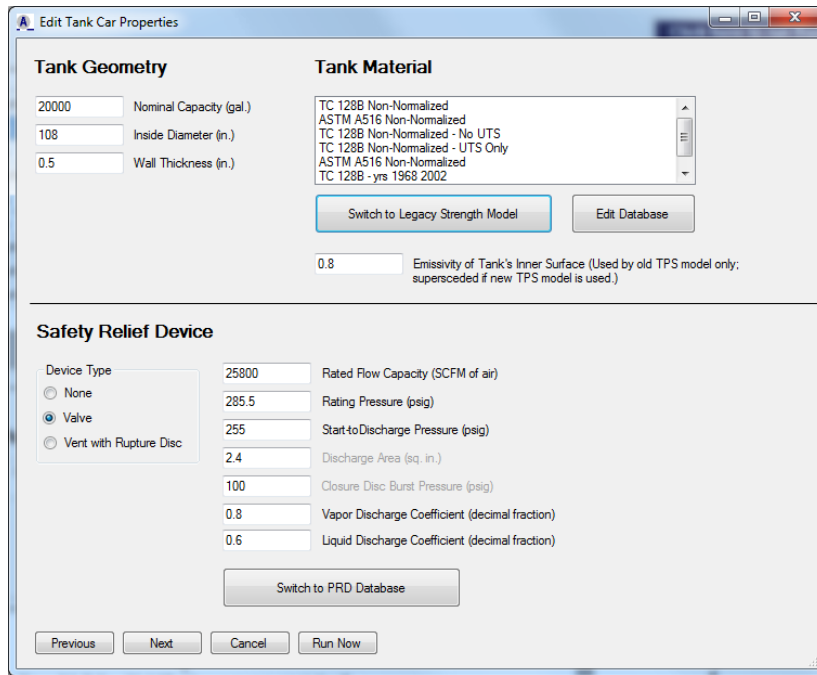


Figure 8.2: The Edit Tank Car Properties window in which the Strength Model Database has been selected.

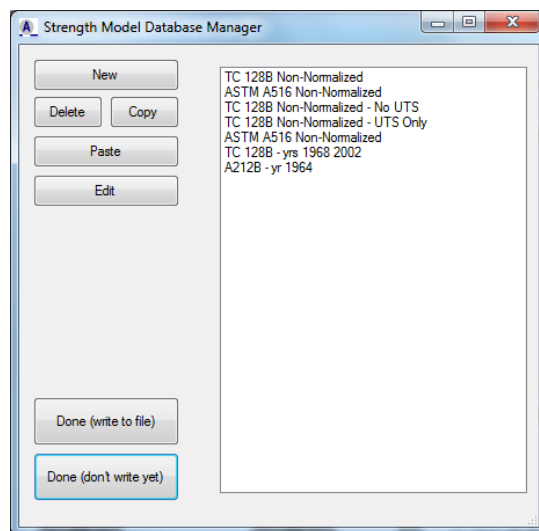
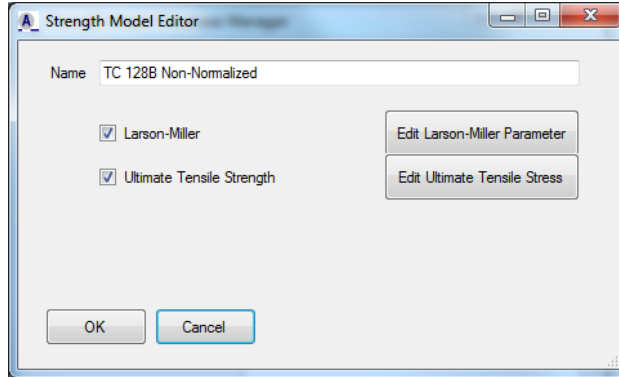


Figure 8.3: Failure Model Database management window.



**Figure 8.4: Editing window for new failure models. Larson-Miller and Ultimate Tensile Strength models are two of a set of future options.**

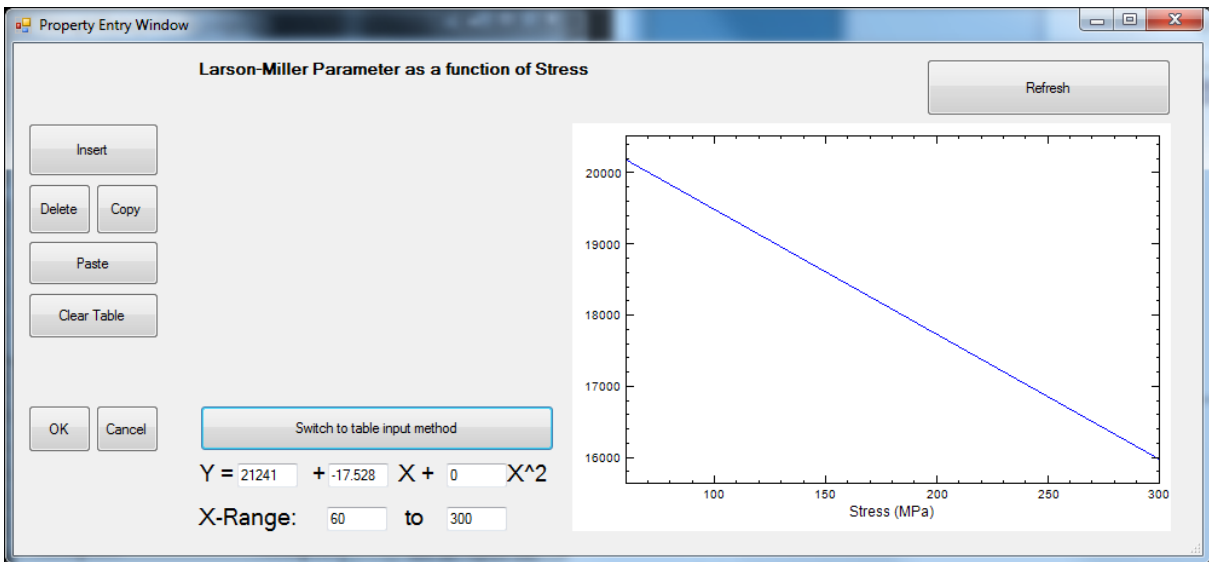
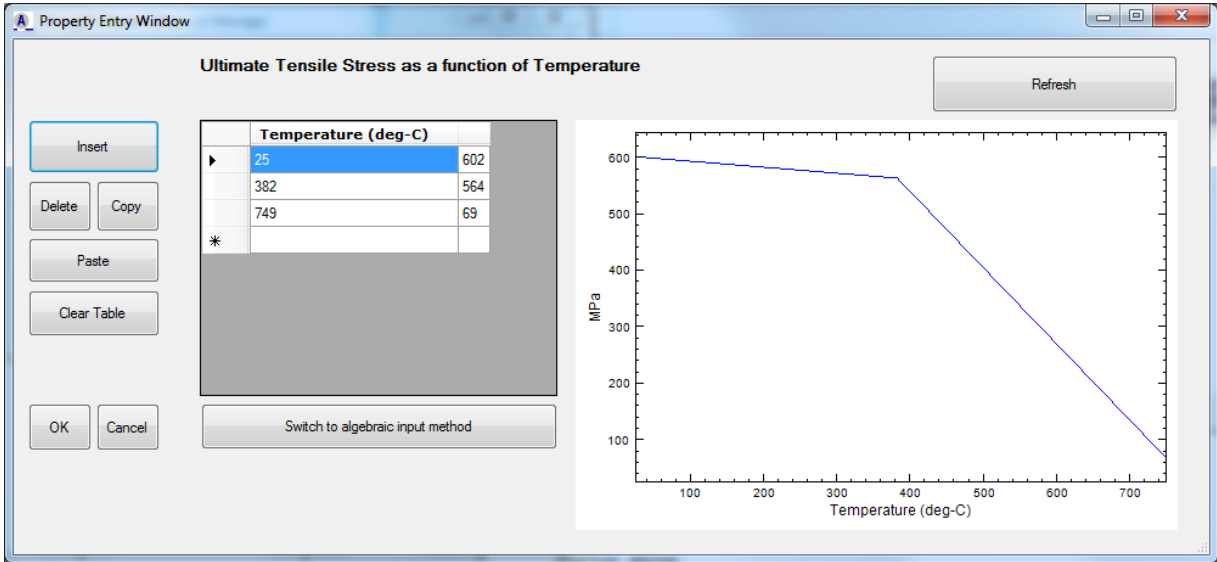
## Validated Entries in the Failure Model Database

AFFTAC comes shipped with a handful of steels that have been successfully validated against the Larson-Miller failure model in recent small-scale experiments. The validation procedure is described in [21]. In that report, the fits to the experimental data are shown. Also, verification tests that are part of the AFFTAC Regression Test Database are described in the *Verification and Validation Testing* document.

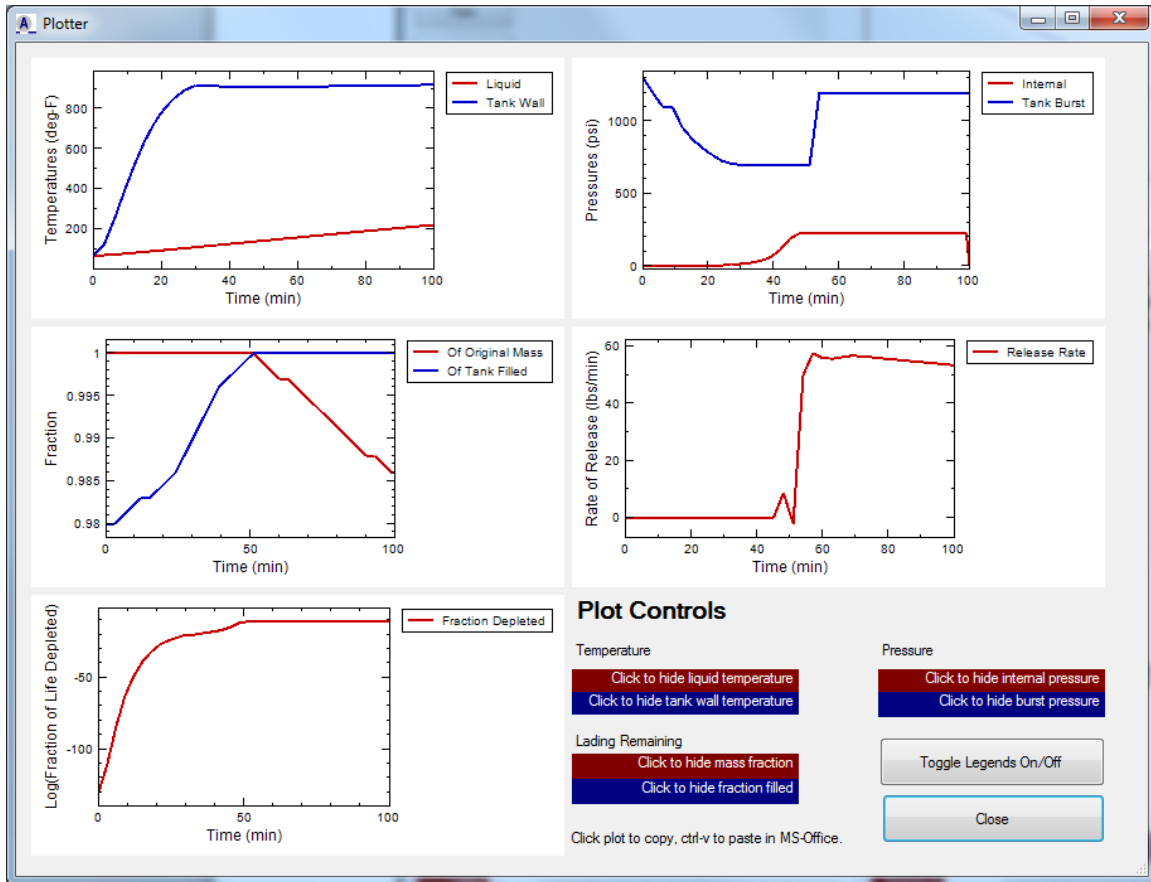
## Larson-Miller Model Theory

High stress at an elevated temperature creates damage in materials that accumulates over time. The damage is due to the migration and production of microscopic defects, both of which occur at higher rates as stress and temperature is increased. As the damage accumulates, the material becomes weaker and it creeps under loading. Eventually, the damage can accumulate to such a high level that the material fails.

Creep is usually discussed using strain as a primary quantity of interest. During a creep-to-failure test, the material is loaded with a constant temperature and stress. Many metals respond by straining at three different rates in distinct stages. The first stage is characterized by a strain rate that is relatively large. But this stage is short lived and quickly gives way to a prolonged second stage where the strain rate is relatively small. The second stage ends by transitioning to a third stage that is relatively short lived and is nonlinear. It is this third stage that ends relatively quickly and abruptly by failure of the material.



**Figure 8.5: Property entry window. The tabular of data entry is still available (top). But this window also accommodates polynomial data entry (bottom). The two modes are activated using the large button between the table and polynomial entry regions of the window.**



**Figure 8.6: New plotting capability that shows “Fraction of Life Depleted” when the Larson-Miller failure model is used**

The second stage is truly much larger than the other two, on the order of a thousand times greater. Thus it is often the exclusive focus of phenomenological failure modeling for engineering applications. The strain rate during that second stage is referred to using different terms including the “secondary strain rate”, the “steady-state strain rate”, and the “minimum strain rate”. All of these terms are correct and appropriate. Here, the term “secondary strain rate” will be used, and the variable will be denoted as  $\dot{\epsilon}_{ss}$ .

In deriving the Larson-Miller phenomenological failure model, it is assumed that the phenomena giving rise to the secondary strain can be modeled using the Arrhenius equation. The Arrhenius equation is empirical but has been found to accurately model several phenomena such as diffusion and reactions where temperature plays a key role. Insofar as the accumulation of damage that leads to ductile failure is like a diffusion process on the macroscopic scale, e.g., the diffusion of voids, it is reasonable to assert that the Arrhenius equation may be a good candidate for a phenomenological model. Experimental data has proven that this assertion is valid.

Therefore, proceeding along those lines of reasoning, it is suggested that the secondary strain rate is governed by the following Arrhenius type equation

$$\dot{\epsilon}_{ss} = Ae^{-\Delta H / RT} \quad 8.3$$

where

- $A$  = a material constant,
- $\Delta H$  = the activation energy of the phenomenon, which here is creep,
- $R$  = the Universal Gas Constant, and
- $T$  = absolute temperature.

Since  $\dot{\epsilon}_{ss}$  is considered to be a constant, it can equally well be expressed as a change in strain over a discrete time,  $\Delta t$ , so that the Arrhenius relation becomes

$$\frac{\Delta \epsilon}{\Delta t} = Ae^{-\Delta H / RT}. \quad 8.4$$

Equation 8.4 can be solved for  $\Delta H/R$  through straightforward algebraic manipulation. Doing so produces

$$\frac{\Delta H}{R} = T \left( \ln \left( \frac{A}{\Delta \epsilon} \right) + \ln(\Delta t) \right). \quad 8.5$$

$R$  is a constant and it is asserted that the activation energy is a function of stress alone. Thus the ratio on the left-hand side of the equation is thought to be a function of stress alone. As will be seen shortly, it is related to the Larson-Miller parameter, which is often abbreviated as *LMP* and will be introduced shortly.

Equation 8.5 applies for each incremental strain occurring over a time step. However, given that the strain rate is assumed constant during this second phase, the above relationship can be used to predict the time increment required for failure to occur. To be precise, if one sets  $\Delta \epsilon = \epsilon_f$ , which is the strain at which failure occurs and  $\Delta t = t_f$ , which is the time at which failure occurs, the above equation becomes

$$\frac{\Delta H}{R} = T \left[ \ln \left( \frac{A}{\epsilon_f} \right) + \ln(t_f) \right]. \quad 8.6$$

The strain at which failure occurs is assumed to represent the damage state that accumulates during creep before failure. It represents the final state at failure, regardless of how that state was achieved and is therefore assumed to be independent of time, temperature, and stress. For this reason, the first term inside the brackets is considered to be a constant for the material. Denoting that constant by  $C'$ , the above equation may be written as

$$\frac{\Delta H}{R} = T[C' + \ln(t_f)] \quad 8.7$$

This equation is very similar to the Larson-Miller relation, the only difference being the use of the natural logarithm as opposed to the base-10 logarithm. The Larson-Miller relation is

$$LMP(\sigma) = T[C + \log(t_f)] \quad 8.8$$

where  $LMP(\sigma)$  is the Larson-Miller parameter which is a function of stress and  $C$  is a constant. It has been found that, by experience,  $C = 20$  for most metals. In experiments that determine the Larson-Miller parameter, this assumption is often made at the outset (i.e.,  $C$  is often not measured). Solving for  $t_f$ ,

$$t_f(\sigma, T) = 10^{\frac{LMP(\sigma) - C}{T}}. \quad 8.9$$

The Larson-Miller parameter is found by loading a material at a constant temperature and stress and measuring the time to failure. In order to apply this value and the above relation in a transient situation, an assertion regarding the secondary strain rate is made. Specifically, it is asserted that while the secondary strain rate ( $\dot{\epsilon}_{ss}$ ) is a constant in time for a fixed temperature and stress, it will change instantaneously to a new fixed value if the temperature and/or stress change, thus  $\dot{\epsilon}_{ss} = \dot{\epsilon}_{ss}[\sigma(t), T(t)]$ .

Using this assertion, the time at which failure occurs during a transient simulation can be determined by integrating  $\dot{\epsilon}_{ss} = \dot{\epsilon}_{ss}[\sigma(t), T(t)]$  over time. When its time integral equals  $\epsilon_f$ , failure will occur. In other words,  $t_f$  is the solution to this equation:

$$\int_0^{t_f} \dot{\epsilon}_{ss}[\sigma(t), T(t)] dt = \epsilon_f \quad 8.10$$

or

$$\int_0^{t_f} \frac{\dot{\epsilon}_{ss}[\sigma(t), T(t)]}{\epsilon_f} dt = 1. \quad 8.11$$

Here it is important to note that

$$\dot{\epsilon}_{ss}[\sigma(t), T(t)] \cdot t_f[\sigma(t), T(t)] = \epsilon_f \quad 8.12$$

which is a way of restating the notion that the secondary strain rate is considered to be temporally invariant for a given stress and temperature, but that it will change in time if

stress and temperature change in time. This notion then results in a failure time that can also change in that same way. From Equation 8.12, the strain ratio is

$$\frac{\varepsilon_f}{\dot{\varepsilon}_{ss}[\sigma(t), T(t)]} = t_f[\sigma(t), T(t)] \quad 8.13$$

Using that in Equation 8.11 produces

$$\int_0^{t_f} \frac{1}{t_f[\sigma(t), T(t)]} dt = 1 \quad 8.14$$

where  $t_f$  is known from experimental data, i.e., Equation 8.9.

In an AFFTAC simulation, the above integral is computed using the rectangle rule. At each time step  $i = 1, 2, 3, \dots, n$ , with  $t = i \cdot \Delta t$  and the summation

$$\sum_{i=1}^n \frac{\Delta t}{t_f(\sigma(t_i), T(t_i))} \quad 8.15$$

is compared to unity. When it equals or surpasses unity, the material is considered to have failed. This quantity is referred to in AFFTAC as the “Fraction of Life Depleted.” When it equals zero, none of the life of the material has been depleted. When it equals unity, it has all been depleted and the tank fails.

### **Burst Pressure for the Larson-Miller Failure Model**

In the legacy failure model, a straightforward algebraic equation relates the material’s temperature to its ultimate tensile strength. From that, using simple geometric considerations described in the “Models for Internal Pressure, Stress, and Strain” chapter, the pressure inside the tank that will lead to bursting can be computed. Thus, when using the legacy models, one of the outputs in AFFTAC is the burst pressure as a function of time. That pressure is plotted on the same plot as the tank internal pressure. When those two lines cross, the tank fails.

In the Larson-Miller model, the relationship between temperature and failure is more complex. It involves time and also the stress history. However, the idea of a “burst pressure” is still extremely valuable and so AFFTAC defines one for the Larson-Miller model to be as follows: “The Larson-Miller burst pressure is the pressure that would cause the tank, given its temperature-stress history and accumulated damage, to fail in one minute.”

To derive the equation for that pressure, we start with the summation in Equation 8.15, above, evaluated at time step  $t_n = n\Delta t$ ,



$$S_n \equiv \sum_{i=1}^n \frac{\Delta t}{t_f(\sigma(t_i), T(t_i))} \quad 8.16$$

We seek a stress,  $\sigma(t_{n+1})$ , such that  $S_{n+1} = 1$  in 1 minute. Or,

$$S_n + \frac{1 \text{ min}}{t_f(\sigma(t_i), T(t_i))} = 1 \quad 8.17$$

Solving for  $t_f$ ,

$$t_f(\sigma(t_i), T(t_i)) = \frac{1 \text{ min}}{1 - S_n} \quad 8.18$$

This value can be used to solve for stress in a two-step process starting first with Equation 8.8, in which the above expression for  $t_f$  is inserted, producing

$$LMP(\sigma) = T \cdot \left[ \log\left(\frac{1 \text{ min}}{1 - S_n}\right) + C \right] \quad 8.19$$

This is the first step in computing the burst strength; it gives a value for the Larson-Miller parameter. The second step to finding the burst stress is to perform an inverse lookup,  $\sigma = \sigma(LMP)$ , of the experimental data or the curve fit to that experimental data. In other words, given the value of LMP from the above equation, the experimental data or curve fit is used to find the corresponding value of  $\sigma$ . Lastly, that value of tensile stress is converted to an internal pressure through geometric considerations described in the chapter entitled “Models for Internal Pressure, Stress, and Strain”.

### Interactions with Other Models

In AFFTAC’s thermal model, the tank wall is divided into different segments. In the simplest applications of AFFTAC, the tank wall is divided into two, with one segment being adjacent to the liquid and the other adjacent to the vapor. In the liquid segment, the tank wall’s temperature is set equal to the lading temperature because of the liquid’s relatively large thermal mass. But in the vapor segment, a thermal model specifically for the wall is used to evolve that part of the tank wall’s temperature over time.

The ability to subdivide those two segments into smaller sub-segments was added to allow you to specify variations in percent coverage of the insulation as a function of angle on the tank in the new, generalized TPS model. While all of the sub-segments adjacent to the liquid are still set to the liquid’s temperature, with the angular dependence

capability, the parts adjacent to the vapor may have temperatures that vary from sub-section to sub-section.

To implement a creep and failure model, it is necessary to keep track of the history for each point on the tank. Or, put another way, it is necessary to sum Equation 8.15 for each distinct angle. Any given point on the tank wall may be adjacent to liquid and then, later, vapor. This history must not be overlooked. Rather, it is tracked for each individual point on the tank.

To meet this requirement, an array with 180 “tracking points” is established where each of the 180 points represent tank material over a span of one degree on the tank wall. The life depleted value for the array is initialized to zero. At each time step, the life-depleted value for each point is incremented using Equation 8.15 with the overall tank wall stress and the temperature at that point on the tank as inputs. After the array is updated, their values are compared to unity. If any of them exceed unity, a flag is set indicating that the tank has failed; the simulation is then terminated.

## **Ultimate Tensile Strength Data**

As mentioned earlier in this chapter, the ultimate tensile strength (UTS) model is implemented in a way very similar to the legacy AFFTAC failure model. In the new UTS model, the input data is queried to determine the UTS of the tank at the highest temperature in the tank wall. Using that value, the internal pressure sustainable by the tank wall is computed. If the actual pressure inside the tank exceeds that computed pressure, failure occurs. The only difference between this model and the legacy version is that you can specify the UTS using polynomial or tabular entry whereas the legacy version uses hard-coded equations. The legacy model is retained in AFFTAC to maintain backward compatibility and for providing benchmark calculations against which the more general failure models can be compared. Both the new UTS model and the Larson-Miller failure model, which are contained in the Strength Model Database can be run simultaneously during a simulation.

# **Pressure Relief Devices and the PRD Database**

There are two ways of specifying the pressure relief device (“PRD”) in an AFFTAC simulation. One is to enter the appropriate values in the Edit Tank Car Properties window, which is the second of the four windows encountered when editing an analysis. Those values relate to the valve’s flow capacity, pressure at which it will open, and certain coefficients that make the flow models more accurate in predicting the discharge rate.

Another way to specify the PRD is to use the PRD Database. As with the other databases in AFFTAC, you can specify all the parameters describing a PRD by simply selecting an entry in the PRD database. When the simulation is run, these parameters are transmitted to the Computational Module.

Regardless of which data entry method is used, the same models are used in the Computational Module. The advantage of entering the values for the PRDs directly is that it can make performing trend studies and sensitivity studies easier. With just a few clicks, you can explore the sensitivity of the simulation to the PRD, e.g., the flow capacity. The advantage of using the database is that it contains PRDs referenced by model number where the parameters have been found through detailed calibration studies. AFFTAC is shipped with 10 entries in the PRD database, all calibrated using recently obtained data. The calibration exercise is described in the accompanying *AFFTAC Verification and Validation Testing* document.

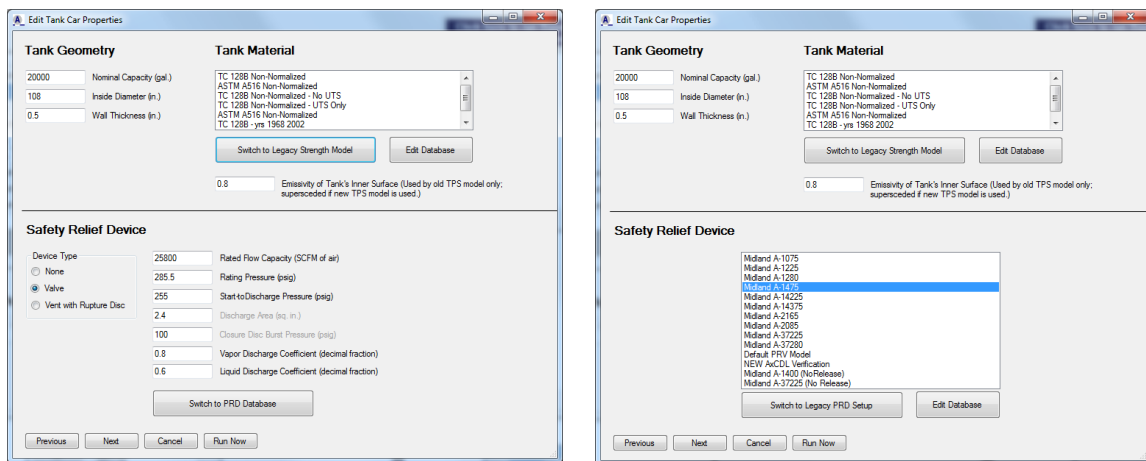
In the following sections, the two methods for entering PRD specifications are described. After that, a detailed description of the theory underpinning the flow models is provided. A description of the input values required to specify a PRD is provided below. A more thorough understanding of these values can be obtained by reading the theory section in this chapter.

<b>Input Value</b>	<b>Applies To</b>	<b>Description</b>
Rated Flow Capacity	Valves	This value describes the amount of air vapor that the PRV can discharge when tested at a specific pressure, which is the “Rating Pressure.”
Rating Pressure	Valves	This is the pressure at which the PRV was tested to determine its rated flow capacity.
Vapor Discharge Coefficient	Valves and Vents	This is a coefficient used to make the flow model more accurate for modeling vapor flow. Because of various obstructions and geometries unique to each PRD, this coefficient is specific to a PRD type.
Liquid Discharge Coefficient	Valves and Vents	This coefficient has the same meaning as the Vapor Discharge coefficient but is for liquid discharge.
Start-to-Discharge Pressure	Valves	This is the value at which the valve will start to open and discharge lading. Note that the valve opening and closing behavior involves other values and hysteresis. Please refer to subsequent sections on PRV opening-closing behavior for more information.
Discharge Area	Vents	This is the area through which the lading flows when a vent is the PRD. Note that for a valve, the area is estimated from the rated flow capacity whereas for vents it is entered directly. This aspect is different and is generalized in the PRD Database.
Closure Disk Burst Pressure	Vents	This is the analog of the start-to-discharge pressure for valves. The difference is that a vent, once ruptures, never closes.

**Table 9.1: Parameters used in modeling PRDs**

## Specifying a PRD Directly during the Editing Sequence

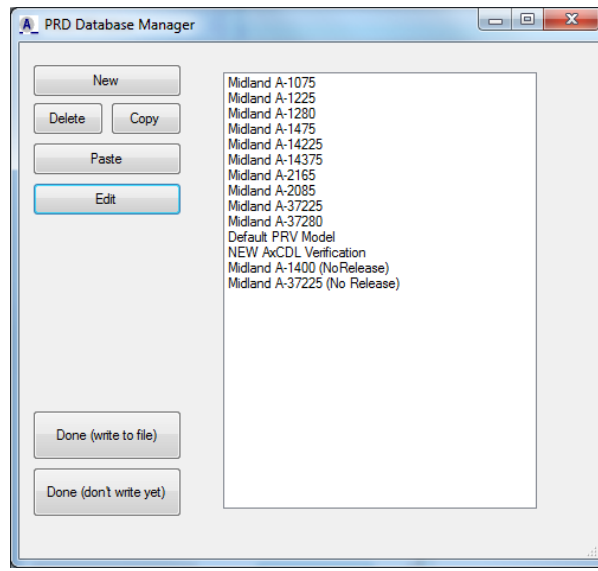
To specify the parameters describing a PRD directly in an analysis, click the **Switch to Legacy PRD Setup** button in the Edit Tank Car Properties window, which is the second of the four-window editing sequence for an analysis. When you click that button, the lower part of the Edit Tank Car Properties window will take on the appearance like that shown in Figure 9.1 (left). As can be seen from the figure, there are two types of PRDs, a valve and a vent with rupture disk. The values specifying their performance were described in Table 9.1 and can be more fully understood by reading the theory section later in this chapter.



**Figure 9.1:** The Edit Tank Car Properties window shown in two modes in the bottom portion of the window. On the left is the traditional, direct entry of PRD values. On the right, is the PRD Database mode.

## Specifying a PRD using the PRD Database

The PRD Database provides pre-calibrated pressure relief valves (PRVs) listed by name. This database can also be expanded to include other PRVs and vents with rupture disks. To use the PRD database, click the **Switch to PRD Database** button in the Edit Tank Car Properties window, which is the second in the four-window editing sequence for an analysis. When you click that button, the lower part of the Edit Tank Car Properties window changes to display the PRD database, as shown in the right part of Figure 9.1. From the list in the lower part of the window, you can select a PRD for your analysis. You can also edit the database by clicking the **Edit Database** button. When you do, the window in Figure 9.2 appears in which you can create new, edit, or delete PRDs.

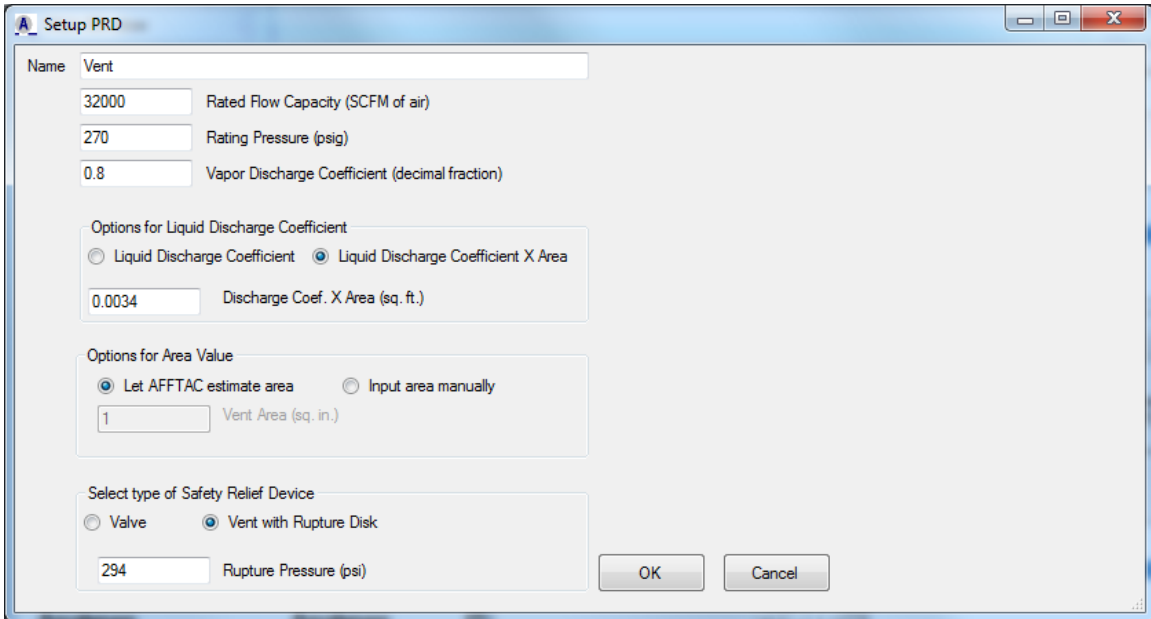
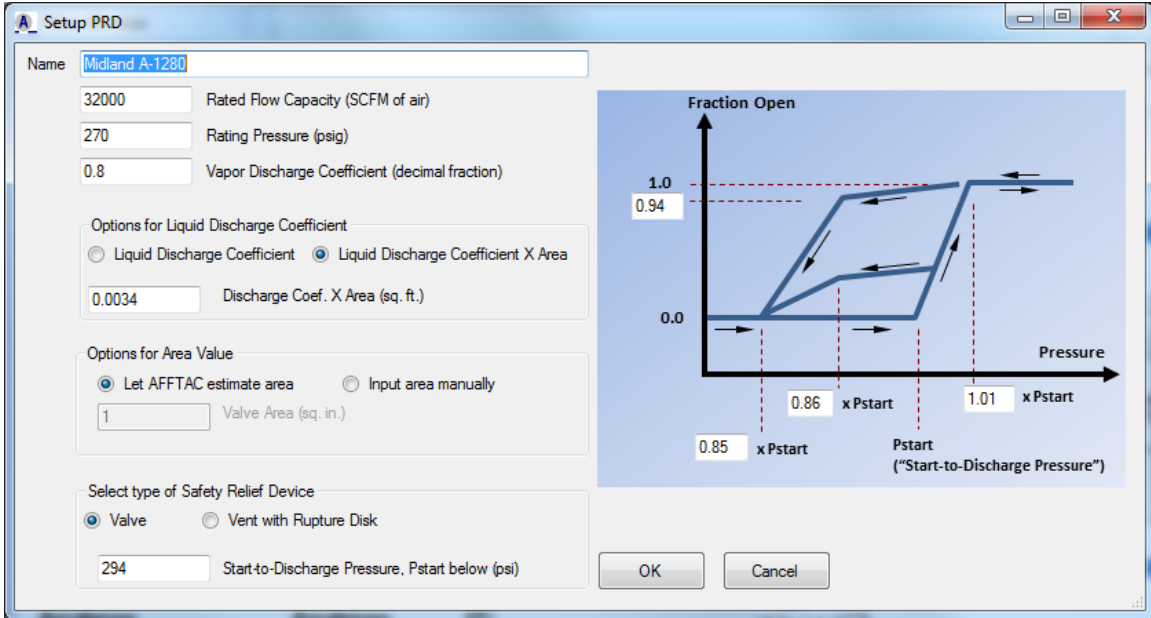


**Figure 9.2: PRD database manager**

To edit a PRD, either double click on the name or highlight it and click the **Edit** button. When you do, a window that resembles the one in Figure 9.3 will appear. The version of the window shown in the upper part of Figure 9.3 is for a PRV while the one in the lower part of the figure is for a vent with rupture disk. The inputs common to both valves and vents will be discussed below, after which specifics to PRVs and vents will be discussed

Similar to the old style of PRD inputs, the window for PRD Database entries has the flow rating and flow rating pressure. However, the PRD Database allows for more flexibility regarding the relationship between the experimental data obtained using vapor flow and the experimental data obtained using liquid/two-phase flow. In the PRD database, the specifications relating vapor flow and liquid flow may be kept separate, if you wish. For example, you may enter a rated flow capacity and rating pressure, which together allow AFFTAC to estimate an area for the PRD. But then you may still choose to enter a value for area times the coefficient of liquid discharge. When vapor is flowing through the PRD, the rated flow capacity and pressure are used. When liquid is flowing through the PRD, the area times coefficient of liquid discharge is used. These two sets of data may be different from each other and, in practice, do not even have to be consistent.

However, you may also choose to link the liquid and vapor discharge inputs. For example, you may request that AFFTAC estimate the PRD area, which uses the flow capacity and pressure you input and then enter only a coefficient of discharge for the liquid flow. Doing so will require AFFTAC to use the area it estimates from the vapor flow data. AFFTAC's method of estimation is described in the theory section of this chapter and more fully in Appendix D.



**Figure 9.3: Window for editing a specific entry in the PRD Database. The mode shown in the upper window is for a valve. The mode shown in the lower window is for a vent.**

## Specifics for a PRV

When you select the type of PRD to be a pressure relief valve (PRV), the window displays a chart showing the nonlinear and hysteresis open-close behavior of the PRV. This behavior is discussed in more detail in “Modeling the Opening and Closing of PRDs” later in this chapter and the process for finding the parameters are in the *AFFTAC Verification and Validation Testing* document.

The primary quantity of interest for the open-close behavior is the start-to-discharge pressure, which is entered on the left-hand side of the window. In the plot, that value is referred to as “P-Start”. The valve begins to open at P-Start and is fully open at a value greater than P-Start. That value is 1.01 in the upper window in Figure 9.3, but you are free to enter whatever value is appropriate for the valve you are modeling. If the pressure decreases at any time after the PRV is open, the closing path is different than the opening path. If it is fully open when the pressure decreases, it follows the upper curve shown in Figure 9.3. If it is not yet fully open, it follows the lower curve. The control points that define the closing paths are all inputs that you are free to specify. Again, this is discussed more fully in the section entitled “Modeling the Opening and Closing of PRDs,” later in this chapter

## Specifics for a Vent with Rupture Disk

For a vent with a rupture disk, the graph of open-close behavior is not present. Instead, the only value of relevance is the start-to-discharge value, which is when the rupture vent bursts.

## Theory for Modeling flow through a PRD

There are four different scenarios in which the tank can lose lading through the PRD. They are illustrated in Figure 9.4. In the two cases where vapor alone is being ejected, the classical model for choked vapor flow, described in a subsequent section, is used. In the two cases where liquid is being ejected, it is assumed that some of the liquid might evaporate during the process resulting in two-phase flow. Therefore, a two-phase isentropic, inviscid flow model is used in some of those cases.

The flow models for choked flow and two-phase flow are discussed in the following subsections. A summary of the mass transport scenarios is tabulated below.

<b>Tank Contents</b>	<b>Flowing Out</b>	<b>Supporting Model</b>
Liquid and Vapor	Vapor	Choked Flow or Low-Speed Flow
Liquid and Vapor	Liquid	Two-Phase Flow
Liquid	Liquid	Liquid or Two-Phase Flow
Vapor	Vapor	Choked Flow or Low-Speed Flow



As mentioned above, AFFTAC has the ability to estimate the discharge area of the PRD, which is the minimum area. The choked flow model, which is used for vapor discharge, is also used for that purpose. Therefore, the choked flow model is described first. Then the liquid and two-phase discharge models, which require information about area, are described.

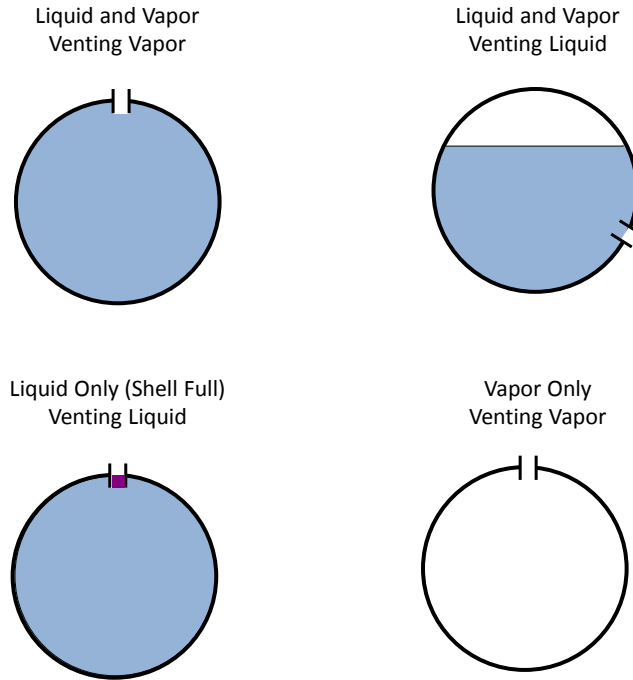


Figure 9.4: Illustration of the four different scenarios for lading release

### Choked Flow Model

If the total pressure within the tank is greater than 27.0 psia, 12.3 psig, the flow of vapor through the relief device can be modeled as choked flow. The value of 12.3 psig is the pressure required to sustain choked flow. The classical equation for choked flow of a compressible gas flow through a nozzle is therefore used. That model is derived in detail in Appendix B and is

$$w = 144C_{DV}A_vP\sqrt{\frac{g\gamma}{ZRT}\left[\frac{2}{\gamma+1}\right]^{\frac{\gamma+1}{\gamma-1}}} \quad 9.1$$

where

- $w$  = mass flow rate (lbs/sec)
- $A_v$  = minimum cross-sectional area of the valve (ft<sup>2</sup>)
- $C_{DV}$  = valve discharge coefficient
- $P$  = upstream gas pressure (psia)

$T$	=	upstream gas temperature (absolute, deg-R)
$g$	=	gravitational constant (ft/sec <sup>2</sup> )
$Z$	=	gas compressibility factor
$R$	=	gas constant, equal to 1,545/(molecular weight) (ft/deg -R)
$\gamma$	=	ratio of specific heats

Most of the terms in the above equation are constants and are therefore separated into a single value. Specifically, the constant  $V_{con}$  is defined as follows:

$$V_{con} \equiv 144 \sqrt{\frac{g\gamma}{R} \left[ \frac{2}{\gamma+1} \right]^{\frac{\gamma+1}{\gamma-1}}} \quad 9.2$$

so that the first equation for the mass flow rate may be written

$$w = V_{con} \frac{C_{DV} A_v p}{\sqrt{ZT}} \quad 9.3$$

The above equation is used for each constituent in the vapor, where  $p$  becomes the constituent's partial pressure,  $p_i$ . The effect of the padding gas on the mass flow rate becomes negligible after a short period of time, because its mass is small compared to that of the lading.

In this model and the ones that follow, the above equation is multiplied by yet one other parameter, the "fraction open", which varies between zero and unity. The fraction open parameter is used to model the opening and closing of valves and has a model of its own, which will be discussed in a subsequent section.

### Estimation of the PRD's Area using the Choked Flow Model

The choked flow model can be used in AFFTAC to compute the minimum cross-sectional area of the PRD. It does it by using experimental data entered by the user, specifically, the "rated flow capacity", "rating pressure", and "coefficient of vapor discharge" as described in Table 9.1. It is assumed that the experimental data was obtained using air at room temperature. For air under those conditions,  $Z = 1.0$ ,  $\gamma = 1.4$ ,  $R = 53.3$  ft-lbf/lbm-deg-R,  $T = 519.7$  deg-R (60 deg-F). In those conditions, the density of air is 0.0763 lbm/ft<sup>3</sup>, which is required because the rated flow capacity is given in cubic feet per minute. Substituting those values into the above equation produces the following estimate for the valve area which appears in this form in the Computational Module:

$$A_v = \frac{m_r}{C_{DV} p_s 2644} \quad 9.4$$

However, there is a non-trivial amount of units conversion embedded in this equation. How this equation is arrived at is described in detail in Appendix D.

### Low Speed Vapor Flow

If the total pressure within the tank is greater than atmospheric pressure (14.7 psia), but less than 12.3 psig, the flow can no longer be considered choked. In these cases, the amount of vapor flow produced during a choked condition is computed and then scaled downward accordingly.

### Two-Phase Flow

When liquid escapes through the pressure relief device, its pressure and temperature drops leading to the creation of some vapor from the liquid state. The resulting situation is known as “two-phase flow” and can occur any time liquid is being ejected.

The model for two-phase flow assumes that the flow is inviscid, which means that the Bernoulli equation can be applied along any streamline. The streamline that flows through the middle of the relief device is chosen for the analysis. For any two points, 1 and 2, on the streamline, the Bernoulli equation states that

$$V_2^2(p_2) = V_1^2 + 2g \int_{p_1}^{p_2} \frac{dp}{\rho} \quad 9.5$$

where  $V$  is the speed at those points and  $p$  is the pressure. Since the pressure is a function of temperature, the above integral may be rewritten as

$$V_2^2(p_2(T)) = V_1^2 + 2g \int_{p(T_1)}^{p(T_2)} \left( \frac{dp}{dT} \right) \frac{dT}{\rho(T)} \quad 9.6$$

For this analysis, Point 1 is assumed to be located far from the opening so that, when there is no padding gas present,  $V_1$  can be assumed to be zero. When padding gas is present, the saturated condition of the liquid flow through the valve will be reached after the fluid has been given some velocity. In this circumstance, the initial velocity is approximated as

$$V_1 = \sqrt{\frac{2gp}{\rho}} \quad 9.7$$

In either case,  $V_1$  is known and so is  $p(T_1)$ , the bulk pressure inside the tank.

For any value  $T_2$ , which corresponds to some unknown position along the streamline, the above integral can therefore be used to compute the speed  $V_2(p_2)$  at a second point. The

objective is to find the temperature  $T_2$  that corresponds to the point along the streamline where the cross-sectional area of the flow is a minimum. When that point is found, it is used to compute the mass flow rate.

Point 2 is found using the above integral with the help of an additional constraint, which is that the entropy of the liquid-vapor mixture is constant. The integral form of the Bernoulli equation, plus the constraint of isentropy provides the theoretical backbone of the algorithm to compute two-phase flow through the relief device. The integral in Equation 9.6 is approximated as this summation:

$$V_2^2 = V_1^2 + 2g \sum_{i=1}^? \frac{1}{\rho(T_1 + i\Delta T)} \frac{dp}{dT} \Delta T \quad 9.8$$

The summation is not carried out at once, but instead in a step-by-step fashion. Because of the temperature-pressure relationship, each addition of a term in the summation represents a small step along the streamline. At each step, the specific entropies (recall  $\Delta S = \Delta Q/T$ ) of the liquid and vapor are computed as follows:

$$\text{Liquid State: } S_L(T) = S_{L1} - c_{p-liq} \frac{T - T_1}{(T + T_1)/2} \quad 9.9$$

$$\text{Vapor State: } S_V(T) = S_L(T) + \frac{H_v}{(T + T_1)/2}$$

Where  $c_{p-liq}$  is the liquid's specific heat. Based on the assumption of isentropy, the

$$\text{Combined total entropy: } S(T) = \lambda S_L(T) + (1 - \lambda) S_V(T) \quad 9.10$$

must remain constant. Therefore requiring

$$S(T) = \lambda S_L(T_i) + (1 - \lambda) S_V(T_i) \quad 9.11$$

at each step allows the ratio  $\lambda$  to be computed at each step. With the value obtained for  $V(T_i)$  and the ratio  $\lambda$ , which allows for the density to be computed, the cross-sectional area at step  $i$  can be computed.

Calculations proceed for  $i = 1, 2, \dots$ , at each step computing  $\lambda$  and the cross-sectional area. When the cross-sectional area reaches a minimum value, the computations are

stopped. That cross-sectional area is used with the speed and density computed at that point to provide the estimate for the mass flow rate for the two-phase flow.

However, as with the other flow models, e.g., the choked vapor flow model, if the PRD is a valve, the resulting cross-sectional area is multiplied by the “fraction open” parameter to represent the opening and closing of the valve. The model for the fraction open parameter is provided in a later section.

For alternative wording describing this model, you might also find it helpful to consult the chapter on PRV flow model validation in the *AFFTAC Verification and Validation Testing* document.

### Liquid Ejection in the Shell Full Condition

The shell full condition occurs when the tank is completely full of liquid. In that scenario, the flow model is used for a different purpose, which is to compute the tank’s internal pressure. The flow rate is already known by computing the difference between the volume of the liquid as it expands due to heating and the volume of the tank. That required flow rate is used as an input into the flow model to compute the amount of pressure that would be required to drive that much flow. That required pressure is then reported as the pressure inside the tank, which is in turn used to help compute the amount of expansion in the tank wall and, more importantly, to determine if the tank has failed under that pressure.

The specific volume, which is specified as a function of temperature by the user, is used to compute the expansion that would occur if the liquid were completely unconstrained. The volume of the tank is subtracted from that volume and divided by the time step length to determine the flow rate. Then, the Bernoulli equation is used to provide an estimate of the pressure required to expel that amount during the time step. For this situation, which is depicted in Figure 9.5, the Bernoulli equation is

$$\frac{1}{2} \rho V_s^2 = g(p_c - p_s) \quad 9.12$$

The velocity  $V_s$  is related to the mass flow rate through the following relationship<sup>2</sup>

$$V_s = \frac{\text{MassFlow Rate (lbs/sec)}}{\text{Liquid Discharge Coefficient} \times \text{Device Opening Area} \times \text{Density (lbs/ft}^3\text{)}} \quad 9.13$$

all of which are known. Therefore, the Bernoulli equation can be used to determine  $p_c$ , the upstream pressure, in terms of  $p_s$ . To provide an estimate<sup>3</sup>,  $p_s$  is assigned the value of the saturated vapor pressure or the atmospheric pressure, whichever is higher. Once  $p_c$  is

<sup>2</sup> See Appendix B for a discussion on the use of the liquid and vapor discharge coefficients.

<sup>3</sup> Consideration of two-phase flow effects for high vapor pressure ladings might result in a slightly lower tank pressure, but the difference would be small.

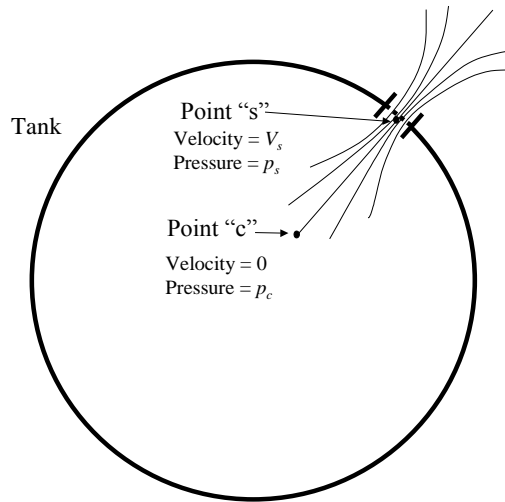
computed, it is used to determine what type of flow conditions exist. The final form of the equation used to compute the pressure required to produce sufficient lading ejection is

$$\hat{p}_{com} \left( \frac{\text{lbf}}{\text{ft}^2} \right) = \hat{p}_{min} \left( \frac{\text{lbf}}{\text{ft}^2} \right) + \frac{1}{64.4 v_{liq}} \left( \frac{Q_{liq}}{720 \cdot C_{DL} \cdot A_{areq}} \right)^2 \left( \frac{\text{lbf}}{\text{ft}^2} \right) \quad 9.14$$

where

$\hat{p}_{min}$	Taken to either atmospheric pressure or the lading vapor pressure, whichever is less
$Q_{liq}$	The amount of lading that must be ejected
$A_{areq}$	The area of the pressure relief device
$C_{DL}$	The liquid discharge coefficient

The hard-coded numbers in the above equation are to handle units and mass-to-volume conversion. A thorough derivation of that equation is given in Appendix E.



**Figure 9.5: Configuration representing the expulsion of liquid due to thermal expansion while in the shell full condition**

In addition to determining the pressure required to expunge the lading, the model attempts to determine if any *additional* lading is expelled during the current time step. In one case, if  $p_s$  is not sufficiently high, the flow through the relief device is assumed to be in the liquid phase. It is assumed that the device will accommodate the amount of mass flow, but no more than that will leave. Therefore, the tank will remain shell full having expelled exactly the amount that is due to thermal expansion. This situation occurs for a

vent if  $p_s < p_{atm}$  (atmospheric pressure) and as a result, the total pressure inside the tank is set to  $p_{atm}$ . Likewise, this situation occurs for a valve if  $p_s < P_{close}$  (valve closing pressure) and as a result, the total pressure in the tank is set to  $P_{close}$ .

If  $p_s$  is sufficiently high (greater than  $p_{atm}$  for a vent or greater than  $P_{close}$  for a valve), it is assumed that two-phase flow occurs. In this situation, the two-phase flow model discussed previously is invoked to determine the mass flow rate. If, in the case of an upright car, enough lading can be expelled in the vapor phase so that the tank will not be shell full at the end of the time step, the tank is no longer considered to be shell full and a logical flag in the program is set to record that fact. Otherwise, the tank remains shell full.

## Modeling the Opening and Closing of PRDs

AFFTAC accommodates two different types of pressure relief devices. The opening and closing models for these two types both have the same purpose, to provide a multiplier (the “fraction open” value) for the flow area available, which is used in the flow models previously described. The models for these two types of devices are described below.

### Spring-Loaded Pressure Relief Valve (PRV)

A pressure relief valve (PRV) is spring loaded so that it remains closed unless a sufficient amount of pressure builds up inside the tank. If a certain pressure is exceeded, the valve opens an amount that is approximately proportional to the excess pressure. As lading is released and the pressure differential decreases, the valve’s spring begins to close it again.

There are some subtleties to how the valve performs, most notably, hysteresis. This subtlety and others are captured in Figure 9.6. The path followed during opening is indicated by the arrows that point towards the right. Once the “Start-to-Discharge” pressure  $P_s$  is reached, the valve begins to open in proportion to the amount that pressure is exceeded. If the pressure continues to increase, the valve will eventually be fully open.

There are two paths that the valve can follow when closing. If the valve is fully open and the pressure drops below the full open pressure ( $F_{full\_open}$  times  $P_s$ ), the valve will begin to close an amount that is proportional to the difference between the full open pressure and a reference closing pressure ( $F_{elbow}$  times  $P_s$ ). The fraction open at  $F_{elbow}$  is  $f_{elbow}$ . Once  $F_{elbow}P_s$  is reached, the valve will become more sensitive; the rate of closure with respect to the pressure increases until it is fully closed at  $F_{full\_close}$  times  $P_s$ . That path is marked “A”. The other path, marked “B”, is followed if the pressure begins to drop before the valve is fully open.

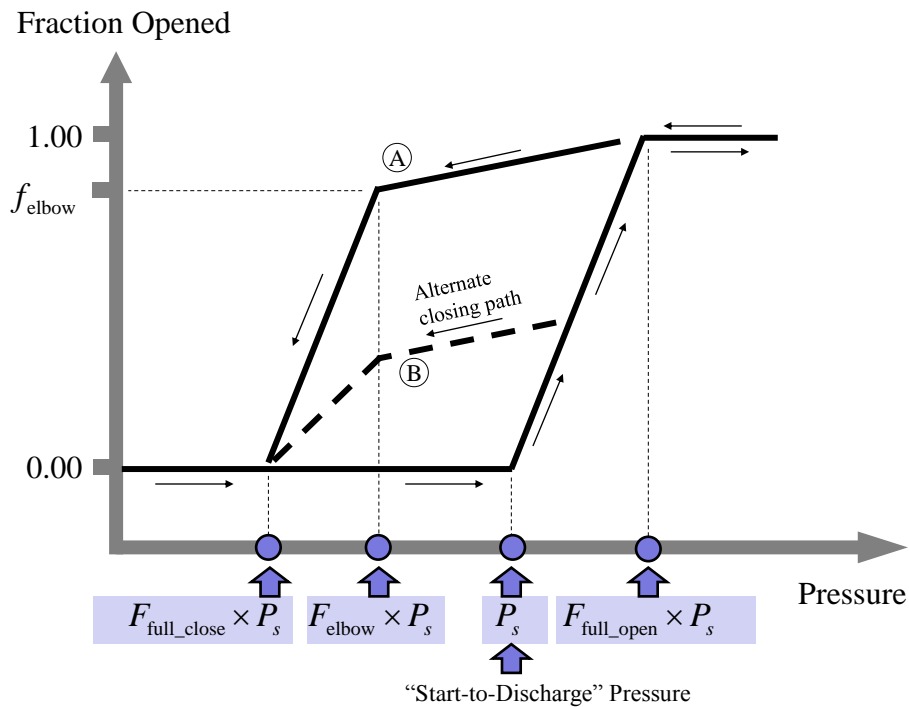
Prior to AFFTAC 4.00, the values  $F_{full\_open}$ ,  $F_{closure}$ ,  $F_{elbow}$ , and  $f_{elbow}$  were hard-coded. When you choose to specify a PRV by typing values directly into the Edit Tank Car Properties window, which is the second in the four-window sequence encountered when

editing an analysis, it is those same hard-coded values that are used. They are shown in the table below.

Hard-Coded PRV Open-Close Modeling Values used in Old Setup Method	
$F_{full\_open}$	1.03
$F_{closure}$	0.82
$F_{elbow}$	0.88
$f_{elbow}$	0.85

**Table 9.2: Default parameters for valve opening and closing model**

However, if you choose to use the PRD Database, you have the freedom to change these values. In a recent experimental and validation exercise described in the *AFFTAC Verification and Validation Testing* document, values for these key parameters as well as areas and coefficients of liquid discharge were determined and used to establish a database of PRVs manufactured by Midland Manufacturing. Those values are shown in the Table 9.3. AFFTAC is shipped with these entries. However, you can edit and expand this database as needed. Very important details regarding how these values were obtained are documented thoroughly in *AFFTAC Verification and Validation Testing*, a companion document to this *User's Manual*. You are encouraged to refer to that document to understand more.



**Figure 9.6: Model for the spring-loaded pressure relief valve**



Model No.	Pressures (psig)		Fraction of the Measured Start-to Discharge Pressure			Fraction Open
	Nominal Start-to-Discharge	Measured Start-to-Discharge	Full Open	Descent	Close	At Descent (Point "A")
A-1075	75	81	1.01	0.69	0.69	0.94
A-1225	225	276	1.03	0.71	0.69	0.95
A-1475	75	81	1.09	1.07	0.91	1.00
A-14225	225	228	1.11	0.89	0.82	0.54
A-14375	375	401	1.05	0.94	0.91	1.00
A-2165	165	156	1.10	1.04	0.85	1.00
A-2085	75	74	1.12	1.03	0.81	0.99
A-37225	225	197	1.03	0.87	0.71	1.00
A-37280	280	280	1.00	0.86	0.54	1.00
A-1280	280	294	1.00	0.86	0.85	0.94

Table 9.3: Results of the model calibration exercise for the valve opening and closing model

### Frangible Disk

The model for the frangible disk is straightforward. If the pressure differential across the disk is less than the user-specified disk burst pressure, there is no opening. However, once the pressure increases beyond that burst pressure, the disk is destroyed and the release area defined by the user is present for the remainder of the simulation (fraction open = 1).



# Models for Internal Pressure, Stress, and Strain

## Modeling Pressure Inside the Tank

The pressure of the vapor is computed using the partial pressures of the vapor's constituents. For ladings that are a pure substance, the total vapor pressure is the sum of the vaporized lading's pressure plus that of the padding gas, if present. For a solution, it is the sum of the partial pressures of the solution's vaporized constituents plus the pressure of the padding gas.

When the quantity of liquid in the tank is very small, the remaining vapor is treated as an ideal gas. The temperature from the previous time step is used, thereby immediately allowing the computation of the vapor pressure  $p_i$ .

When the quantity of liquid in the tank is not small, the vapor is assumed to be saturated. The partial pressures of the lading's constituents are computed using pressure-versus-temperature data that you enter in tabular form in the Ladings Database. That data is queried through quadratic interpolation during the simulation.

It is assumed that the padding gas first achieves an initial state of equilibrium before the fire, but after that no further mass exchange occurs between the padding gas in the vapor and the liquid lading, which is to say that the padding gas is assumed to never diffuse into or out of the liquid, regardless of the pressure. Once the relief device has opened, the

padding gas pressure is calculated from the mass of the padding gas remaining in the tank and its temperature.

Aside:

The assumption described above is believed to have little or no impact on the simulation results. The primary reason for it is the little likelihood that equilibrium conditions could ever be attained during the course of the fire. There would not be sufficient time for the effect of the padding gas' partial pressure to be communicated to all portions of the liquid within the tank for the gas to be absorbed or liberated quickly enough.

Additionally, the assumption is believed to produce a conservative estimate for the padding gas pressure even though it has counteracting impacts. Specifically, during the initial stages of heating, allowing mass exchange to maintain equilibrium would cause there to be an increase in the amount of gas in the liquid phase caused by the initial expansion of the liquid phase due to heating. That dissolution into the liquid phase would lead to a decrease in the padding gas' partial pressure. However, counteracting that effect is the fact that, if mass exchange were allowed, then after the initial opening of the safety relief device, the decrease in pressure would lead to liberation of the padding gas from the liquid phase, causing an increase in vapor pressure and an increased flow rate through the valve.

Therefore, no mass exchange of the padding gas between the vapor and liquid phases would on the one hand delay the time at which the relief device opens, but on the other hand increase the pressure after the lading begins to flow through it. To some extent, these effects would probably counteract each other. Regardless, when the space occupied by the vapor reaches approximately 10%, the effect of the padding gas becomes insignificant on the prediction of flow through the relief device.

As mentioned above, since the amount of liquid is small, the pressure of the padding gas is computed using the ideal gas law, still holding to the assumption of no mass exchange between the liquid and vapor phases. The user's inputs for the padding gas' initial pressure, initial volume occupied by the vapor, and initial temperature are used in conjunction with the current volume and current temperature to compute the current pressure. The embodiment of this law is expressed in:

$$P_{pad}(t) = P_{pad}(0) \times \frac{1-f(0)}{1-f(t)} \times \frac{T_{lading}(t)}{T_{lading}(0)} \times \frac{w_{pad}(t)}{w_{pad}(0)} \quad 10.1$$

where  $p_{pad}(t)$  is the pressure of the padding gas at time,  $t$ ,  $f(t)$  is the fraction of the tank filled with liquid at time,  $t$ , and  $w(t)$  is the weight of the padding gas at time,  $t$ . In all cases, the pad gas pressure is never allowed to be negative.

## Modeling Tank Deformation

### Thermal Expansion

When the tank heats up, its volume increases due to thermal expansion of the tank wall. Although this expansion is relatively small, in a shell-full condition it has an impact because as the liquid heats, it also expands and needs more room. A linear thermal expansion law is used as the basis for the tank expansion computation. It is that

$$L(T) = L_{ref} [1 + \alpha(T - T_{ref})] \quad 10.2$$

where  $L(T)$  is length as a function temperature  $T$ ,  $L_{ref}$  is the length at a reference temperature  $T_{ref}$ , and  $\alpha$  is the coefficient of thermal expansion. The ratio of lengths at two different temperatures is therefore

$$\frac{L(T_2)}{L(T_1)} = \frac{1 + \alpha(T_2 - T_{ref})}{1 + \alpha(T_1 - T_{ref})} \quad 10.3$$

$T_{ref}$  can be taken to be zero with no loss of generality. Therefore, the relationship reduces to

$$\frac{L_2}{L_1} = \frac{1 + \alpha T_2}{1 + \alpha T_1} \quad 10.4$$

If  $T_1$  is taken to be the initial temperature of the tank, then the above ratio represents the thermal strain,

$$\varepsilon_T(T) = \frac{1 + \alpha T}{1 + \alpha T_{init}} \quad 10.5$$

The tank can also expand due to internal stresses imposed through the pressure build up inside. As shown in Figure 10.1, the pressure differential represented as  $p$  in the figure is balanced by the circumferential stress inside the tank wall. Through geometrical considerations the following stress balance in the radial direction can be written:

$$2\sigma_c t_w \frac{\Delta\theta}{2} = pr \frac{\Delta\theta}{2} \quad 10.6$$

Canceling terms and using half the diameter ( $d/2$ ) instead of radius,  $r$ , produces

$$\sigma_c = \frac{pd}{2t_w} \quad 10.7$$

In a similar way, the axial strain can be related to the internal pressure by writing a stress balance in the axial direction. Referring to Figure 10.2, the balance of stresses requires that

$$(\pi r^2)p = \sigma_a t_w (2\pi r) \quad 10.8$$

In terms of diameter,  $d$ , the result is

$$\sigma_a = \frac{dp}{4t_w} \quad 10.9$$

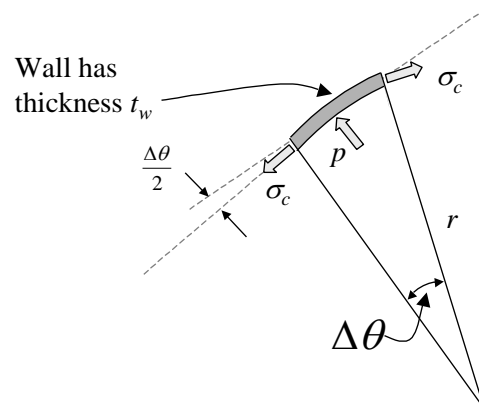


Figure 10.1: Circumferential stress in the tank wall and its relationship to the pressure differential

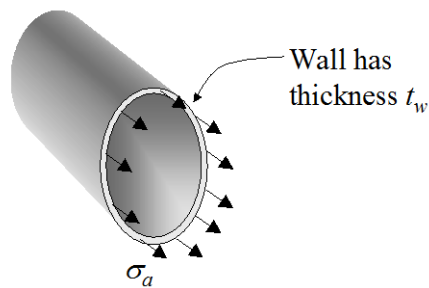


Figure 10.2: Axial stress in the tank wall

### Elastic Strain

The axial and circumferential stresses derived above are related to the corresponding strains through Hooke's law of elasticity

$$\begin{aligned}\varepsilon_c &= \frac{\sigma_c}{E} - \nu \frac{\sigma_a}{E} \\ \varepsilon_a &= \frac{\sigma_a}{E} - \nu \frac{\sigma_c}{E}\end{aligned}\tag{10.10}$$

where  $E$  is Young's modulus and  $\nu$  is Poisson's ratio.

### Plastic Strain

The plastic strain that occurs and is modeled using the Larson-Miller model is not yet implemented in the volume change calculation.

### Combined Strain

The thermal strain, circumferential strain, and axial strain all contribute to a change in volume of the tank car. The thermal strain acts in all three directions and so the change in volume depends on it to the third power. The circumferential strain will act only on the circular cross section and so the change in volume depends on it to the second power. The axial strain only acts in one direction. Therefore, the new volume is due to these effects is modeled as

$$V = V_{init} (1 + \varepsilon_c)^2 (1 + 2\varepsilon_a) \left( \frac{1 + \alpha T}{1 + \alpha T_{init}} \right)^3\tag{10.11}$$





# Numerics

Some of the core conservation models in AFFTAC manifest themselves as first order ordinary differential equations. For example, Equation (5.12) is the transient equation for the lading temperature.

AFFTAC uses a step-wise transient approach known as the Forward Euler method with nonlinear lagging to solve this transient equation, as well as the other transient heat and mass conservation equations. In the Forward Euler method, the derivative is estimated as follows, for example:

$$\frac{dT_{lading}}{dt} \approx \frac{T_{lading}^{new} - T_{lading}^{old}}{\Delta t} \quad 11.1$$

By substituting this approximate derivative, an equation for  $T_{lading}^{new}$  is obtained. That equation uses values of the other temperatures from the previous time step, e.g.,  $T_{lading}^{old}$ . The overall conceptual flow chart of the AFFTAC computations is shown in Figure 2.1, which illustrates the presence of the Forward Euler method.

## Dampening

The advantages and disadvantages of the Forward Euler method have been clearly discussed in the literature. The advantages are that it eliminates the need to solve nonlinear equations. Specifically, at each time step, the previous time step's solution is used to extrapolate forward in time, also described in "The Scope and Interaction of AFFTAC's Models". The disadvantage is that if the time step is too large, the extrapolation can cause the solution to overshoot acceptable bounds.

As a simple example of this phenomenon, consider two stacked blocks of wood, A and B, where A is hotter than B. Because A is hotter, heat flux will flow from it to B. The

amount of heat flux is proportional to their temperature difference. So, in reality, as B warms up and A cools off, the heat flux falls off to zero. In a Forward Euler scheme, the initial temperature difference would be used to compute an initial flux between them. That flux would be multiplied by a time step and used to extrapolate to determine the temperatures at the end of the time step. If the time step is not too big, the result will be that B is a little warmer and A is a little cooler. In that case, the method works fine. But if the time step is too big, the initial flux will be extrapolated out in time too long, causing B to actually become warmer than A, and A cooler than B.

This scenario is unstable and causes the simulation to fail catastrophically. One approach to solving this problem is to continue to use a larger time step but arbitrarily reduce the result obtained. The effect is to dampen the transient behavior. Although there are errors associated with this approach, often an appropriate dampening factor can be used that causes the solution to be stable. Although the transient solution will be in error, the steady state solution will still be correct, unless nonlinear effects play a dominant role.

AFFTAC makes heavy use of this approach. It is manifested in the source code as a weighted average between the previous time step's solution for, say, temperature, and the prediction for the temperature at the new time step, e.g.,

$$T^{new} = \alpha T^{old} - (1 - \alpha) \hat{T}^{new} \quad 11.2$$

where  $\hat{T}^{new}$  is the value predicted without dampening. Typically,  $0.25 < \alpha < 0.5$ . In addition to the thermal solution values, dampening is also used for the auxiliary models. For example, in computing the change in volume due to thermal expansion and the pressure differential, the new value for the volume is dampened using  $\alpha = 1/3$ .

### **Overshoot**

A problem similar to the instability problem discussed above is that of overshoot. For example, during the choked flow computations, if the resulting pressure after discharge during the time step would be less than atmospheric in the case of a vent, or less than the valve closing pressure in the case of a safety relief valve, the out-flows are arbitrarily reduced. This compensation is required because of the consequences due to the finite time step, which may not be sufficiently accurate for rapidly changing conditions. The effect is significant only as the shell full condition is approached.

# Tutorial 1: A Simple Analysis

To begin this tutorial, start the AFFTAC GUI. When you do, the Main Window should appear, where the Analysis Database is displayed. In its distributed version, AFFTAC's Analysis Database comes preloaded with several regression tests, including the example problems in [1]. For this tutorial, one of these example problems (Example 1.1) will be recreated from scratch.

Click **New** in AFFTAC's Main Window. Doing so will create a new entry at the bottom of the Analysis Database and will also display the first of the four editing windows. In this first window select the **Standard Pool Fire** option and enter 100 for the **Length of the Simulation** entry. Leave zero as the entry for the rollover angle. When you are finished making those adjustments, the window should look like that shown in Figure 12.1.

When it does, click **Next**. Doing so displays the Edit Tank Car Properties window. Enter the following information:

Nominal Capacity:	33000
Inside Diameter:	112
Wall Thickness:	0.5625

Then select **AAR TC128-70, Grs. A & B Min. Tensile Strength 81 Kpsi** from the pull-down arrow. Enter the following data for the material:

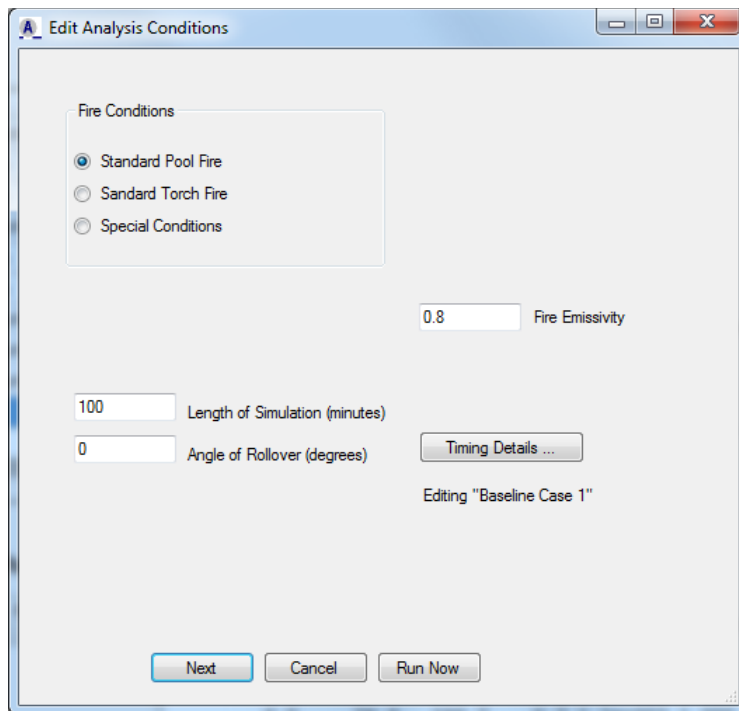
Nominal Burst Strength:	750
Tensile Strength:	81000
Emissivity:	0.8

In the lower half of the window, select the “Valve” option under **Device Type** for the **Safety Relief Device** option and enter the following information:

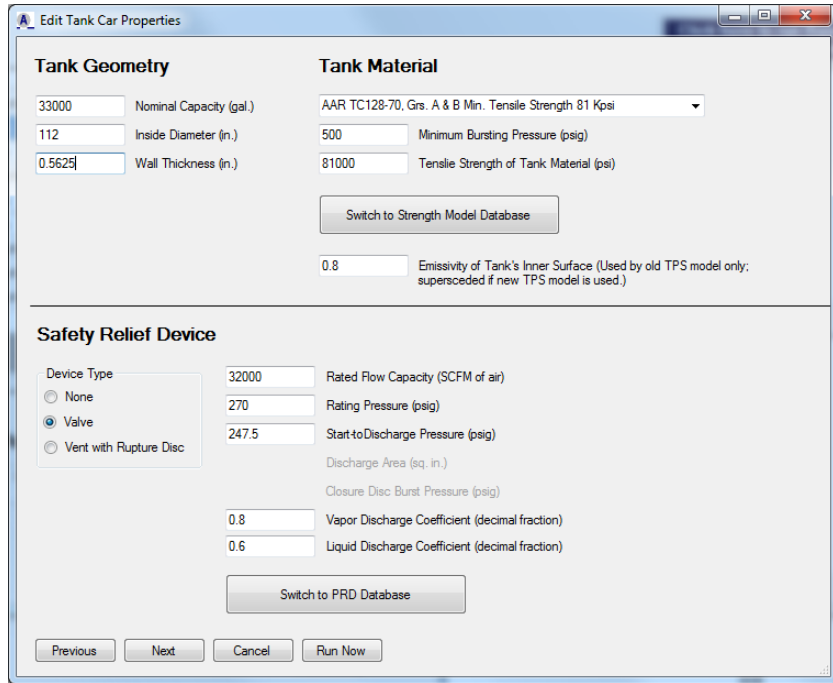
Rated Flow Capacity: 32000  
Rating Pressure: 270  
Start-to-Discharge Pressure: 247.5  
Vapor Discharge Coefficient: 0.8  
Liquid Discharge Coefficient: 0.6

When you have finished making these entries, the window should look like that shown in Figure 12.2. When it does, click **Next**. Doing so will leave you in the Select TPS Model window.

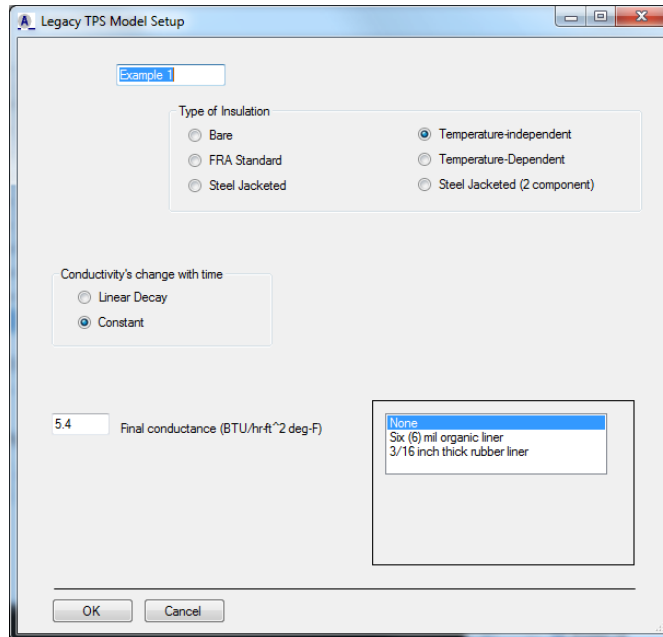
For this tutorial, highlight Example 1, which is a pre-loaded TPS type. To see the data describing the insulation named “Example 1,” double click on it. Doing so displays the window shown in Figure 12.3. The Example 1 insulation type is a temperature-independent thermal protection system that is constant in time. The value of the conductance is 5.4 BTU/hr-ft<sup>2</sup> deg-F.



**Figure 12.1: Analysis conditions for Tutorial 1**



**Figure 12.2: Tank car properties for Tutorial 1**



**Figure 12.3: Legacy TPS Model for Tutorial 1**

Now, click **OK** to return to the Select TPS Model window. To add or delete TPS types in the database, the Legacy TPS Database can be accessed by clicking the **Manage Legacy TPS Database** button in the Select TPS Model window. It can also be accessed through the Main Window under the **Edit Databases-Legacy TPS Model** menu option.

Highlight Example 1 in the Select TPS Model window and click **Next**, which will display the fourth in the series of four editing windows. Select the lading named Butane and enter the following data:

Fraction of Tank Filled: 0.96  
Initial Temperature: 60.

The Ladings Database can be accessed through the **Manage Ladings Database** button, or the menu option **Edit Databases-Ladings** in the Main Window.

The inputs you have provided in the past three windows may be reviewed using the **Previous** and **Next** buttons that are shown at the bottom of each of the four editing windows. Clicking **Cancel** would erase these changes and return you to the Main Window. At this point, the Setup Lading window should look like that shown in Figure 12.4.

When it does, click **Run Now**, which will execute the analysis and return you to the Main Window. To review the input as echoed by the Computational Module, scroll through the information in the top right pane of the Main Window.

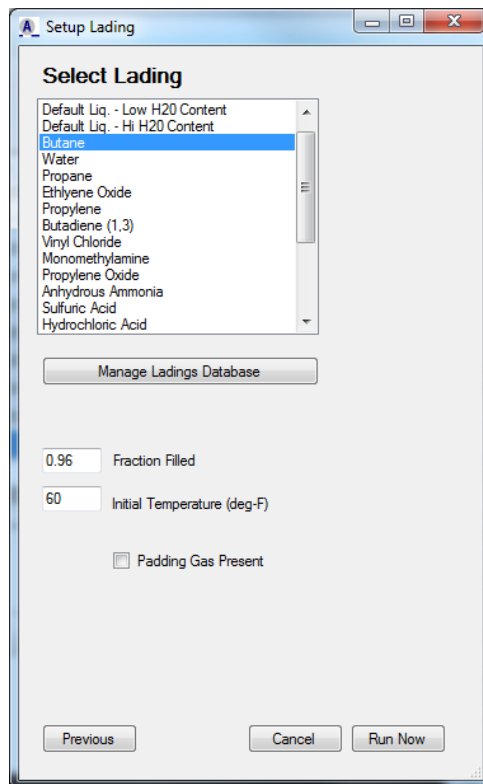


Figure 12.4: Lading setup for Tutorial 1

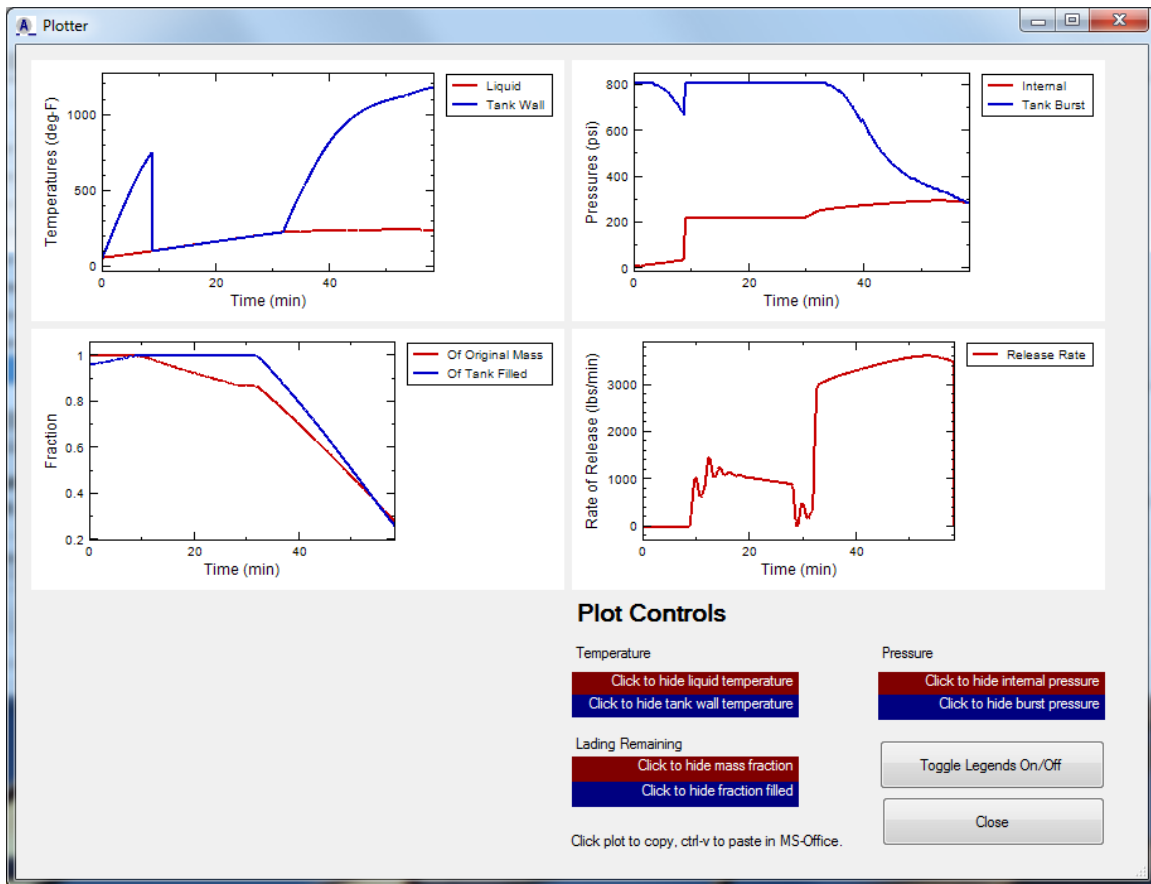
In the left pane of the Main Window, look at the list of analyses. Notice that this analysis is listed at the bottom. However, it has not yet been saved to the Analysis Database file. Before it can be saved there, the administrative information must be added. Likewise, to print the results of this analysis, the administrative information must be added. In the lower part of the Main Window, click the **Edit Admin Data** button. Enter the following information:

Job Number: My First Tutorial  
 Customer: N/A

Click **OK** and then you can save the analysis and print the results.

Note that the default information for your name and your company name may be defined through the Main Window, under the menu option **Options-User Information**.

In the Main Window click the **Plot Displayed Results** button.. Doing so displays the plot window shown in Figure 12.5. These plots can be cut and pasted into other Microsoft Office applications.



**Figure 12.5: Graphical results for Tutorial 1**





# Tutorial 2: Adding a Lading

In this tutorial, you will be guided through the process of adding a new lading to the Ladings Database. Run the AFFTAC GUI and, once in the Main Window, select the menu option **Edit Databases-Ladings**. Upon doing so, a window like that shown in Figure 13.1 will appear. In that window are listed the various ladings that are already contained in the database file.

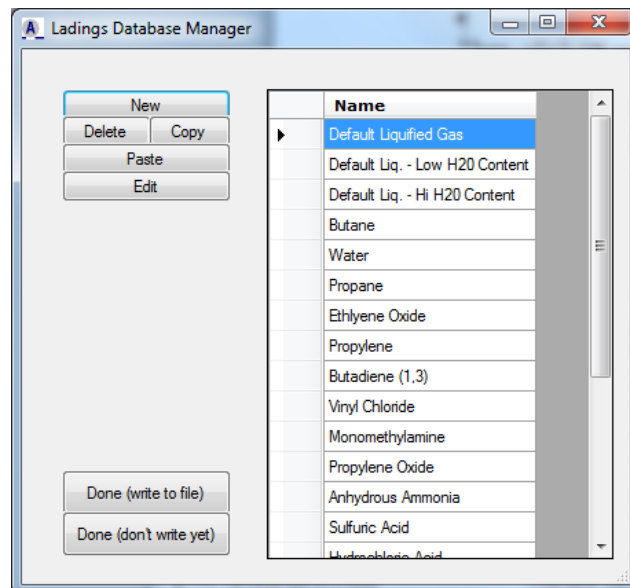
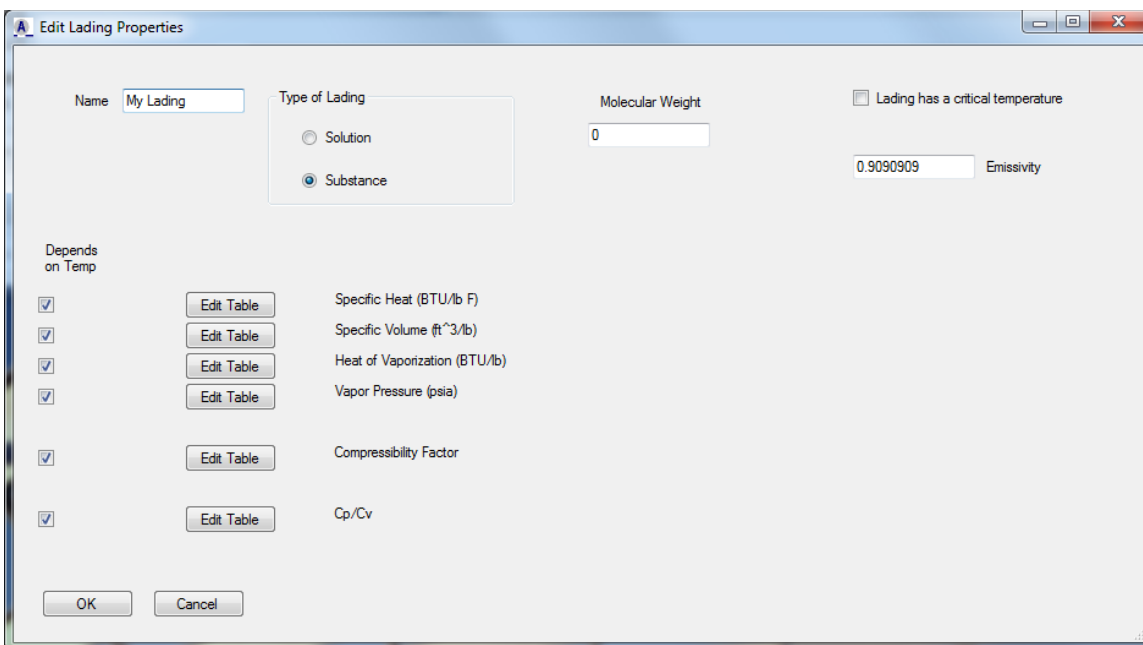


Figure 13.1: Ladings Database

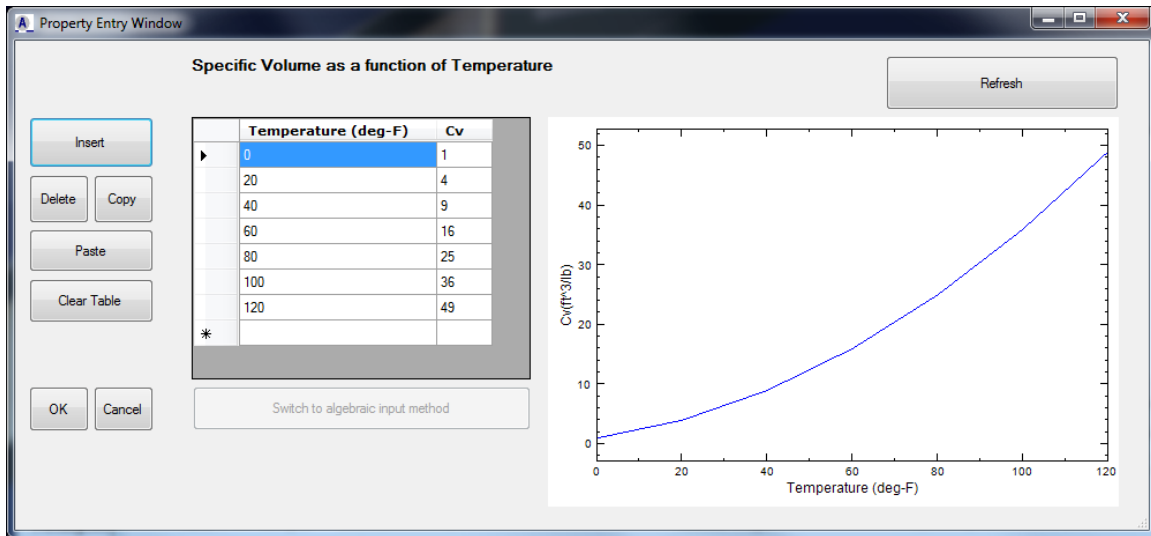
Click **New**. When you do, a new lading is added to the list and is displayed as the last entry. This new lading is merely a placeholder. It does not yet have any real data associated with it. To provide the necessary data, highlight it and click the **Edit** button.

Doing so displays the window shown in Figure 13.2. In this window, the various properties required by the AFFTAC Computational Module are displayed. First, type in the name “My Lading” in the **Name** entry box. Next, make sure that the **Substance** button is selected. Note that if **Solution** is selected (try it) there are some properties that require values for both the solvent and solute, and some values are required at two concentration levels.

Now it will be demonstrated how to provide the data for one of the properties. Click on the **Edit Table** button next to the **Specific Heat** label. When you do, the window shown in Figure 13.3 appears.



**Figure 13.2: Configuration of Edit Lading Properties window for Tutorial 2**



**Figure 13.3: Property Entry Window**

Although there are values supplied in that window, they are not to be taken as legitimate, but rather, placeholders to demonstrate how the window should look once data is entered. For now, click **Clear Table**, which will remove these entries and prepare the table for fresh data.

After you have cleared the placeholder data, click on the left cell, in the temperature column. Using the numeric keypad on your keyboard, type the value 30 and press **ENTER**. Next type 120 and press **ENTER**. Repeat this process to enter 210 and 260 (do not press **ENTER** after 260).

Now, click on the top right cell, under the Cp column. Type 0.5546 and press **ENTER**. Type 0.5946 and press **ENTER** again. Continue, entering 0.7141 and 0.9619 (do not press **ENTER** after 0.9619).

Click **Refresh** to view the updated graph. You may edit the data by clicking directly over the cell you wish to change. You can also copy, cut, and paste rows using the buttons provided. When you are finished, the window should look like that shown in Figure 13.4.

Once the data has been entered correctly, click **OK**. This same process may be repeated for all of the properties listed. Note that the current version of the Computational Module has certain requirements regarding the number of data points that should be provided for each property. If those requirements are not met, the AFFTAC GUI will inform you when you click **OK** in the Edit Lading window.

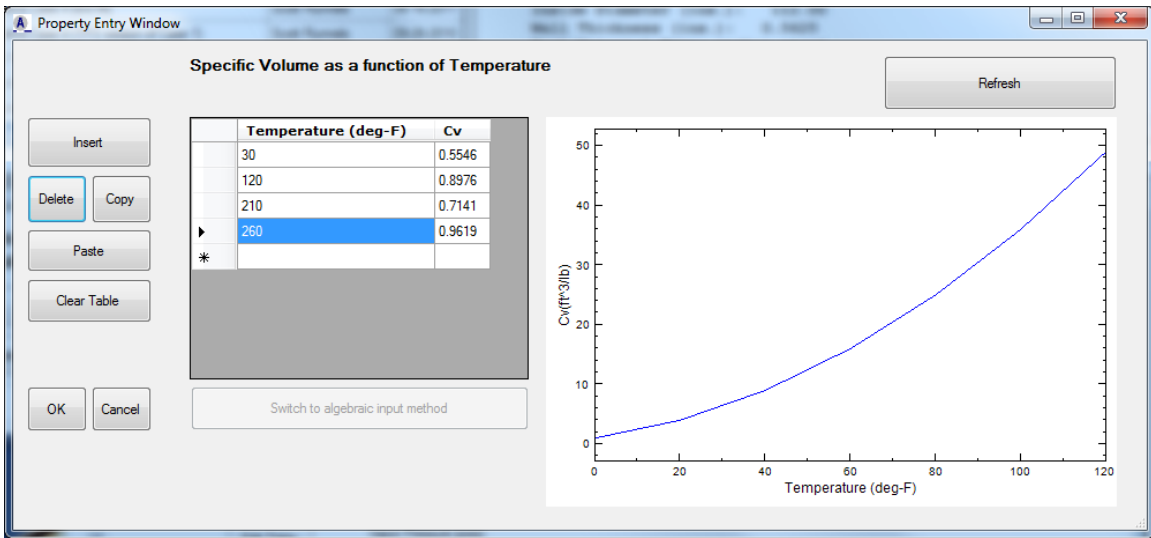


Figure 13.4: Specific volume for Tutorial 2

# Bibliography

1. Johnson, Milton (IIT Research Institute, Chicago, IL 60616), *Tank Car Thermal Analysis, Volume I, User's Manual for Analysis Program (final report)*, for the U.S. Department of Transportation, Federal Railroad Administration, Office of Research and Development, Washington, D.C. 20590, DOT/FRA/ORD-98/09A, November 1998.
2. Johnson, Milton (IIT Research Institute, Chicago, IL 60616), *Tank Car Thermal Analysis, Volume II, Technical Documentation Report for Analysis Program (final report)*, for the U.S. Department of Transportation, Federal Railroad Administration, Office of Research and Development, Washington, D.C. 20590, DOT/FRA/ORD-98/09B, November 1998.
3. Johnson, M. R., "Temperatures, Pressures and Liquid Levels of Tank Cars Engulfed in Fires, Volume 1, Results of Parametric Analyses", and "Volume II Description of Analytic Procedure", Federal Railroad Administration Report No. DOT/FRA/OR&D-84/08.II, June 1984.
4. "Specifications for Tank Cars", Association of American Railroads, Mechanical Division.
5. McAdams, W. H., *Heat Transmission*, 2<sup>nd</sup> Edition, McGraw-Hill Book Company, 1942, pp. 133-141 and 294-337.
6. Townsend, W.; Anderson, C.; Zook, J. and Cowgill, G., "Comparison of Thermally Coated and Uninsulated Rail Tank cars filled with LPG Subjected to a Fire Environment," Federal Railroad Administration Report No. FRA-OR&D 75-32, December 1974.
7. Braker, W. and Mossman, A. L., *The Matheson Unabridged Gas Data Book*, 1974.

8. Gallant, R. W., *Physical Properties of Hydrocarbons, Volume 1*, Gulf Publishing Co., Houston, Texas, 1968.
9. Macriss, R. A., "Liquid and Vapor Phase Enthalpy of Monomethylamine," *Journal of Chemical and Engineering Data*, Volume 12, No. 1, January 1967, pp. 28-33.
10. Gallant, R. W., "Physical Properties of Hydrocarbons, Part 12, C<sub>2</sub>-C<sub>4</sub> Oxides," *Hydrocarbon Processing*, Vol. 46, No. 3, March 1967, pp 143-150.
11. *International Critical Tables of Numerical Data, Physics, Chemistry and Technology*, Volume III.
12. Kirk and Othermer, *Encyclopedia of Chemical Technology*, Interscience Publishers, 3<sup>rd</sup> Edition, John Wiley & Sons.
13. Slack, A. V., editor, *Phosphoric Acid*, Marcel Depper, Inc., New York, 1968.
14. *Properties and Selection: Non-Ferrous Alloys and Pure Metals*, Metals Handbook, Ninth Edition, Volume 2, 1979.
15. "Report on a Study of Metal Specimens Removed from Tank Car Tanks Involved in a Derailment and Explosions at Laurel, Mississippi," Association of American Railroads Report No. MR-453, July 1969.
16. *Properties and Selection: Irons and Steels*, Metals handbook, Ninth Edition, Volume 1, 1979.
17. "Design Guidelines for the Selection and Use of Stainless Steel," AISI Committee of Stainless Steel Producers, 1977.
18. Chapman, Alan J, *Heat Transfer Fourth Edition*, Macmillan Publishing Company, New York, 1984, ISBN 0-02-321470-8.
19. Shames, Irving H., *Mechanics of Fluids, Second Edition*, McGraw-Hill, Inc., New York, 1982
20. ASME Handbook on Certification of Capacity of Pressure Relief Devices, Section VIII – Division I.
21. Trostel, Bryan, "Pressure Relief Valve Testing for US Dept. of Transportation," 10RN-CE10015 Rev. 1, Nov. 29, 2010.

# Appendix A: Default Ladings

By Milton Johnson, Ph.D.

The use of default values for the thermal properties is not recommended. If at all possible, a search for the thermal properties of a lading should be conducted and the values that are obtained entered into the AFFTAC database. If this is not feasible, then the default lading templates may be used, keeping in mind the following guidelines that have been followed to estimate their thermal properties. These guidelines do not apply to tank cars transporting cryogenic liquids, compressed gases such as helium, or slurries/products, such as liquid sulfur, which solidify upon heating. If the product being considered is a solution, it should be treated as though it were a substance for the purpose of obtaining default values and the following guidelines should be used.

## Vapor Pressure

The test pressure of the tank car class authorized to transport a product is often an indication of the vapor pressure of the product. Therefore, two sets of values for default vapor pressure data are provided, one for products that would be shipped in non-pressure cars having a test pressure of 100 psi and the other for products that must be shipped in pressure tank cars having a test pressure of 300 psi or greater. Some products that have low vapor pressures, e.g. products classified as poison by inhalation, must be shipped in pressure tank cars even though they may have low vapor pressures. This is done to require the use of a stronger tank car providing added safety in the shipment of the product. The suggested vapor pressures given below could be substantially over estimated for those ladings.

Assuming that liquefied gases are shipped in pressure cars and liquids are shipped in non-pressure cars, the vapor pressure property values are estimated as follows:

Liquids (non-pressure cars)

Temperature (°F)	Vapor Pressure (psia)
60	5
150	40
240	125

Liquefied gasses (pressure cars)

Temperature (°F)	Vapor Pressure (psia)
60	140
120	300
180	570

Some products, such as bromine, chlorine and hydrogen cyanide, must be shipped in tank cars having a test pressure of 500 psi or greater. This is done not because they have high vapor pressures, but to insure they are shipped in stronger, safer cars. The vapor pressures given above for pressure tank cars would be conservative for these products.

## Specific Heat

There is a wide range of values for the specific heat of the liquid for products shipped in tank cars. Values can range from over 1.00 BTU/lb-°F, for solutions containing a large percentage of water, to as low as 0.10 BTU/lb-°F for bromine at about 200 °F. Also, for most products the specific heat tends to rise with increasing temperature, but for some products (e.g. bromine) it decreases. This makes it difficult to suggest default properties for specific heat that are conservative, but not overly conservative. Since the specific heat of the liquid determines the rate of temperature increase of the product with a given heat input, it is obvious that lower values for this parameter will lead to more conservative analyses. The following default values are suggested, although they may not always lead to conservative results:

Temperature (°F)	Specific Heat (BTU/lb-°F)
60	0.40
300	0.70

## Specific Volume

It is assumed that the density of the product is known. The specific volume is simply the inverse of this value expressed in ft<sup>3</sup>/lb. Since the density of materials tend to decrease



with increasing temperature, the specific volume will increase with increasing temperature.

Again, there is a considerable variation of this rate of increase among products shipped in tank cars making it difficult to suggest default properties. Values range from an increase in specific volume of 13 percent for chlorosulfonic acid in the temperature range from 50 to 302 °F to a 70 percent increase for hydrogen fluoride in the same temperature range. The rate of increase in specific volume with temperature is an important parameter when the tank car becomes shell full and liquid is being expelled through the valve, a larger valve capacity for liquid flow being required when the rate of increase is higher. Tentative values are suggested as follows.

Liquids (non-pressure cars) or Liquefied Gases Containing at least 50% water

Temperature (°F)	Percentage increase in Specific Volume from Ambient Value
60	Ambient Value
180	10%
300	30%

Liquefied gasses (pressure cars)

Temperature (°F)	Percentage increase in Specific Volume from Ambient Value
60	Ambient Value
150	20%
240	50%

## Heat of Vaporization

There is also considerable variation in the heat of vaporization among products shipped in tank cars ranging from about 1000 BTU/lb for solutions containing a high percentage of water to less than 100 BTU/lb, for products such as bromine, methyltrichlorosilane, titanium tetrachloride and phosphorus trichloride. Other factors being equal, a lower heat of vaporization will result in the generation of greater volume of vaporized product requiring a larger capacity pressure relief valve. The heat of vaporization decreases with increasing temperature. The following default values are suggested although they may not be conservative in all cases:

Temperature (°F)	Heat of Vaporization BTU/lb
60	300
240	100

If the product is a solution containing at least 50 percent water as the solvent, the

following values are suggested:

Temperature ( $^{\circ}$ F)	Heat of Vaporization BTU/lb
60	800
240	300

## **Compressibility Factor**

This parameter does not have a major influence on the calculations. A default value of 0.9 is suggested for the compressibility factor of product vapor. It would be entered into the program at two values for temperature (e.g. 60 and 300  $^{\circ}$ F).

## **Ratio of Specific Heats**

This parameter does not have a major influence on the calculations. A default value of 1.1 is suggested for the ratio of specific heats of product vapor. It would be entered into the program at two values for temperature (e.g. 60 and 300  $^{\circ}$ F).

# **Appendix B: Choked Vapor Flow**

## **Derivation and Area Estimation Method**

The primary reference for these derivations is given in [19].

### **Applications of the First Law of Thermodynamics**

#### **Application to Quasi-Static Process**

In this section, thermodynamic relationships are derived that describe intrinsic responses of the fluid, without consideration of a system. To derive these relationships, consider fluid in a quasi-static process, where pressure,  $p$ , is uniform. The differential form of the First Law of Thermodynamics (hereafter, “First Law”) reduces to

$$dq - dw = du \qquad \text{B.1}$$

where  $u$  is the internal energy of the fluid,  $q$  is the heat transferred into the fluid, and  $w$  is the work done by the fluid.

If this process is adiabatic, reversible (isentropic),  $dq = 0$ . Also, fluid alone can only do work intrinsically through expansion, so  $dw = pdv$ , where  $dv$  is the infinitesimal change in volume. Therefore, the First Law for the fluid is

$$du = -pdv. \quad \text{B.2}$$

The specific heat at constant volume,  $c_v$ , is defined as

$$c_v \equiv \frac{du}{dT} \quad \text{B.2}$$

or

$$du = c_v dT \quad \text{B.4}$$

so that

$$c_v dT = -pdv. \quad \text{B.5}$$

Returning to Equation B.2 and adding  $pdv$  to both sides,

$$du + pdv + vdp = vdp \quad \text{B.6}$$

which means that

$$d(u + pv) = vdp \quad \text{B.7}$$

or

$$dh = vdp \quad \text{B.8}$$

where  $h = u + pv$  is enthalpy. The specific heat at constant pressure,  $c_p$ , is defined as

$$c_p \equiv \frac{dh}{dT} \quad \text{B.9}$$

or

$$dh = c_p dT \quad \text{B.10}$$

so that

$$c_p dT = vdp. \quad \text{B.11}$$

Divide Equation B.11 by B.5, to get

$$\frac{c_p}{c_v} = -\frac{v dp}{p dv} \quad \text{B.12}$$

Rearrange,

$$-\frac{c_p dv}{c_v v} = -\frac{dp}{p}, \quad \text{B.13}$$

and define the ratio of specific heats as  $k=c_p/c_v$ , so that

$$-k \frac{dv}{v} = \frac{dp}{p} \quad \text{B.14}$$

Assume a constant ratio ( $k$ ) of specific heats, and integrate:

$$-\int k \frac{dv}{v} = \int \frac{dp}{p} \quad \text{B.15}$$

$$pv^k = \text{constant} \quad \text{B.16}$$

The above equation means that the product of pressure and specific volume is everywhere constant in the quasi-static process. Introducing “ $i$ ” to denote an inlet and “ $o$ ” to denote an outlet, the above equation implies that

$$p_i v_i^k = p_o v_o^k \quad \text{B.17}$$

$$\frac{p_i}{p_o} = \left( \frac{v_o}{v_i} \right)^k \quad \text{B.18}$$

For an ideal gas,  $p v = RT$  so that the above equation may be written as

$$\frac{T_i v_o}{T_o v_i} = \left( \frac{v_o}{v_i} \right)^k \quad \text{B.19}$$

or

$$\frac{T_i}{T_o} = \left( \frac{v_o}{v_i} \right)^{k-1} \quad \text{B.20}$$

The ideal gas law,  $p\nu=RT$ , can be applied again, to produce

$$\frac{T_i}{T_o} = \left( \frac{RT_o / p_o}{RT_i / p_i} \right)^{k-1} = \left( \frac{T_o p_i}{T_i p_o} \right)^{k-1} \quad \text{B.21}$$

Manipulation of the above equation results in

$$\frac{T_i}{T_o} = \left( \frac{p_i}{p_o} \right)^{k-1/k} \quad \text{B.22}$$

### Application to a Control Volume

The differential form of the First Law of Thermodynamics for a system (“First Law”) is as follows,

$$dQ - dW = dE \quad \text{B.23}$$

where

$$Q = \text{heat transferred in to the system} \quad \text{B.24}$$

$$W = \text{work done by the system}$$

$$E = \text{energy in the system}$$

The right-hand side has to do with the state of the fluid in the system. Since fluid can move through the system, it is helpful to highlight that fact when writing the First Law as time derivatives. In particular, the energy time derivative must be a “substantial” derivative (i.e., follows the substance which is the fluid). Capital “ $D$ ” is used for that purpose, and the time-derivative form of the First Law may be written as

$$\frac{dQ}{dt} - \frac{dW}{dt} = \frac{DE}{Dt} \quad \text{B.25}$$

It is necessary at this point to more firmly establish the notion of a control volume, which will be denoted here by  $\Omega$ . The Reynolds Transport Theorem accounts for the fact that the substance (fluid) flows through the control volume. In taking the flow into account, the First Law, which is meant to apply to a system, can be made to handle the situation where fluid flows through the system. The derivation of the Reynold’s Transport Theorem can be made from geometrical considerations and can be applied to any material state variable. For energy, it is stated as follows:

$$\frac{DE}{Dt} = \int_{\partial\Omega} e\rho\mathbf{V} \cdot \hat{\mathbf{n}}dA + \frac{\partial}{\partial t} \int_{\Omega} e\rho d\nu \quad \text{B.26}$$

where  $\partial\Omega$  is the boundary of  $\Omega$ ,  $e$  is the material-intensive energy,  $\mathbf{V}$  is the velocity vector at the boundary, and  $\hat{\mathbf{n}}$  is the outward normal at the boundary.

For steady-state flow, the second term on the right-hand side is zero. Using the resulting expression for  $DE/Dt$  in the First Law,

$$\frac{dQ}{dt} - \frac{dW}{dt} = \int_{\partial\Omega} e\rho\mathbf{V} \cdot \hat{\mathbf{n}}dA. \quad \text{B.27}$$

It is helpful to separate the work term on the left-hand side into two parts:

$$\frac{dW}{dt} = \frac{dW_s}{dt} + \int_{\partial\Omega} \mathbf{T} \cdot \mathbf{V}dA = \text{"Shaft work rate"} + \text{"Flow work rate"} \quad \text{B.28}$$

where  $\mathbf{T}$  is the stress tensor. The product of  $\mathbf{T}$  and  $\mathbf{V}$  represent stress through a distance, per time. When integrated over an area, it represents the rate of work done by the fluid.

The first term is the rate of work done on the fluid by moving parts inside the control volume (e.g., a fan). For flow through the pressure relief device, there are no moving parts that do any appreciable work on the fluid, so the “shaft work rate” is zero, which leaves only the flow work rate, so that

$$\frac{dW}{dt} = \int_{\partial\Omega} \mathbf{T} \cdot \mathbf{V}dA. \quad \text{B.29}$$

In flow through the pressure relief device, it is assumed the flow is frictionless, so the only stress at the surface is normal stress. In other words,

$$\mathbf{T} = p\hat{\mathbf{n}} \quad \text{B.30}$$

So, the flow work rate is

$$\frac{dW}{dt} = \int_{\partial\Omega} \mathbf{T} \cdot \mathbf{V}dA = \int_{\partial\Omega} p\mathbf{V} \cdot \hat{\mathbf{n}}dA \quad \text{B.31}$$

Substituting this expression for the work term on the left-hand side of the First Law produces the following form of the First Law:

$$\frac{dQ}{dt} - \int_{\partial\Omega} p\mathbf{V} \cdot \hat{\mathbf{n}}dA = \int_{\partial\Omega} e\rho\mathbf{V} \cdot \hat{\mathbf{n}}dA \quad \text{B.32}$$

In the release of vapor through the safety relief device, the flow is sufficiently fast to completely neglect any heat exchanged between the fluid and the valve. Hence, the flow is adiabatic/isentropic and the  $dQ/dt$  term is zero, and the First Law becomes

$$-\int_{\partial\Omega} p\mathbf{V} \cdot \hat{\mathbf{n}}dA = \int_{\partial\Omega} e\rho\mathbf{V} \cdot \hat{\mathbf{n}}dA \quad \text{B.33}$$

The term on the left-hand side can be combined with the term on the right-hand side by inserting  $\rho v$ , which is unity. Doing so produces

$$-\int_{\partial\Omega} pv\rho\mathbf{V} \cdot \hat{\mathbf{n}}dA = \int_{\partial\Omega} e\rho\mathbf{V} \cdot \hat{\mathbf{n}}dA \quad \text{B.34}$$

Then, combining the two integrals,

$$\int_{\partial\Omega} \rho(e + pv)\mathbf{V} \cdot \hat{\mathbf{n}}dA = 0 \quad \text{B.35}$$

The energy of the material is comprised of kinetic, gravitational potential, and internal energy. In other words,

$$e = \frac{V^2}{2} + gz + u \quad \text{B.36}$$

where  $g$  is the acceleration due to gravity,  $z$  is the height above a datum, and  $u$  is the internal energy. Inserting this expression for energy into the preceding equation produces the following form of the First Law:

$$\int_{\partial\Omega} \rho \left( \frac{V^2}{2} + gz + u + pv \right) \mathbf{V} \cdot \hat{\mathbf{n}}dA = 0 \quad \text{B.37}$$

In flow through the pressure relief device, there is no appreciable altitude change. Therefore, the total surface integral of  $gz$  can be neglected. And so the First Law becomes

$$\int_{\partial\Omega} \rho \left( \frac{V^2}{2} + u + pv \right) \mathbf{V} \cdot \hat{\mathbf{n}}dA = 0 \quad \text{B.38}$$

Using enthalpy, which is defined as  $h = u + pv$ , the First Law can be expressed as

$$\int_{\partial\Omega} \rho \left( \frac{V^2}{2} + h \right) \mathbf{V} \cdot \hat{\mathbf{n}}dA = 0 \quad \text{B.39}$$



At this point, the surface integral can be simplified in two ways:

- (1) In the present application, the surface area is comprised of only one inlet and one outlet. The areas for the inlet and outlet are  $A_i$  and  $A_o$ , respectively.
- (2) An approximation is made concerning the direction of the flow at the inlet and outlet. It is assumed that the flow is normal to the control volume ( $A_i$  and  $A_o$ ), which means that the dot product between velocity and the surface normal vector is simply the magnitude of the velocity ( $V$ ).

Under these assumptions,

$$\left(\frac{V_o^2}{2} + h_o\right) \rho_o A_o V_o = \left(\frac{V_i^2}{2} + h_i\right) \rho_i A_i V_i \quad \text{B.40}$$

The products of density, area, and velocity that appear on both sides of the above equation are expressions of mass flow rate. Conservation of mass therefore means that these two products must be equal and therefore cancel. And so the First Law becomes,

$$\frac{V_o^2}{2} + h_o = \frac{V_i^2}{2} + h_i \quad \text{B.41}$$

The control volume for this application is chosen to be such that the velocity at the inlet is very small such that  $V_i^2$  is negligible. Under that assumption, the First Law is

$$\frac{V_o^2}{2} + h_o = h_i \quad \text{B.42}$$

Next, it is assumed that the specific heats are constant, i.e., that

$$c_p \equiv \frac{dh}{dT} \quad \text{B.43}$$

is a constant. With  $c_p$  being a constant, the above equation may be integrated such that

$$h - h_d = c_p (T - T_d) \quad \text{B.44}$$

Here,  $(h_d, T_d)$  is an arbitrary datum. Substituting this expression into the First Law produces

$$\frac{V_o^2}{2} + c_p (T_o - T_d) = c_p (T_i - T_d) \quad \text{B.45}$$

The  $T_d$  terms cancel, and thus

$$\frac{V_o^2}{2} + c_p T_o = c_p T_i \quad \text{B.46}$$

Dividing by  $T_o$ ,

$$\frac{V_o^2}{2T_o} + c_p = c_p \frac{T_i}{T_o} \quad \text{B.47}$$

and then by  $c_p$ ,

$$\frac{V_o^2}{2c_p T_o} + 1 = \frac{T_i}{T_o} \quad \text{B.48}$$

In Appendix C, it is shown that for an ideal gas,  $c_p = \left(\frac{k}{k-1}\right)R$ . Using that fact, the First Law becomes

$$\frac{V_o^2}{kRT_o} \frac{(k-1)}{2} + 1 = \frac{T_i}{T_o} \quad \text{B.49}$$

Also, for an ideal gas,  $c^2 = kRT$ , and this term appears in the above equation. Therefore, the ratio  $\frac{V_o^2}{kRT_o} = \frac{V_o^2}{c^2} = M^2$ , where  $M$  is the Mach number (the ratio of speed to the speed of sound). The First Law in terms of  $M$  is

$$M^2 \frac{(k-1)}{2} + 1 = \frac{T_i}{T_o} \quad \text{B.50}$$

Inverting the above equation,

$$\frac{T_o}{T_i} = \frac{1}{1 + M^2 \frac{(k-1)}{2}} \quad \text{B.51}$$

Using Equation B.22, the First Law may be written as

$$\left(\frac{p_o}{p_i}\right)^{k-1/k} = \frac{1}{1 + \frac{(k-1)}{2} M^2} \quad \text{B.52}$$

or

$$\frac{p_o}{p_i} = \frac{1}{\left(1 + \frac{(k-1)}{2} M^2\right)^{k/(k-1)}} \quad \text{B.53}$$

## Mass Flow for an Ideal Gas

The mass flow rate is

$$G = \rho VA \quad \text{B.54}$$

where

$$\rho = \text{density} \quad \text{B.55}$$

$$V = \text{average velocity}$$

$$A = \text{area of flow}$$

For an ideal gas,

$$\rho = p / RT \quad \text{B.56}$$

where

$$p = \text{pressure} \quad \text{B.57}$$

$$R = \text{gas constant}$$

By substitution of the ideal gas law into the mass flow rate equation,

$$G = \frac{p}{RT} VA \quad \text{B.58}$$

The following step is simple algebra. The  $RT$  term is split into two square roots and a form of unity ( $k/k$ ) is introduced. The value  $k$  is the ratio of the vapor's specific heats, as was described in the previous sub-section (Equations B.13-B14).

$$G = pA \frac{V}{\sqrt{kRT}} \sqrt{\frac{k}{RT}} \quad \text{B.59}$$

For an ideal gas, the speed of sound,  $c$ , is

$$c = \sqrt{kRT} . \quad \text{B.60}$$

For an ideal gas the Mach number is

$$M = \frac{V}{c} = \frac{V}{\sqrt{kRT}} \quad \text{B.61}$$

The Mach number can therefore be used in the expression for the mass flow rate as follows:

$$G = pAM \sqrt{\frac{k}{RT}} \quad \text{B.62}$$

Introducing the subscript “o” for “outlet,” the above equation may be used to express the mass flow rate at the outlet of a control volume,

$$G = p_o AM \sqrt{\frac{k}{RT_o}} \quad \text{B.63}$$

Into this equation, pressures and temperatures at the inlet (subscript “i”) will be introduced in ratios that equal unity. Then the terms are rearranged:

$$G = p_o AM \sqrt{\frac{k}{RT_o}} \left( \sqrt{\frac{T_i}{T_o}} \sqrt{\frac{p_i}{p_o}} \right) \quad \text{B.64}$$

or

$$G = \frac{p_o}{p_i} AM \sqrt{\frac{k}{R}} \sqrt{\frac{T_i}{T_o}} \frac{p_i}{\sqrt{T_i}} \quad \text{B.65}$$

Into this equation, the relationships derived earlier for  $p_o/p_i$  and  $T_o/T_i$  (Equations B.51 and B.53) are substituted:

$$G = \frac{MA}{\left(1 + \frac{(k-1)}{2} M^2\right)^{(k+1)/2(k-1)}} \sqrt{\frac{k}{R}} \frac{p_i}{\sqrt{T_i}} \quad \text{B.66}$$

For  $M=1$ ,

$$G|_{M=1} = p_i A \left( \frac{2}{(k+1)} \right)^{(k+1)/2(k-1)} \sqrt{\frac{k}{RT_i}} \quad \text{B.67}$$

Or, combining terms,

$$G|_{M=1} = p_i A \sqrt{\frac{k}{RT_i} \left( \frac{2}{k+1} \right)^{k+1/k-1}} \quad \text{B.68}$$

## **AFFTAC's Sub-Sonic Vapor Flow Model**

If the pressure is not sufficiently high, then it is assumed choked flow has not occurred, and so  $M < 1$ . Therefore, the applicable equation is not Equation B.68, but rather its predecessor, Equation B.66, which modified to include the vapor discharge coefficient results in

$$G_{\text{sub-sonic}} = \frac{M(AC_{Dc})}{\left( 1 + \frac{(k-1)}{2} M^2 \right)^{(k+1)/2(k-1)}} \sqrt{\frac{k}{R}} \frac{p_i}{\sqrt{T_i}} \quad \text{B.73}$$

However, it is noted here that AFFTAC instead uses a simplified linear model for sub-sonic flow. Specifically, AFFTAC computes the flow rate as if the flow is choked, and then linearly scales it according to pressure. This simplification in AFFTAC is probably unneeded, since the compact analytical form is readily available in Equation B.72.



# Appendix C: Thermodynamic Identities for an Ideal Gas

By definition,

$$c_p = \frac{dh}{dT} = \frac{d}{dT}(u + pv) \quad \text{C.1}$$

For an ideal gas,

$$pv = RT \quad \text{C.2}$$

And so

$$c_p = \frac{d}{dT}(u + RT) = c_v + R \quad \text{C.3}$$

Therefore,

$$c_p - c_v = R \quad \text{C.4}$$

Dividing both sides by  $c_v$ ,

$$\frac{c_p}{c_v} - 1 = \frac{R}{c_v} \quad \text{C.5}$$

The ratio of specific heats appears often and is defined here as  $k$ ,

$$k \equiv \frac{c_p}{c_v} \quad \text{C.6}$$

Therefore, using this definition,

$$\begin{aligned} k - 1 &= \frac{R}{c_v} \\ &= \frac{Rk}{c_p} \end{aligned} \quad \text{C.7}$$

so that

$$c_p = \left( \frac{k}{k-1} \right) R \quad \text{C.8}$$



# Appendix D: Derivation of PRD Area Estimation Formula

In the initialization part of AFFTAC's main routine, the vapor discharge coefficient is used with the choked flow model to compute the area of the valve. The line in the code is as follows:

```
avlv =  
User.ValveFlowCapacity/(User.DischargeCoef_Vap*pasd*2644.0)  
; //discharge area of safety relief valve (sq ft)
```

Derivation of that line of code starts with B.72, here labeled D.1:

$$A = \frac{G_{\text{exp}}}{C_{Dv} p_{\text{exp}} \sqrt{\frac{k}{ZRT_{\text{exp}}} \left( \frac{2}{k+1} \right)^{k+1/k-1}}} \quad \text{D.1}$$

With units,

$$A(\text{ft}^2) = \frac{G_{\text{exp}} \left( \frac{\text{lbm}}{\text{min}} \right)}{C_{Dv} P_{\text{exp}} \left( \frac{\text{lbf}}{\text{ft}^2} \right) \sqrt{ZR \left( \frac{\text{ft} \cdot \text{lbf}}{\text{lbm} \cdot ^\circ \text{R}} \right) T_{\text{exp}} (^{\circ} \text{R}) \left( \frac{2}{(k+1)} \right)^{k+1/k-1}}} \quad \text{D.2}$$

In the line of code shown above, pressure is in psi instead of the units given above, and volumetric flow rate is used instead of mass flow rate. Thus, the following substitutions are made into Equation D.2:

$$G_{\text{exp}} \left( \frac{\text{lbm}}{\text{sec}} \right) = Q_{\text{exp}} \left( \frac{\text{ft}^3}{\text{min}} \right) \cdot \rho \left( \frac{\text{lbm}}{\text{ft}^3} \right) \cdot \frac{1}{60} \left( \frac{\text{min}}{\text{sec}} \right) = \frac{Q_{\text{exp}} \rho}{60} \left( \frac{\text{lbm}}{\text{sec}} \right) \quad \text{D.3}$$

and

$$P_{\text{exp}} \left( \frac{\text{lbf}}{\text{ft}^2} \right) = \hat{P}_{\text{exp}} \left( \frac{\text{lbf}}{\text{in}^2} \right) \cdot 144 \left( \frac{\text{in}^2}{\text{ft}^2} \right) = \hat{P}_{\text{exp}} \cdot 144 \left( \frac{\text{lbf}}{\text{ft}^2} \right) \quad \text{D.4}$$

Making these substitutions,

$$A(\text{ft}^2) = \frac{\frac{Q_{\text{exp}} \rho}{60} \left( \frac{\text{lbm}}{\text{sec}} \right)}{C_{Dv} \hat{P}_{\text{exp}} \cdot 144 \left( \frac{\text{lbf}}{\text{ft}^2} \right) \sqrt{ZR \left( \frac{\text{ft} \cdot \text{lbf}}{\text{lbm} \cdot ^\circ \text{R}} \right) T_{\text{exp}} (^{\circ} \text{R}) \left( \frac{2}{(k+1)} \right)^{k+1/k-1}}} \quad \text{D.5}$$

or

$$A(\text{ft}^2) = \frac{Q_{\text{exp}} \left( \frac{\text{lbm}}{\text{sec}} \right)}{C_{Dv} \hat{P}_{\text{exp}} \cdot \frac{60 \cdot 144}{\rho} \left( \frac{\text{lbf}}{\text{ft}^2} \right) \sqrt{ZR \left( \frac{\text{ft} \cdot \text{lbf}}{\text{lbm} \cdot ^\circ \text{R}} \right) T_{\text{exp}} (^{\circ} \text{R}) \left( \frac{2}{(k+1)} \right)^{k+1/k-1}}} \quad \text{D.6}$$

Now, the remaining units may be considered. First, inside the radical, the fact that

$$\frac{1 \cdot \text{lbf}}{1 \cdot \text{lbm}} = g \frac{\text{ft}}{\text{sec}^2} \quad \text{D.7}$$

is used. Making that substitution,

$$A(\text{ft}^2) = \frac{Q_{\text{exp}} \left( \frac{\text{lbm}}{\text{sec}} \right)}{C_{Dv} \hat{p}_{\text{exp}} \cdot \frac{60 \cdot 144}{\rho} \left( \frac{\text{lbf}}{\text{ft}^2} \right) \sqrt{g \frac{\text{ft}}{\text{sec}^2} ZR \left( \frac{\text{ft}}{^{\circ}\text{R}} \right) T_{\text{exp}} (^{\circ}\text{R}) \left( \frac{2}{(k+1)} \right)^{k+1/k-1}}} \quad \text{D.8}$$

The Rankine units cancel, leaving  $\text{ft}^2/\text{sec}^2$  in the denominator inside the radical. Bringing those units outside the radical results in

$$A(\text{ft}^2) = \frac{Q_{\text{exp}} \left( \frac{\text{lbm}}{\text{sec}} \right)}{C_{Dv} \hat{p}_{\text{exp}} \cdot \frac{60 \cdot 144}{\rho} \left( \frac{\text{lbf}}{\text{ft}^2} \right) \left( \frac{\text{sec}}{\text{ft}} \right) \sqrt{g ZR T_{\text{exp}} \left( \frac{2}{(k+1)} \right)^{k+1/k-1}}} \quad \text{D.9}$$

Simplifying produces

$$A(\text{ft}^2) = \frac{Q_{\text{exp}} \left( \frac{\text{lbm}}{\text{lbf}} \right) \left( \frac{\text{ft}^3}{\text{sec}^2} \right)}{C_{Dv} \hat{p}_{\text{exp}} \cdot \frac{60 \cdot 144}{\rho} \sqrt{g ZR T_{\text{exp}} \left( \frac{2}{(k+1)} \right)^{k+1/k-1}}} \quad \text{D.10}$$

Using again that

$$\frac{1 \cdot \text{lbm}}{1 \cdot \text{lbf}} = \frac{1 \text{ sec}^2}{g \text{ ft}} \quad \text{D.11}$$

results in

$$A(\text{ft}^2) = \frac{Q_{\text{exp}} \left( \frac{1}{g} \right) \left( \frac{\text{sec}^2}{\text{ft}} \right) \left( \frac{\text{ft}^3}{\text{sec}^2} \right)}{C_{Dv} \hat{p}_{\text{exp}} \cdot \frac{60 \cdot 144}{\rho} \sqrt{g ZR T_{\text{exp}} \left( \frac{2}{(k+1)} \right)^{k+1/k-1}}} \quad \text{D.12}$$

Pulling  $g$  inside the radical and coalescing units, produces

$$A(\text{ft}^2) = \frac{Q_{\text{exp}}}{C_{Dv} \hat{p}_{\text{exp}} \cdot \left\{ \frac{60 \cdot 144}{\rho} \sqrt{\frac{gk}{ZRT_{\text{exp}}} \left( \frac{2}{(k+1)} \right)^{k+1/k-1}} \right\}} (\text{ft}^2) \quad \text{D.13}$$

The term in curly braces evaluates as follows:

$$\frac{60 \cdot 144}{\rho} \sqrt{\frac{gk}{ZRT_{\text{exp}}} \left( \frac{2}{(k+1)} \right)^{k+1/k-1}} = \frac{60 \cdot 144}{0.0763} \sqrt{\frac{(32.2) \cdot (1.4)}{(1) \cdot (53.3533) \cdot (60 + 459)} \left( \frac{2}{(1.4+1)} \right)^{1.4+1/1.4-1}} = 2644 \quad \text{D.14}$$

which is what is used in the code, i.e., the line originally presented in this appendix, rewritten as

$$A(\text{ft}^2) = \frac{Q_{\text{exp}}}{C_{Dv} \hat{p}_{\text{exp}} \cdot 2644} (\text{ft}^2) \quad \text{D.15}$$

# Appendix E: Derivation of Shell- Full Liquid Expulsion Pressure

In the ShellFull routine, the discharge coefficient is used to compute the pressure required to discharge the required amount of liquid, where the required amount is computed using a volume comparison. The line of code to compute the required pressure is shown below.

```
pcom = pmin +  
      ( pow(reql/(720.0*DischargeCoef_Liq*areq),2)  
      )/(64.4*splq);
```

The volume to be expelled is computed as follows:

```
reql = 0.9*reql+0.1*(TotalMass*splq-TankVolume_cuft)/delt.
```

Ignoring for the moment the 0.9-0.1 relaxation factors, this equation may be rewritten as

$$\text{req1} = \frac{\text{TotalMass} \cdot v_{liq} - V_{\text{tank}}}{\Delta t} \quad \text{E.1}$$

Here, req1 is the required liquid volumetric flow rate in a shell full condition. Renaming that variable to  $Q_{liq} \left( \frac{\text{ft}^3}{\text{min}} \right)$ , the pcom equation from the line of code above may be written as

$$p_{com} = p_{\min} + \frac{\left( \frac{Q_{liq}}{720 \cdot C_{D_{liq}} \cdot A_{areq}} \right)^2}{64.4 \cdot v_{liq}} \quad \text{E.2}$$

The derivation of this equation starts with the Bernoulli equation,

$$p_{com} = p_{\min} + \frac{1}{2} \rho_{liq} V^2 \quad \text{E.3}$$

With units, it is

$$p_{com} \left( \frac{\text{lbf}}{\text{ft}^2} \right) = p_{\min} \left( \frac{\text{lbf}}{\text{ft}^2} \right) + \frac{1}{2} \rho_{liq} \left( \frac{\text{lbm}}{\text{ft}^3} \right) V^2 \left( \frac{\text{ft}^2}{\text{sec}^2} \right) \quad \text{E.4}$$

The fact that

$$(1 \cdot \text{lbm}) = (1 \cdot \text{lbf}) \frac{1 \text{ sec}^2}{g \text{ ft}} \quad \text{E.5}$$

may be substituted to produce

$$p_{com} \left( \frac{\text{lbf}}{\text{ft}^2} \right) = p_{\min} \left( \frac{\text{lbf}}{\text{ft}^2} \right) + \frac{1}{2} \frac{\rho_{liq}}{g} \left( \frac{\text{lbf}}{\text{ft}^3} \cdot \frac{\text{sec}^2}{\text{ft}} \right) V^2 \left( \frac{\text{ft}^2}{\text{sec}^2} \right) \quad \text{E.6}$$

Coalescing units, leaves

$$p_{com} \left( \frac{\text{lbf}}{\text{ft}^2} \right) = p_{\min} \left( \frac{\text{lbf}}{\text{ft}^2} \right) + \frac{1}{2} \frac{\rho_{liq}}{g} V^2 \left( \frac{\text{lbf}}{\text{ft}^2} \right) \quad \text{E.7}$$

However, in the code, pressure is in psi, thus,

$$P_{com} \left( \frac{\text{lbf}}{\text{ft}^2} \right) = \hat{P}_{com} \left( \frac{\text{lbf}}{\text{in}^2} \right) \cdot 144 \left( \frac{\text{in}^2}{\text{ft}^2} \right) = \hat{P}_{com} \cdot 144 \left( \frac{\text{lbf}}{\text{ft}^2} \right) \quad \text{E.8}$$

is substituted to produce

$$\hat{P}_{com} \cdot 144 \left( \frac{\text{lbf}}{\text{ft}^2} \right) = \hat{P}_{min} \cdot 144 \left( \frac{\text{lbf}}{\text{ft}^2} \right) + \frac{1}{2} \frac{\rho_{liq}}{g} V^2 \left( \frac{\text{lbf}}{\text{ft}^2} \right) \quad \text{E.9}$$

Dividing through by 144 and expressing 144 as 12 squared,

$$\hat{P}_{com} \left( \frac{\text{lbf}}{\text{ft}^2} \right) = \hat{P}_{min} \left( \frac{\text{lbf}}{\text{ft}^2} \right) + \frac{1}{2} \frac{\rho_{liq}}{g} \left( \frac{V}{12} \right)^2 \left( \frac{\text{lbf}}{\text{ft}^2} \right) \quad \text{E.10}$$

Or, using specific volume instead while substituting  $g = 32.2$ ,

$$\hat{P}_{com} \left( \frac{\text{lbf}}{\text{ft}^2} \right) = \hat{P}_{min} \left( \frac{\text{lbf}}{\text{ft}^2} \right) + \frac{1}{64.4 v_{liq}} \left( \frac{V}{12} \right)^2 \left( \frac{\text{lbf}}{\text{ft}^2} \right) \quad \text{E.11}$$

The units of velocity, V, is ft/min. It is the required volumetric flow rate divided by the area and the liquid discharge coefficient, with factors to provide the appropriate conversion of units:

$$V \left( \frac{\text{ft}}{\text{sec}} \right) = \frac{Q_{liq} \left( \frac{\text{ft}^3}{\text{min}} \right)}{60 \left( \frac{\text{sec}}{\text{min}} \right) \cdot C_{D_{liq}} \cdot A_{areq} (\text{ft}^2)} = \frac{Q_{liq}}{60 \cdot C_{D_{liq}} \cdot A_{areq}} \left( \frac{\text{ft}}{\text{min}} \right) \quad \text{E.12}$$

Substituting that equation into Equation E.11 yields

$$\hat{P}_{com} \left( \frac{\text{lbf}}{\text{ft}^2} \right) = \hat{P}_{min} \left( \frac{\text{lbf}}{\text{ft}^2} \right) + \frac{1}{64.4 v_{liq}} \left( \frac{Q_{liq}}{60 \cdot 12 \cdot C_{D_{liq}} \cdot A_{areq}} \right)^2 \left( \frac{\text{lbf}}{\text{ft}^2} \right) \quad \text{E.13}$$

or

$$\hat{P}_{com} \left( \frac{\text{lbf}}{\text{ft}^2} \right) = \hat{P}_{min} \left( \frac{\text{lbf}}{\text{ft}^2} \right) + \frac{1}{64.4 v_{liq}} \left( \frac{Q_{liq}}{720 \cdot C_{D_{liq}} \cdot A_{areq}} \right)^2 \left( \frac{\text{lbf}}{\text{ft}^2} \right) \quad \text{E.14}$$

which corresponds to the line of code originally cited,

```
pcom = pmin+( pow(reql/(720.0*DischargeCoef_Liq*areq),2) )  
/  
          (64.4*splq);
```



# **Appendix F: Governing Equations for the Generalized TPS Model**

## **Convection and Radiation Communication Areas**

The assumptions in the introduction to “The Generalized TPS Model and Database” mean that an equation can be written that describes the area of exposure between any two adjacent areas. To begin,  $A$  is the total area represented.  $Ac_i$  is the area of Layer  $i$  that is without voids while  $A(1 - c_i)$  is the area of Layer  $i$  that has voids. When considering the right-hand side of Layer  $i$ , the area that is exposed to layers beyond Layer  $i+1$  is  $Ac_i(1 - c_{i+1})$ . Here, the first  $c_i$  represents the non-void part of Layer  $i$ , where the  $(1 - c_{i+1})$  represents the part of Layer  $i+1$  that is void. Through this area,  $Ac_i(1 - c_{i+1})$ , Layer  $i$  can exchange heat and radiation with Layer  $i+2$ . But if Layer  $i+2$  also has voids in it, Layer  $i$  will exchange heat with Layer  $i+3$ , and so on. For each layer  $j$  to the right of Layer  $i$ , the area of communication between  $i$  and  $j$  is reduced by the amount of coverage of the layers between them. In general, the communication area between the right side of Layer  $i$  and the left side of Layers  $i+2$ ,  $i+3$ , etc. are as follows:

$$A_{R_i L_{i+2}} = Ac_i (1 - c_{i+1}) c_{i+2} \quad \text{F.1}$$

where  $A_{R_i L_j}$  is the communication area between the right side of  $i$  and the left side of  $j$ .  
The communication area between  $i$  and the left side of  $i + 3$  is

$$A_{R_i L_{i+3}} = Ac_i (1 - c_{i+1}) (1 - c_{i+2}) c_{i+3} \quad \text{F.2}$$

Likewise, for  $i$  and  $i + 4$  it is

$$A_{R_i L_{i+4}} = Ac_i (1 - c_{i+1}) (1 - c_{i+2}) (1 - c_{i+3}) c_{i+4} \quad \text{F.3}$$

In general, the communication area between the right side of Layer  $i$  and the left side of Layer  $j$  ( $j > i + 1$ ) is

$$A_{R_i L_j} = Ac_i c_j \prod_{k=i+1}^{j-1} (1 - c_k) \quad \text{F.4}$$

A similar exercise can be performed for the left side of Layer  $i$  and the right side of Layer  $i-2$ . Their communication area is

$$A_{L_i R_{i-2}} = Ac_i (1 - c_{i-1}) c_{i-2} \quad \text{F.5}$$

Likewise, for  $i$  and  $i-3$ ,

$$A_{L_i R_{i-3}} = Ac_i (1 - c_{i-1}) (1 - c_{i-2}) c_{i-3} \quad \text{F.6}$$

And for Layer  $i-4$ , it is

$$A_{L_i R_{i-4}} = Ac_i (1 - c_{i-1}) (1 - c_{i-2}) (1 - c_{i-3}) c_{i-4} \quad \text{F.7}$$

So, in general, the communication area between the left side of Layer  $i$  and the right side of Layer  $j$  is

$$A_{L_i R_j} = Ac_i c_j \prod_{k=j+1}^{i-1} (1 - c_k) \quad \text{F.8}$$

## Conduction Communication Areas

All areas, including the area in contact and the areas exposed to radiation and convective heat transfer, experience conduction. The areas over which each of the three temperatures exist may be computed by considering the fractional coverages as

probabilities. For example, the probability at any point in the  $i$  interface of Layers  $i$  and  $i+1$  being in contact is the product of the probability of there being material present on Layer  $i$  ( $c_i$ ) with the probability of there being material present on Layer  $i+1$  ( $c_{i+1}$ ). Scaling this product by the total area considered yields the area of the region in contact,  $Ac_i c_{i+1}$ . In a similar fashion, the area over which  $T_{R_i}$  exists is the product of the probability that material in Layer  $i$  is present ( $c_i$ ) with the probability that material in Layer  $i+1$  is not present ( $1-c_{i+1}$ ). In summary, the areas are as follows:

Temperature	Joint Probability at a Point	Scaled to Obtain Area	
$T_i$	$c_i c_{i+1}$	$Ac_i c_{i+1}$	(F.8a)
$T_{R_i}$	$c_i (1 - c_{i+1})$	$Ac_i (1 - c_{i+1})$	(F.8b)
$T_{L_i}$	$c_i (1 - c_{i-1})$	$Ac_i (1 - c_{i-1})$	(F.8c)

**Table F.1 Computing Areas of Contact and Exposure Using a Joint Probability Approach**

To determine the communication areas between two areas, one multiplies the two joint probabilities together because doing so represents the probability of overlap. Table F.2 summarizes the results of this approach. The left column describes the two areas that are overlapping; the third column is the area of overlap. The ‘‘Nomenclature’’ column establishes a simpler notation that is used in subsequent equations. There are some subtleties to the notation. First, the area connecting  $T_i$  and  $T_{i-1}$ , is reversible, e.g.,  $A_{i,i-1} = A_{i-1,i}$ . Using this fact, the  $A_{i,i-1}$  variable can be used to represent other combinations. Substituting  $i+1$  for  $i$ ,  $A_{i+1,i} = Ac_{i+1}^2 c_{i+2} c_i = A_{i,i+1}$ . Another subtlety is that the  $i$  index on  $L$  and  $R$  in  $A_{L,R}$  is omitted since that conduction *must* occur on layer  $i$ . Likewise, the  $i$  subscript is omitted on  $R$  in  $A_{i,R}$  since it that conduction must be  $i+1$ . And note that if the area connecting  $T_{i-1}$  and  $T_{R_i}$  is needed,  $i-1$  can be substituted for  $i$ , giving the quantity  $A_{i-1,R} = Ac_{i-1} c_i^2 (1 - c_{i+1})$ . Finally, the  $i$  subscript on  $L$  is omitted in  $A_{i,L}$  since that conduction must be on  $i$ .

Conduction Path Connecting	Joint Probability at a Point of Overlap Occuring	Scaled to Obtain Area	Nomenclature	
$T_i$ and $T_{i-1}$	$c_i^2 c_{i+1} c_{i-1}$	$Ac_i^2 c_{i+1} c_{i-1}$	$A_i$	(F.8d)
$T_i$ and $T_{R_{i+1}}$	$c_i c_{i+1}^2 (1 - c_{i+2})$	$Ac_i c_{i+1}^2 (1 - c_{i+2})$	$A_{i,R}$	(F.8e)
$T_{L_i}$ and $T_{R_i}$	$c_i^2 (1 - c_{i+1})(1 - c_{i-1})$	$Ac_i^2 (1 - c_{i+1})(1 - c_{i-1})$	$A_{L,R}$	(F.8f)
$T_i$ and $T_{L_i}$	$c_i^2 c_{i+1} (1 - c_{i-1})$	$Ac_i^2 c_{i+1} (1 - c_{i-1})$	$A_{i,L}$	(F.8g)

**Table F.2 Computing Conduction Communication Areas Using a Joint Probability Approach**

It is worthwhile to make special notation for how these values change at endpoints. Specifically,  $c_0$  and  $c_{n+1}$  represent the “coverage” of the non-existent layers adjacent to the innermost and outermost layers, respectively. Hence,  $c_0 = c_{n+1} = 0$ . Thus, the above area values for these endpoints are:

Area Value	$1 < i < n$	$i = 1$	$i = n$	
$A_i$	$Ac_i^2 c_{i+1} c_{i-1}$	0	0	(F.8h)
$A_{i,R}$	$Ac_i c_{i+1}^2 (1 - c_{i+2})$	$Ac_i c_{i+1}^2 (1 - c_{i+2})$	0	(F.8i)
$A_{L,R}$	$Ac_i^2 (1 - c_{i+1})(1 - c_{i-1})$	$Ac_i^2 (1 - c_{i+1})$	$Ac_i^2 (1 - c_{i-1})$	(F.8j)
$A_{i,L}$	$Ac_i^2 c_{i+1} (1 - c_{i-1})$	$Ac_i^2 c_{i+1}$	0	(F.8k)

**Table F.3 Endpoint values for area**

## Heat Balance Equations

### Area in Contact

For generality, consider interface  $i$ , which is the interface between Layer  $i$  and Layer  $i+1$ . Since this area is in contact, conduction is the only mechanism for heat transfer. A heat balance on the interface states that the heat flowing into it must equal the heat flowing out of it. That requirement is embodied in the following equation:

$$\frac{k_i}{w_i} A_i (T_i - T_{i-1}) + \frac{k_i}{w_i} A_{i,L} (T_i - T_{L_i}) + \frac{k_{i+1}}{w_{i+1}} A_{i+1} (T_i - T_{i+1}) + \frac{k_{i+1}}{w_{i+1}} A_{i,R} (T_i - T_{R_{i+1}}) = 0 \quad \text{F.9}$$

### Right Side's Exposed Area

Consider again interface  $i$ , but this time, the part of that interface that is exposed due to a lack of coverage in Layer  $i+1$ . Heat conduction still occurs to the left, but radiative and convective heat transfer occurs to the right. Again, a heat balance on the interface states that the heat flowing into it must equal the heat flowing out of it. That requirement is embodied in the following equation, where heat conduction to the left is represented in the first terms and radiative plus convective heat flow is represented in the last terms:

$$\begin{aligned} & \frac{k_i}{w_i} A_{i-1,R} (T_{R_i} - T_{i-1}) + \frac{k_i}{w_i} A_{L,R} (T_{R_i} - T_{L_i}) + \\ & \sum_{k=i+1}^n A_{R_i,L_k} h_{i,k} (T_{R_i} - T_{L_k}) + \sum_{k=i+1}^n A_{R_i,L_k} \frac{\sigma(T_{R_i}^4 - T_{L_k}^4)}{1/\varepsilon_{R_i} + 1/\varepsilon_{L_k} + 1} = 0 \end{aligned} \quad \text{F.10}$$

In the above equation, the radiative exchange is modeled as the exchange between two infinite parallel planes. Behind this choice are the assumptions that the distance separating them is small compared to the communication area. Along with that assumption, the radiative and convective exchange between layers based on exposure of the walls surrounding the voids is neglected.

### Left Side's Exposed Area

Now consider the layer on the right of interface  $i$ . Part of that layer will be exposed due to voids in Layer  $i$ . Analogous to the above equation, heat conduction will occur to the *right*, while radiative and convective heat transfer will occur to the *left*. The heat balance is in the following analogous equation:

$$\begin{aligned} & \frac{k_i}{w_i} A_{i,L} (T_{L_i} - T_i) + \frac{k_i}{w_i} A_{L,R} (T_{L_i} - T_{R_i}) + \\ & \sum_{k=1}^{i-1} A_{L_i,R_k} h_{i,k} (T_{L_i} - T_{R_k}) + \sum_{k=1}^{i-1} A_{L_i,R_k} \frac{\sigma(T_{L_i}^4 - T_{R_k}^4)}{1/\varepsilon_{L_i} + 1/\varepsilon_{R_k} + 1} = 0 \end{aligned} \quad \text{F.11}$$

The same assumptions regarding radiative exchange for Equation F.10 apply here in an analogous way.

### Boundary Conditions

Following the same methodology that is currently in AFFTAC, the following two boundary conditions are applied to the above equations:

- (1) Inner Boundary Known Temperature Condition: This condition is applied by setting  $T_{L_1} = T_{known}$ . Note that a requirement of the model is that the innermost and

outermost layers have 100% coverage. The value of  $T_{known}$  is taken as the inner layer's inner temperature from the previous time-step. The process of using this old value is part of the current nonlinear lagging methodology in AFFTAC. So for Layer 1, Equations F.11 is replaced with

$$T_{L_1} = T_{known} \quad \text{F.12}$$

- (2) Outer Boundary Flux Condition: This condition replaces the conduction, radiation, and convection occurring towards the right for Layer  $n$  with a heat flux that is based on the flame temperature and outermost layer temperature. Thus, Equation F.10 for  $i = n$  is replaced with

$$\frac{k_i}{w_i} A_{i-1,R} (T_{R_i} - T_{i-1}) + \frac{k_i}{w_i} A_{L,R} (T_{R_i} - T_{L_i}) + A \sigma (\varepsilon_{R_n} T_{R_n}^4 - \varepsilon_f \varepsilon_{R_n} f T_f^4) = 0 \quad \text{F.13}$$

The factor  $f$  is a shape configuration factor as discussed in the chapter entitled "Details of the Overall Thermal Model". Also, it is noted that because there is 100% coverage on this outer surface,  $T_n = T_{R_n}$ . This equation replaces Equation F.11 for  $i = n$ .

- (3) Zero Coverage: Because no lateral conduction is built into the model, the model breaks down for small coverage values. However, the model recovers its accuracy in the limit of zero coverage by setting the conduction region temperatures equal to the radiating temperatures on the same surface (Equations F.14, below) and by setting the exposed area temperatures for the layer with zero coverage equal to their counterparts on the neighboring surfaces (Equations F.15, below).

So when  $c_i = 0$  in place of the conduction equations, we have:

$$\begin{aligned} T_i - T_{L_{i+1}} &= 0 \\ T_{i-1} - T_{R_{i-1}} &= 0 \end{aligned} \quad \text{F.14}$$

And in place of the exposed areas' radiation and convection equations, we have

$$\begin{aligned} T_{L_i} - T_{R_{i-1}} &= 0 \\ T_{R_i} - T_{L_{i+1}} &= 0 \end{aligned} \quad \text{F.15}$$

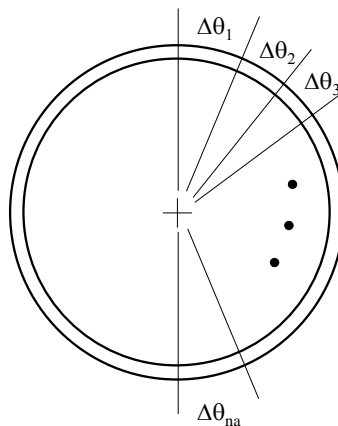
## Angular Dependence

There are two aspects in which the TPS model is in effect in the AFFTAC operator split methodology. First, the TPS model is used to compute the updated outer surface

temperature. In this situation, the interior boundary condition is applied as a known value and the outer surface temperature ( $T_I$ ) is determined by solving the system of equations described above. Second, the TPS model is used in a heat balance equation for the innermost surface. In this second application, the inner surface temperature  $T_n$  is not known. But in this situation, the most recent value for  $T_{n-1}$  is used in with the thermal conductivity and thickness to compute the heat flux entering the innermost surface from the outside. This heat flux is balanced with the heat flux from the innermost surface to the vapor and liquid to compute  $T_n$ .

In this the generalized TPS model, these two areas of application remain unchanged in principle. However, this model also admits the possibility that the coverage terms ( $c_i$ , above) may vary with angle. Specifically, the user is allowed to set up  $n_a$  segments of the tank car wherein the  $c_i$  array may have different values for each layer,  $i$  (see Figure F.1). Therefore, in the implemented algorithm, the coverage array has two subscripts, the first for the angle region and the second for the layer;  $c_{ai}$  is the coverage for Layer  $i$  in angle region  $a$ .

The angular dependence of the TPS does not affect the assumption that the inner tank wall temperature adjacent to the liquid lading, which is equal to the liquid temperature, is uniform. However, it does affect the assumption that the inner tank wall temperature adjacent to the vapor lading is uniform. Rather, an array of innermost temperatures is introduced in AFFTAC; these values are determined using the procedure described in the first paragraph of this section. Likewise, an array of outermost temperatures for this region are introduced; these are determined using the procedure described in that same paragraph.



**Figure F.1: Illustration of how the coverage values ( $c_i$ ) can vary based on a user-specified number of angle bins.**

## Nonlinear Solver

Equation F.9-F.11 with boundary conditions F.12-F.13 constitute  $3n$  simultaneous nonlinear equations for the  $3n$  temperatures,  $T_i$ ,  $T_{Li}$ , and  $T_{Ri}$ ,  $i = 1, 2, 3, \dots, n$ , where  $n$  is the number of layers. As is currently done in AFFTAC, these temperatures are determined using the Newton-Raphson iterative method. To formulate the solver, functions are defined using the heat balance and boundary conditions described earlier. In other words,

Exposed Left Side Balance

F.16

$$f_i^1(T_{L_i}, T_{R_i}, T_i) = \begin{cases} T_{L_i} - T_{known} & i = 1 \\ T_{L_i} - T_{R_{i-1}} & \text{if } c_i = 0 \\ \frac{k_i}{w_i} [A_{i,L}(T_{L_i} - T_i) + A_{L,R}(T_{L_i} - T_{R_i})] + \sum_{k=1}^{i-1} A_{L,R_k} \left[ h_{i,k}(T_{L_i} - T_{R_k}) + \frac{\sigma(T_{L_i}^4 - T_{R_k}^4)}{1/\varepsilon_{L_i} + 1/\varepsilon_{R_k} + 1} \right] & 2 < i < n \end{cases}$$

Exposed Right Side Balance

F.17

$$f_i^2(T_{L_i}, T_{R_i}, T_i) = \begin{cases} \frac{k_i}{w_i} [A_{i-1,R}(T_{R_i} - T_{i-1}) + A_{L,R}(T_{R_i} - T_{L_i})] + \sum_{k=i+1}^n A_{R_i L_k} \left[ h_{i,k}(T_{R_i} - T_{L_k}) + \frac{\sigma(T_{R_i}^4 - T_{L_k}^4)}{1/\varepsilon_{R_i} + 1/\varepsilon_{L_k} + 1} \right] & 1 \leq i < n \\ T_{R_i} - T_{L_{i+1}} = 0 & \text{if } c_i = 0 \\ \frac{k_i}{w_i} [A_{i-1,R}(T_{R_i} - T_{i-1}) + A_{L,R}(T_{R_i} - T_{L_i})] + A \sigma(\varepsilon_{R_n} T_{R_n}^4 - \varepsilon_f \varepsilon_{R_n} f T_f^4) & i = n \end{cases}$$

Contact Balance

F.18

$$f_i^3(T_{L_i}, T_{R_i}, T_i) = \begin{cases} \frac{k_i}{w_i} [A_i(T_i - T_{i-1}) + A_{i,L}(T_i - T_{L_i})] + \frac{k_{i+1}}{w_{i+1}} [A_{i+1}(T_i - T_{i+1}) + A_{i,R}(T_i - T_{R_{i+1}})] = 0 & 1 \leq i < n \\ T_i - T_{L_{i+1}} \text{ and } T_{i-1} - T_{R_{i-1}} & c_i = 0 \\ T_i - T_{R_i} & i = n \end{cases}$$

In so doing, the simultaneous nonlinear equations may be written as



$$\begin{aligned}
f_i^1(T_{L_i}, T_{R_i}, T_i) &= 0, \quad i = 1, 2, 3, \dots, n \\
f_i^2(T_{L_i}, T_{R_i}, T_i) &= 0, \quad i = 1, 2, 3, \dots, n \\
f_i^3(T_{L_i}, T_{R_i}, T_i) &= 0, \quad i = 1, 2, 3, \dots, n
\end{aligned}
\tag{F.19}$$

and the Newton-Raphson algorithm for this system may be written as follows. Let  $I$  denote the iteration number, then

$$\begin{aligned}
T_{L_i}^{I+1} &= T_{L_i}^I + \delta_{L_i}^I, \quad i = 1, 2, 3, \dots, n-1 \\
T_{R_i}^{I+1} &= T_{R_i}^I + \delta_{R_i}^I, \quad i = 1, 2, 3, \dots, n-1 \\
T_i^{I+1} &= T_i^I + \delta_i^I, \quad i = 1, 2, 3, \dots, n-1
\end{aligned}
\tag{F.20}$$

The deltas are the solution to the following linear system:

$$\begin{bmatrix} J^{11} & J^{12} & J^{13} \\ J^{21} & J^{22} & J^{23} \\ J^{31} & J^{32} & J^{33} \end{bmatrix}_I \begin{bmatrix} \delta_{L_i}^{I+1} \\ \delta_{R_i}^{I+1} \\ \delta_i^{I+1} \end{bmatrix} = - \begin{bmatrix} \mathbf{f}^1 \\ \mathbf{f}^2 \\ \mathbf{f}^3 \end{bmatrix}_I
\tag{F.21}$$

where the Jacobian entries are given by

$$\begin{aligned}
J_{ij}^{11} &= \frac{\partial f_j^1}{\partial T_{L_j}} & J_{ij}^{12} &= \frac{\partial f_j^1}{\partial T_{R_j}} & J_{ij}^{13} &= \frac{\partial f_j^1}{\partial T_j} \\
J_{ij}^{21} &= \frac{\partial f_j^2}{\partial T_{L_j}} & J_{ij}^{22} &= \frac{\partial f_j^2}{\partial T_{R_j}} & J_{ij}^{23} &= \frac{\partial f_j^2}{\partial T_j} \\
J_{ij}^{31} &= \frac{\partial f_j^3}{\partial T_{L_j}} & J_{ij}^{32} &= \frac{\partial f_j^3}{\partial T_{R_j}} & J_{ij}^{33} &= \frac{\partial f_j^3}{\partial T_j}
\end{aligned}
\tag{F.22}$$

These entries may be evaluated analytically using Equations F.9-F.11. To assist with notation, it is helpful to review and define the following to functions. The Kronecker delta,  $\delta_{ij}$ , is unity if  $i=j$  and zero otherwise. Second, the integer unit step function,  $u_{i,j}$ , is unity if  $j \geq i$  and zero otherwise. The entries of the Jacobian will now be derived below.

First, to assist in the taking of partial derivatives, the functions are re-written with each term split apart and made separate. To assist with the algebra, the following terms are defined:

F.23

$$F_{R_i L_k} \equiv A_{R_i L_k} \frac{\sigma}{1/\varepsilon_{R_i} + 1/\varepsilon_{L_k} + 1}$$

$$F_{L_i R_k} \equiv A_{R_i L_k} \frac{\sigma}{1/\varepsilon_{L_i} + 1/\varepsilon_{R_k} + 1}$$

$$G_{R_i L_k} \equiv A_{R_i L_k} h_{i,k}$$

$$G_{L_i R_k} \equiv A_{L_i R_k} h_{i,k}$$

Exposed Left Side Balance

F.24

$$f_i^1(T_{L_i}, T_{R_i}, T_i) = \begin{cases} \left( \frac{k_i}{w_i} (A_{i,L} + A_{L,R}) + \sum_{k=1}^{i-1} G_{L_i R_k} \right) T_{L_i} + \left( \sum_{k=1}^{i-1} F_{L_i R_k} \right) T_{L_i}^4 & 1 < i \leq n \\ - \left( \frac{k_i}{w_i} A_{L,R} \right) T_{R_i} - \sum_{k=1}^{i-1} G_{L_i R_k} T_{R_k} - \sum_{k=1}^{i-1} F_{L_i R_k} T_{R_k}^4 - \left( \frac{k_i}{w_i} A_{i,L} \right) T_i & \\ T_{L_i} - T_{R_{i-1}} = 0 & c_i = 0 \\ T_{L_i} - T_{known} & i = 1 \end{cases}$$

Exposed Right Side Balance

F.25

$$f_i^2(T_{L_i}, T_{R_i}, T_i) = \begin{cases} - \sum_{k=i+1}^n G_{R_i L_k} T_{L_k} - \sum_{k=i+1}^n F_{R_i L_k} T_{L_k}^4 - \left( \frac{k_i}{w_i} A_{L,R} \right) T_{L_i} + \left( \frac{k_i}{w_i} (A_{i-1,R} + A_{L,R}) + \sum_{k=i+1}^n G_{R_i L_k} \right) T_{R_i} & 1 \leq i < n \\ + \left( \sum_{k=i+1}^n F_{R_i L_k} \right) T_{R_i}^4 - \left( \frac{k_i}{w_i} A_{i-1,R} \right) T_{i-1} & \\ T_{R_i} - T_{L_{i+1}} = 0 & c_i = 0 \\ \frac{k_i}{w_i} (A_{i-1,R} + A_{L,R}) T_{R_i} - \left( \frac{k_i}{w_i} A_{L,R} \right) T_{L_i} - \left( \frac{k_i}{w_i} A_{i-1,R} \right) T_{i-1} + (A \varepsilon_{R_n}) T_{R_n}^4 - A \varepsilon_f \varepsilon_{R_n} f T_f^4 & i = n \end{cases}$$

Contact Balance

F.26

$$f_i^3(T_{L_i}, T_{R_i}, T_i) = \begin{cases} -\left(\frac{k_i}{w_i} A_{i,L}\right) T_{L_i} - \left(\frac{k_{i+1}}{w_{i+1}} A_{i,R}\right) T_{R_{i+1}} + \left(\frac{k_i}{w_i} A_i + \frac{k_i}{w_i} A_{i,L} + \frac{k_{i+1}}{w_{i+1}} A_{i+1} + \frac{k_{i+1}}{w_{i+1}} A_{i,R}\right) T_i & 1 \leq i < n \\ -\left(\frac{k_i}{w_i} A_i\right) T_{i-1} - \left(\frac{k_{i+1}}{w_{i+1}} A_{i+1}\right) T_{i+1} = 0 \\ T_i - T_{L_{i+1}} \text{ and } T_{i-1} - T_{R_{i-1}} & c_i = 0 \\ T_i - T_{R_i} & i = n \end{cases}$$

Using the functions expressed as above, the Jacobian can now be written as follows:

First row of blocks:

$$J_{ij}^{11} = \frac{\partial f_i^1}{\partial T_{L_j}} = \begin{cases} \left(\frac{k_i}{w_i} (A_{i,L} + A_{L,R}) + \sum_{k=1}^{i-1} G_{L_i, R_k}\right) \delta_{i,j} + 4 \left(\sum_{k=1}^{i-1} F_{L_i, R_k}\right) T_{L_i}^3 \delta_{i,j} & 1 < i \leq n \\ \delta_{i,j} & c_i = 0 \\ \delta_{i,j} & i = 1 \end{cases} \quad \text{F.27}$$

$$J_{ij}^{12} = \frac{\partial f_i^1}{\partial T_{R_j}} = \begin{cases} -\left(\frac{k_i}{w_i} A_{L,R}\right) \delta_{i,j} - G_{L_i, R_j} (1 - u_{i,j}) - (4F_{L_i, R_j}) T_{R_j}^3 (1 - u_{i,j}) & 1 < i \leq n \\ \delta_{i,j-1} & c_i = 0 \\ 0 & i = 1 \end{cases} \quad \text{F.28}$$

$$J_{ij}^{13} = \frac{\partial f_i^1}{\partial T_j} = \begin{cases} -\frac{k_i}{w_i} A_{i,L} \delta_{i,j} & 1 < i \leq n \\ 0 & i = 1 \end{cases} \quad \text{F.29}$$

Second row of blocks:

$$J_{ij}^{21} = \frac{\partial f_i^2}{\partial T_{L_j}} = \begin{cases} -\left(G_{R,L_j}\right)u_{i,j-1} - \left(4F_{R,L_j}\right)T_{L_j}^3 u_{i,j-1} - \left(\frac{k_i}{w_i} A_{L,R}\right)\delta_{i,j} & 1 \leq i < n \\ \delta_{i,j} & c_i = 0 \\ -\left(\frac{k_i}{w_i} A_{L,R}\right)\delta_{i,j} & i = n \end{cases} \quad \text{F.30}$$

$$J_{ij}^{22} = \frac{\partial f_i^2}{\partial T_{R_j}} = \begin{cases} \left(\frac{k_i}{w_i} (A_{i-1,R} + A_{L,R}) + \sum_{k=i+1}^n G_{R,L_k}\right)\delta_{i,j} + 4\left(\sum_{k=i+1}^n F_{R,L_k}\right)T_{R_j}^3 \delta_{i,j} & 1 \leq i < n \\ \delta_{i,j+1} & c_i = 0 \\ \frac{k_i}{w_i} (A_{i-1,R} + A_{L,R})\delta_{i,j} + 4A\sigma\varepsilon_{R_j} T_{R_j}^3 \delta_{i,j} & i = n \end{cases} \quad \text{F.31}$$

$$J_{ij}^{23} = \frac{\partial f_i^2}{\partial T_j} = \begin{cases} -\frac{k_i}{w_i} A_{i-1,R} \delta_{i-1,j} & 1 \leq i < n \\ -\frac{k_i}{w_i} A_{i-1,R} \delta_{i-1,j} & i = n \end{cases} \quad \text{F.32}$$

Third row of blocks:

$$J_{ij}^{31} = \frac{\partial f_i^3}{\partial T_{L_j}} = \begin{cases} -\frac{k_i}{w_i} A_{i,L} \delta_{i,j} & 1 \leq i < n \\ 0 & i = n \\ -\delta_{i,j+1} & c_i = 0 \end{cases} \quad \text{F.33}$$

$$J_{ij}^{32} = \frac{\partial f_i^3}{\partial T_{R_j}} = \begin{cases} -\frac{k_{i+1}}{w_{i+1}} A_{i,R} \delta_{i,j-1} & 1 \leq i < n \\ -\delta_{i,j-1} & i = n \text{ or if } c_i = 0 \end{cases} \quad \text{F.34}$$

$$J_{ij}^{33} = \frac{\partial f_i^3}{\partial T_j} = \begin{cases} \frac{k_i}{w_i} (A_i + A_{i,L}) \delta_{i,j} + \frac{k_{i+1}}{w_{i+1}} (A_{i+1} + A_{i,R}) \delta_{i,j} - \frac{k_i}{w_i} A_i \delta_{i,j+1} - \frac{k_{i+1}}{w_{i+1}} A_{i+1} \delta_{i,j-1} & 1 \leq i < n \\ \delta_{i,j} \text{ and } \delta_{i,j-1} & c_i = 0 \\ \delta_{i,j} & i = n \end{cases}$$

The above expressions for the Jacobian are cumbersome from a programming standpoint. A more helpful representation is as follows:

First row of blocks:

$$J_{ij}^{11} = \begin{cases} \text{Diagonal entry: } \left( \frac{k_i}{w_i} (A_{i,L} + A_{L,R}) + \sum_{k=1}^{i-1} G_{L_i, R_k} \right) + 4 \left( \sum_{k=1}^{i-1} F_{L_i, R_k} \right) T_{L_i}^3 & 1 < i \leq n \\ \text{Diagonal entry: } 1 & c_i = 0 \\ \text{Diagonal entry: } 1 & i = 1 \end{cases} \quad \text{F.36}$$

$$J_{ij}^{12} = \begin{cases} \text{Diagonal entry: } - \left( \frac{k_i}{w_i} A_{L,R} \right) & \text{Before the diagonal: } -G_{L_i, R_j} - 4F_{L_i, R_j} T_{R_j}^3 & 1 < i \leq n \\ \text{Before the diagonal: } -1 & c_i = 0 \\ 0 & i = 1 \end{cases} \quad \text{F.37}$$

$$J_{ij}^{13} = \begin{cases} \text{Diagonal entry: } - \frac{k_i}{w_i} A_{i,L} & 1 < i \leq n \\ 0 & i = 1 \end{cases} \quad \text{F.38}$$

Second row of blocks:

$$J_{ij}^{21} = \begin{cases} \text{Diagonal entry: } -\left(\frac{k_i}{w_i} A_{L,R}\right) & \text{After the diagonal: } -(G_{R_i L_j}) - 4F_{R_i L_j} T_{L_j}^3 & 1 \leq i < n \\ \text{After the diagonal: } -1 & & c_i = 0 \\ \text{Diagonal entry: } -\left(\frac{k_i}{w_i} A_{L,R}\right) & & i = n \end{cases} \quad \text{F.39}$$

$$J_{ij}^{22} = \begin{cases} \text{Diagonal entry: } \frac{k_i}{w_i} \left( A_{i-1,R} + A_{L,R} + \sum_{k=i+1}^n G_{R_i L_k} \right) + 4 \left( \sum_{k=i+1}^n F_{R_i L_k} \right) T_{R_j}^3 & 1 \leq i < n \\ \text{Diagonal entry: } 1 & & c_i = 0 \\ \text{Diagonal entry: } \frac{k_i}{w_i} (A_{i-1,R} + A_{L,R}) + 4A\alpha_{R_j} T_{R_j}^3 & & i = n \end{cases} \quad \text{F.40}$$

$$J_{ij}^{23} = \begin{cases} \text{One entry before the diagonal: } -\frac{k_i}{w_i} A_{i-1,R} & 1 \leq i < n \\ \text{One entry before the diagonal: } -\frac{k_i}{w_i} A_{i-1,R} & i = n \end{cases} \quad \text{F.41}$$

Third row of blocks:

$$J_{ij}^{31} = \begin{cases} \text{Diagonal entry: } -\frac{k_i}{w_i} A_{i,L} \delta_{i,j} & 1 \leq i < n \\ 0 & i = n \\ \text{Diagonal entry: } -1 & \text{if } c_{i-1} = 0 \end{cases} \quad \text{F.42}$$

$$J_{ij}^{32} = \begin{cases} \text{One after the diagonal: } -\frac{k_{i+1}}{w_{i+1}} A_{i,R} & 1 \leq i < n \\ \text{Diagonal entry: } -1 & i = n \\ \text{Diagonal entry: } -1 & \text{if } c_i = 0 \end{cases} \quad \text{F.43}$$

$$J_{ij}^{33} = \begin{cases} \text{Diagonal entry: } \frac{k_i}{w_i}(A_i + A_{i,L}) + \frac{k_{i+1}}{w_{i+1}}(A_{i+1} + A_{i,R}) & \text{One before: } -\frac{k_i}{w_i} A_i & \text{One after: } -\frac{k_{i+1}}{w_{i+1}} A_{i+1} & 1 \leq i < n \\ \text{Diagonal entry: } 1 & & & i = n \text{ or if } c_i = 0, \\ & & & \text{or if } c_{i-1} = 0, \end{cases} \quad \text{F.44}$$